VYSOKÉ UČENÍ TECHNICKÉ V BRNĚ
FAKULTA ELEKTROTECHNIKY A KOMUNIKAČNÍCH TECHNOLOGIÍ
ÚSTAV BIOMEDICÍNSKÉHO INŽENÝRSTVÍ

Ing. Marina Ronzhina

STUDY OF ELECTROPHYSIOLOGICAL FUNCTION OF THE HEART IN EXPERIMENTAL CARDIOLOGY

STUDIUM ELEKTROFYZIOLOGICKÝCH PROJEVŮ SRDCE V EXPERIMENTÁLNÍ KARDIOLOGII

ZKRÁCENÁ VERZE DISERTAČNÍ PRÁCE

ABRIDGED DOCTORAL THESIS

Obor: Biomedicínská elektronika a biokybernetika

Školitel: doc. Ing. Jana Kolářová, Ph.D.

Rok obhajoby: 2016

ABSTRACT

Isolated heart is widely used in experimental cardiology to study myocardial ischemia and infarct, left ventricular hypertrophy, myocarditis, etc. Nevertheless, the standardized criteria for assessment of above disorders in animal models are missing that complicates interpretation of the results obtained in such studies. It is of special importance, if several pathologies are presented simultaneously, when possible co-effects cannot be simply identified and analysed. Besides the condition of the heart, there are many other factors playing important role in data acquisition and analysis. In this work, electrophysiological effects of increased left ventricular mass (intrinsic factor) and voltage-sensitive dye di-4-ANEPPS (external factor) are evaluated on rabbit isolated hearts under non-ischemic and ischemic condition. Although both phenomena are quite frequent in animal studies, their effects on ischemia manifestations and electrogram-based ischemia detection accuracy have not been quantitatively described yet. Results of quantification of ischemia-induced changes in heart function (under normal conditions, increased LV or dye administration) by analysis of various EG and VCG parameters are summarized. Such important aspects as recording electrodes placement, method of parameters calculation (using or without outcomes of manual EG delineation) and definition of the beginning of 'true' ischemic injury in preparation (methodological factors) are also addressed. Along with it, different tools for automatic detection of ischemia in data are presented. According to the results of statistical analysis of parameters and testing the detectors on different data, all above mentioned phenomena (both heart-related and methodological) should be taken into account to ensure successful study of the heart electrical activity.

KEYWORDS

Rabbit isolated heart; electrogram; vectorcardiogram; global myocardial ischemia; left ventricle size; di-4-ANEPPS; feature selection; automatic classification.

ABSTRAKT

Srdeční poruchy, jejichž příkladem je ischemie myokardu, infarkt, hypertrofie levé komory a myokarditida, jsou v experimentální kardiologii obvykle studovány na modelu izolovaného srdce. Kritéria pro detekci srdečních poruch však nejsou pro zvířecí modely standardizována, což komplikuje srovnání a interpretaci výsledků různých experimentálních studií. Obzvlášť složitá situace nastává při současném výskytu několika patologických jevů, jejichž vzájemná součinnost komplikuje rozpoznání jejich individuálních účinků. Korektní posouzení stavu srdce vyžaduje také zohlednění mnoha faktorů spojených s akvizicí dat. Tato práce je věnována kvantitativnímu hodnocení elektrofyziologických změn způsobených globální ischemií myokardu. Vliv ischemie byl hodnocen pro fyziologická srdce a srdce se zvětšenou levou komorou a dále pro srdce nabarvená napěťově-citlivým barvivem di-4-ANEPPS. Přestože jsou oba fenomény často zastoupeny v animálních studiích, nebyl dosud popsán jejich vliv na manifestaci ischemie v elektrogramech (EG), ani nebyl kvantifikován jejich vliv na přesnost detekčních algoritmů pro identifikaci ischemie. Práce shrnuje kvantitativní změny srdeční funkce vyvolané ischemií (v normálních podmínkách, při hypertrofii levé komory, a při administraci barviva) založené na hodnocení EG a VKG parametrů. Dále práce obsahuje rozbor důležitých aspektů akvizice záznamů, jako je umístění snímacích elektrod, způsob výpočtu deskriptorů z EG a VKG (s použitím výsledků manuálního rozměření záznamů, nebo bez něj) a identifikace okamžiku vývoje ischemie v preparátu. Nedílnou součást práce tvoří návrh, realizace a ověření metod pro automatickou detekci ischemie v experimentálních záznamech. Výsledky práce dokazují, že dosažení opakovatelných a věrohodných výsledků je podmíněno zohledněním všech výše uvedených faktorů souvisejících jak se stavem srdce, tak s metodikou záznamu a analýzy dat.

KLÍČOVÁ SLOVA

Izolované králičí srdce; elektrogram; vektorkardiogram; globální ischemie myokardu; velikost levé komory srdeční; di-4-ANEPPS; výběr příznaků; automatická klasifikace.

TABLE OF CONTENTS

Introduction **5**

1 Brief summary of electrophysiological studies of myocardial ischemia **5**

1.1 Electrocardiography 5
1.2 ECG based diagnostics of myocardial ischemia 5
1.3 Study of myocardial ischemia using rabbit model 7

2 Aims of the doctoral thesis **9**

3 Experiments with rabbit isolated hearts **9**

4 Electrical activity of the heart under normal and ischemic conditions **15**

4.1 General characteristics of electrogram 15
4.2 Effects of left ventricle mass on electrogram 20
4.3 Effects of voltage-sensitive dye di-4-ANEPPS on electrogram 24

5 Automatic detection of ischemia in electrograms **30**

5.1 Feature selection 31
5.2 Data classification 33
5.3 Evaluation of classification performance 34
5.4 Binary classification: single-feature decision rule method 34
5.5 Binary classification: multi-feature supervised techniques 37
5.6 4-class classification: single-feature decision tree 38
5.7 4-class-classification: multi-feature supervised techniques 39
5.8 11-class classification 40

Overall conclusions **41**

References **44**

Selected author publications **49**

Appendix A – Parameters calculated from electrograms and vectorcardiograms **50**

INTRODUCTION

Although ischemic and reperfusion injury has been intensely studied, it is worth of further interest, since the coronary artery disease still represents one of the major causes of morbidity and mortality in many countries around the world. Particularly, in Europe region, coronary heart disease (which is a result of coronary artery disease) caused 19 % of deaths in men and 20 % of deaths in woman last year [1]. Myocardial ischemia and concomitant arrhythmias result in incorrect electrical and mechanical activity of the heart and often lead to the sudden death.

Mechanisms of various heart disorders are well known due to available diagnostic tools such as electrocardiography, echocardiography, heart catheterization, etc. First two techniques are fundamental methods widely used for clinical diagnostics of heart diseases in both acute and chronic forms by assessment of the pathological changes in electrical conduction system, morphological structure and function of the heart. There are standardized guidelines for diagnostics and management of heart diseases reported by American Heart Association (AHA), American College of Cardiology Foundation (ACCF) and Heart Rhythm Society (HRS) [2]. Recommendations from the guidelines are regularly updated according to the results of new studies. Nevertheless, there are still areas requiring an improvement of available methods and/or development of new ones with sufficient sensitivity and specificity.

Open questions in the development of the disease, its diagnostics and corresponding treatment may be successfully solved using various animal models, from subcellular level to that of the whole organism. The isolated heart perfused according to Langendorff is possible predominant model used to study myocardial ischemia and infarction [3],[4]. In experimental cardiology, above and many other aspects are usually examined by means of electrophysiological, biochemical and histological techniques. The first methods are mainly represented by analysis of heart electrical activity recorded as electrocardiogram (ECG, in animal *in vivo*), electrogram (EG, in isolated heart) or cardiac action potential (AP, any model including tissue and cells). Although the animals have been used in electrophysiological studies for a long time, the standardized criteria for assessment of cardiac disorders in animal models are missing, which often complicates interpretation of achieved results and their comparison with other reports. Particularly, lack of criteria for ischemia manifestation in rabbit heart (one of the most frequently used model [5]) may lead to discrepancy in obtained study results due to differences in the definition of ischemia beginning in preparation and/or in ECG or EG patterns used for ischemia assessment. This is of special importance, when there are several coexisting factors (such as LV enlargement, myocardial ischemia, drug effects, etc.) which may affect cardiac activity in different or similar way. The identification and elimination of such co-effects is rather difficult and requires performing more detailed analysis of recorded data or additional investigating of the phenomena on control group/s.

Besides above aspects, there are many others not associated with the heart or used diagnostics rules rather than with technical or methodological concept of the method, such as: placement, size and material of recording electrodes, the content and temperature of the solutions (*in vitro* studies), type of anaesthesia, administration of some drugs (heparin, electric-mechanical uncoupler, etc.), duration of stabilization period and the whole experiment, utilizing of some methods with potential undesirable effects (e.g. phototoxic effects of voltage-sensitive dye used for AP recording by optical way, etc.). All of them may affect the quality of obtained data and the reliability of study results. Thus, successful study of the heart electrical activity under normal as well as pathological condition is only possible in case of comprehensive approach, when heart-related factors and other methodological aspects are taken into account.

1 BRIEF SUMMARY OF ELECTROPHYSIOLOGICAL STUDIES OF MYOCARDIAL ISCHEMIA

1.1 ELECTROCARDIOGRAPHY

Heart is a pump that drives a blood through the vasculature. This mechanical function of the heart is the result of coordinated contractions of atria and ventricles which occur in response to the conduction electrical signal, so called action potential (AP). Various pathological conditions lead to dysregulation of the excitation-contraction coupling [6]. For example, ischemic heart is characterized by slow conduction and non-uniform excitability that make it more predisposed to ventricular fibrillation [7].

AP origins in the pacemaker cells of sinoatrial (SA) node and then is passing to the other sites of the heart through conduction system. APs from different heart locations have a specific morphology, which also varies with species and heart rate and can be affected with drugs or hormones. In contrast to the cell of SA node (and other peacemaker cells) which have the smooth APs, non-peacemaker ones (for instance, AP of ventricular myocytes) are characterized by AP with longer plateau phase (see below) that prevents re-excitation and generating the heart beat without preceding relaxation [6]. The upstroke of AP corresponds with the onset of QRS complex and end of AP with the end of T wave [8]. ECG curve describes the depolarization and repolarization of the heart, where the P wave and QRS complex represent the depolarization of atria and ventricles, respectively, and T wave represents the repolarization of the ventricles.

Non-invasive measurement of electrical activity of the heart – electrocardiography – is the basic diagnostic method in cardiology. The standard clinical surface ECG includes recordings from 12 leads: three bipolar (lead I, II, III), six unipolar precordial leads (V1 through V6) and three modified unipolar limb leads (aVR, aVL and aVF) [9]. Other lead system – Frank system – consists of only three orthogonal leads (X, Y and Z) used for construction of so called vectorcardiogram (VCG). Although the standard 12-lead system is widespread used in clinic, the latter can better reflect the anatomic changes in the heart (e.g. providing better sensitivity and specificity than conventional ECG in the diagnosis of left ventricular enlargement), bring unique or additional 3D information about cardiac electrical activity [10],[11].

1.2 ECG BASED DIAGNOSTICS OF MYOCARDIAL ISCHEMIA

Various cardiac diseases may be indicated on ECG as characteristic changes of its shape (including amplitude and/or time interval changes). ECG alterations during myocardial ischemia – the most common type of cardiovascular disease – originate from the changes in metabolic as well as electrophysiological systems. The lack of O_2 leads to the switching the oxidative phosphorylation to glycolysis for ATP production. Some ATP energy may be used to maintain the mitochondrion membrane potential, which may lead to fall in ATP and increasing ADP. Under these conditions, sarcolemmal ATP-sensitive K^+ channels have a greater probability to being open and produce an outward K^+ current (plateau phase). This results in shortening APD, depolarization (decrease from -85 mV to -60 mV) of the resting membrane potential and, consequently, in reduction in excitability and conduction block. [12]

Reperfusion restores the delivery of oxygen and substrates required for aerobic ATP generation and washes accumulated H^+ out, which results in the normalization of extracellular pH; external K^+ is also reduced by washout and resting potential quickly restores to normal values; the systolic and diastolic $[Ca^{2+}]_i$ level increases to the control values within approx. 15 min of reperfusion, which enables the normalization of heart mechanical function [7],[13],[14].

Corresponding ECG changes may be indicated by leads facing the ischemic region. Initial shortening of APD in ischemic zone without concurrent changes in conduction velocity (usually in subepicardial region) leads to *tall*, *symmetrical* and *peaked T wave*. Decreased APD also results in *shortening of QT* interval. ST segment corresponds with the period when the ventricles are depolarized, i.e. the ventricular APs are all in the plateau phase. If all regions of ventricles have the same transmembrane potential, such as in healthy

heart, this period is isoelectric in ECG. However, above changes over the myocardium (mainly shortening and decreased amplitude of AP and depolarization – i.e. less negative resting membrane potential) are not homogenous (especially at the border zone) and a voltage gradient between normal and ischemic zones appears, which results in flow of the current (so called injury current) between these regions. On the surface ECG, these currents are represented by *deviation of ST segment* above (ST segment elevation) or below (ST segment depression) the baseline. ST elevation or depression appears in ECG, if the injury currents are directed toward or away from the recording electrode. After about 5 minutes of ischemia, the ST segment becomes further elevated because of the shorter AP in ischemic region of the heart and later, the ST becomes markedly elevated due to delayed activation in ischemic region. This can be accompanied by pronounced inverted T wave. When cells in the middle of infarct zone become unexcitable, the *'monophasic patterns'* are presented in ECG. The changes in depolarization leads to slowed conduction of electrical impulses through the ventricles, which is manifested in ECG as *widening of QRS* or/and *reduction of R peak steepness*.

In a clinical setting, myocardial ischemia is identified from the ECG according to the AHA/ACCF/HRS recommendations primarily based on ST segment changes that occur during the early acute phase of acute coronary syndromes [2]. Furthermore, hypertrophy, effects of some drugs, electrolyte abnormalities and other factors may also cause ST segment deviation which may result in false positive diagnosis of ischemia and complicate differentiation between these abnormalities and acute ischemia. Other source of wrong ECG interpretation is the absence of ST changes in patients with ischemic chest pain, which may be explained by different mechanisms, such as perpendicular orientation of ST vector to the recording plane, cancellation of electrical forces caused by ischemia at opposites sites, absence of coronary occlusion and corresponding ST changes at the time of ECG recording [15]. The changes in electrical activation within ischemic or infarcted region are also reflected in the changes of QRS complex. Particularly, the magnitude and extent of QRS alterations depend on the size and location of the ischemic region (and, consequently, on the vessel occluded) and the mutual placement of this region and recording lead [2].

The most frequently used tool for diagnosis of cardiac artery disease is *stress test* including physical exercise which leads to increased oxygen demand in myocardium and, therefore, may unmask the disease during test. Simultaneously with the exercise, ECG is recorded and ST segment is evaluated. According to the previously reported results of meta-analysis, the sensitivity (Se) and specificity (Sp) of stress-induced ST deviations in ischemia detection reach 50-68 % and 77-90 %, respectively [16].

The accuracy (Acc) of ischemia detection using ST-deviation criteria can be verified by coronary angiography, at autopsy or by modern non-invasive technologies, such as nuclear scintigraphy, echocardiography or magnetic resonance imaging. These methods are used as a *gold standard* and the results of ECG detection are compared with finding obtained using such tests. However, the diagnostic Acc of the detection of myocardial ischemia by nuclear and echocardiographic imaging test is only 75-90 %. Thus, the diagnosis of ischemia in ECG may possible be correct, even if the presence of ischemic injury was not detected by the imaging techniques, which complicates interpretation of the results. [17]

Various aspects of ischemia assessment by ECG have been recently studied with the purpose of improving the detection Acc: the effect of definition of the point used for ST level measurement on the stability of ST-segment elevated myocardial infarction diagnosis [18]; number and placement of ECG leads [19],[20]; evaluation of other ECG criteria. The latter is of special interest because of quite low diagnostic ability of ST criteria. It led to the development of new methods based on analysis of other parts of ECG (mainly QRS complex) or discriminators derived from ST-T interval. In the first group of studies, potential use of QRS prolongation as a marker of myocardial ischemia was investigated [21],[22]. Many various studies were inspired by the concept of so called high-frequency (HF) QRS complex. Decrease of the amplitude of HF-QRS components can be evaluated by corresponding HF parameters (the root-mean-square value – RMS [23], reduced amplitude zone [24] and HF morphology index [25]). In more recent study with stress-induced ischemia confirmed by myocardial perfusion imaging, it was found, that the diagnostic

performance of HF-QRS analysis (Se = 69 %, Sp = 86 %) was enhanced as compared to conventional ST segment method (Se = 39 %, Sp = 82 %) [26]. Other group of QRS-related methods is based on the analysis of QRS slopes (upward and downward) [27]-[29]. However, according to the highly variable Acc of this method, QRS slope information to detect ischemia is disputable; it can, nevertheless, be used as an adjunct to the conventional ST segment analysis.

Standard guidelines for assessment of myocardial condition are defined for only standard ECG and not available for VCG [2],[30]. Nevertheless, many new VCG descriptors have been proposed in recent studies for ischemia and myocardial infarction detection. In most cases, the new parameters allowed improving detection performance, such as in: ST (at J point) and ventricular gradient (VG) difference vectors (relative to the reference) [31], QRS-loop parameters (volume, maximum vector magnitude, planar area, maximum distance between centroid and loop, angle between XY and optimum plane, perimeter, and area-perimeter ratio) [32], combination of QRS-loop parameters with standard ST-change vector magnitude, QRS-vector difference and spatial ventricular gradient [33], etc.

In view of the above, still further enhancement of myocardial ischemia detection using ECG is possible by improvement of conventional approach or by development of new methods employing new descriptors and more advanced techniques for data analysis.

1.3 STUDY OF MYOCARDIAL ISCHEMIA USING RABBIT MODEL

Many various aspects of the development of heart disease, its diagnostics and treatment may be successfully investigated using animals. Among various species, rabbit is one of the most popular models used in studies of cardiovascular system due to low cost, short time for disease progression, short gestation time, the similarity of physical dimensions of the hart to that of human, etc. [5]. Moreover, the cardiac physiology of rabbit is similar to that of human, namely: a) similar basic cardiac electrophysiological parameters [34]; b) the same repolarizing ionic currents in the ventricles influencing AP duration (delayed rectifier K^+ currents I_{Kr} and I_{Ks}) [35]; c) similar transport of Ca^{2+} [6]. The two last observations are especially relevant for the study of arrhythmias [36].

Isolated rabbit heart is used in a wide range of studies including biochemical, pathophysiologic, metabolic and pharmacological studies. One of the main areas is the study of ischemia-reperfusion injury and mechanisms of ischemic or pharmacological preconditioning [37]. Three *types of ischemia* can be induced in isolated heart: 1) by complete stopping of coronary flow (global ischemia), 2) by partially restricting coronary flow (low-flow ischemia), 3) by occluding a coronary artery (mostly the left anterior descending artery, LAD) (regional ischemia). The first and the third approaches are most widely used and each of them has both advantages and limits. In human, in most cases ischemia affects a specific region of the myocardium because of stenosis in a coronary artery. This situation can be simulated by animal model of regional ischemia, where the coronary flow is reduced by various ways, such as use of hydraulic occluder positioned around the coronary artery, intracoronary placement of a hollow plug attached to a catheter or other mechanical devices [3]. Significant benefits of above method is that they can be performed in open- and even closed-chest preparations *in situ* and may mimic ischemia of different degree: severe in case of complete occlusion and mild or moderate in case of reduction of coronary flow to some percentage of value at rest. The simplest (and the most frequently used) way to induce severe regional ischemia is complete cessation of a coronary flow by ligating of a coronary artery. However, the anatomy of the heart coronary system should be taken into account in case of regional ischemia model. Significant intraspecies differences in anatomy of rabbit coronary system have been found previously [37],[38]: since the left coronary artery is always dominant, both bifurcation and trifurcation of the atria coronaria sinistra may be observed in the population. Thus, the reproducibility of experiments with regional ischemia in rabbit is quite low and strongly depends on the experience and knowledge of the investigator about the coronary arteries distribution.

Difficulties associated with the regional ischemia inducing can be avoided by using the global ischemia model. Global ischemia can be simply induced by stopping of the heart perfusion. In this case, the presence or absence of collateralisation is irrelevant; thus, highly reproducible results may be achieved. Generally, this model of ischemia mimics severe hypotension in patients or the situation, where the whole heart becomes ischemic during open-heart surgery with aortic-cross clamping [39]. Despite the fact that above phenomena are relatively rare, use of the heart model of global ischemia is of interest in heart surgery field and in ventricular fibrillation study. Since there are some important differences between the global ischemia model and human heart undergoing arrest for the surgery (particularly, method used for heart arresting – cold cardioplegia in human *vs* full stopping of perfusion in animal model, cold *vs* warm or cold ischemia in human and isolated heart, respectively, etc.), the use of isolated heart is only way to obtain valuable information about ischemia-reperfusion injury at the molecular and genomic level [40]. Rabbit isolated heart model is intensively used to study the evolution of arrhythmias and to test antiarrhythmic or proarrhythmic effects of available and new drug compounds [5],[41]. In cardiac arrhythmia studies, global ischemia is of interest especially due to its effects on the activation patterns of ventricular fibrillation [42]-[46]. In all above investigation fields, the study of potential *preconditioning effect* of global ischemia is still topical. Ischemic preconditioning is defined as a delay and decrease of irreversible damage of cardiac tissue in response to ischemia after previous one or several short-term periods of reversible myocardial ischemia [47]. It can be easily examined in isolated heart model, where 3-10 minutes long global ischemia (or 3-5 ischemia-reperfusion repetitions) is frequently used as the preconditioning stimulus followed by the period of intermittent reperfusion and long-term (30 minutes or longer) test ischemia (global or regional) [48]-[52].

For *quantitative assessment of ischemia*, various electrophysiological variables and biochemical markers with prominent changes during ischemia can be used in experimental cardiology. Besides such advantages as the absence of neurohumoral regulation and possibility of fully controlled experimental conditions, isolated heart preparation provides good direct access to the epicardium, which makes it suitable for simultaneous monitoring of heart mechanical function and electrical activity under 'physiological' as well as pathological conditions. The most common electrophysiological records providing in experiments on isolated hearts are EG and monophasic AP (MAP). Cardiac electrical activity is usually measured using epicardial, endocardial or transmural electrodes attached to the tissue or inserted into the ventricular wall ([5],[48],[49],[53]) or by electrodes placed in the heart bath filled with the conductive physiological solution ([54]). More advanced – touch-less – techniques are based on recording of MAP using potentiometric voltage-sensitive dyes (VSDs) and corresponding optical devices [5],[44],[46],[53]-[58]. Different approaches can be applied simultaneously with aim to comprehensively investigate the relationships between various physiological parameters, that is important in experiments focused on the study of effects of electrical stimuli or the drugs on heart electrical activity, the mechanisms of onset and evolution of serious cardiac arrhythmias (including the study of ventricle conduction velocity and pathways), etc. [3],[43],[59]-[62].

As in human, ECG/EG remains the most frequent tool used in experimental studies. However, to best of our knowledge, ECG criteria for detection of ischemia in animals are not available. Probably the only document summarizing some guidelines for ECG assessment of arrhythmias (such as ventricular premature beat VPB, atrioventricular (AV) block, etc.) associated with ischemia, infarction and reperfusion in animal studies is the Lambeth Conventions, which were recently updated [63]. According to the Conventions, qualitative assessment of severity of ischemia includes following indexes: visual inspection for cyanosis and dyskinetic regional wall motion; ST segment elevation and ST-T alternans; regional increasing of extracellular potassium and venous lactate concentration.

2 AIMS OF THE DOCTORAL THESIS

An electrophysiological study in the rabbit isolated heart is one of the basic tools in experimental cardiology, which particularly allows investigation of myocardial ischemia and other cardiac disorders. However, there are still many arguable aspects (methodological, technical, etc.) in this area, which are worthy of attention. Therefore, dissertation is mainly focused on the investigation of some factors which may affect various phases of animal study and on the summarizing of corresponding suggestions with aim to improve reliability of experimental data, analysis results and their interpretation. Particular main tasks addressed in this work can be formulated as follows:

1. to describe patterns of EG recorded in rabbit isolated heart under normal conditions (i.e. fully perfused heart without drug administration – control group);
2. to quantify the response of the heart to short-term repeated perfusion stopping (so called global ischemia) by means of various parameters derived from EGs and VCG and to determine the most appropriate placement of electrodes for monitoring ischemia-induced alterations in recorded electrograms;
3. to assess possible effects of increased LV mass on cardiac electrical activity under non-ischemic and ischemic conditions (including describing manifestations of increased LV in recorded data, developing the method for increased LV mass detection and quantifying ischemia-induced changes by means of EG and VCG parameters);
4. to validate the suitability of the voltage-sensitive dye di-4-ANEPPS administration in experiments with rabbit isolated heart (including assessment of possible electrophysiological effects of the dye on the heart under non-ischemic and ischemic conditions by analysis of recorded data);
5. to develop the tools for automatic detection of myocardial ischemia and to assess possible effects of above experimental conditions (changed LV mass or dye administration) on detection accuracy (including evaluating discrimination ability of EG and VCG parameters and selecting the most reliable of them for further classification, implementing single- and multi-feature approaches based on simple human-like decision rules as well as more advanced supervised techniques and testing them on real data from control group, hearts with increased LV mass and hearts stained with the dye, evaluating the effect of definition of ischemia beginning in preparation and the effect of parameters calculation method – using or without outcomes of manual EG delineation – on classification performance).

3 EXPERIMENTS WITH RABBIT ISOLATED HEARTS

Experimental setup

Electrograms of rabbit isolated heart recorded in the framework of the thesis are the part of database of animal electrocardiographic signals available at the Department of Biomedical Engineering, BUT [64].

The experiments on adult New Zealand rabbits (both sexes, weight 1.9 – 3.45 kg) were carried out in collaboration with research team from Physiology Department of Faculty of Medicine (Masaryk University, Brno) in accordance with the guidelines for animal treatment approved by local authorities and conformed to the EU law. The heart was excised from anesthetized animal, placed in the bath, filled with Krebs-Henseleit (K-H) solution (1.25 mM Ca^{2+}, 37° C), and retrogradely perfused with the solution according to Langendorff in the mode of constant perfusion pressure 85 mmHg and temperature 37° C.

Data acquisition

Three main types of experimental protocols were included in the study as follows:

A. For general study of electrical activity of rabbit isolated heart under normal and ischemic conditions, five and eleven experiments were carried out according to the protocols from Fig. 1a and Fig. 1c (bottom), respectively. The first protocol allows recording of EG from different areas of LV using only two orthogonal bipolar leads due to the rotation of the heart about its longitudinal axis during recording, when the electrodes are fixed in the same position. However, the cardiac electrical activity cannot be monitored continuously in this case. In the second protocol, EGs are recorded from the heart which is fixedly placed relative to the electrodes. As a result, continuous EGs can be recorded during the whole experiment, which is required for detailed evaluation of ischemia-induced changes.

B. For evaluation of the effects of increased LV mass on electrical activity of rabbit isolated heart under normal and non-ischemic conditions, sixteen experiments were carried out according to the protocol from Fig. 1b. Already during the preparation, visible enlargement of LV was observed in some hearts. According to the results of retrospective analysis, LV weight to heart weight (LVW/HW) ratio – representing the LV fraction in the whole heart mass – was the only index suitable for dividing the animals into two groups. The discrimination threshold value of LVW/HW ratio (0.57) was found by analysis of ROC curve. Thus, animals with LVW/HW ratio below or equal threshold were assigned to group L and animals with the ratio above threshold to group H (LVW/HW 0.53 ± 0.03 and 0.61 ± 0.03, respectively; $p < 0.001$, Mann-Whitney U-test; $n = 8$ in each group).

C. For assessment of the effects of VSD di-4-ANEPPS on electrical activity of the rabbit isolated heart under normal and ischemic conditions, twenty experiments were carried out. In the first type of experiments (Fig. 1, c, top, n = 9), di-4-ANEPPS (di-4-amino-naphthyl-ethenylparidiunium, Molecular Probes, Inc., USA) was added to the perfusing solution to the final concentration of 2 μmol/l for recording AP from the middle of LV by optical method simultaneously with EG. Such a "slow" staining allows use low-concentrate dye solution and consequently reduces possible undesired effects of the dye on the heart. The second protocol (Fig. 1c, bottom, n = 11; only hearts with low LVW/HW ratio) did not include VSD administration; thus, only EGs were recorded. In both cases, three consecutive periods of ischemia and reperfusion (each 10 min long) were carried out. Experiments focused on the verification of the effects of the dye on sodium channels were additionally performed. Briefly, differentiated NG108-15 cells with sodium channels expression similar to those in cardiac myocytes were included in the study. Two experimental protocols – with acute application of the dye and 30 min long incubation of the cell in presence of this VSD – were used to test the response of sodium channels to the dye. Possible effect of DMSO (commonly used for dye dilution) was also evaluated in dye-free experiments. I_{Na} was measured in the whole-cell patch clamp configuration. Arrhythmias (junctional rhythm NOD and atrioventricular block AVB of the 2nd and 3rd degree) were evaluated manually through the whole data set; ventricular premature beats (VPBs) and supraventricular extrasystols (SVES) were counted within particular experimental periods.

EGs were recorded by three pairs of Ag-AgCl disc electrodes placed orthogonally on the inner surface of the bath filled with conductive K-H solution. Recorded EGs were digitized by 16-bit AD converters with sampling rate of 2 kHz and stored on PC. At the beginning of the experiments, the hearts were oriented relative to the electrodes in the same way, which is shown in left and middle parts of Fig. 2. In this case, horizontal leads (lead I and lead II) "look" at the middle part of LV and boundary region of LV. In some protocols, the heart was rotated around its longitudinal axis from initial position 0° to 90° (Fig.2, right) in 10° steps in the direction depicted with light grey arrow in Fig. 2. The orientation of the heart at the end of rotation session is shown in right part of Fig. 2. Rotation in this way allows to record data from whole LV region. Totally, five rotation sessions were performed during ischemia (i1-i5) and reperfusion (r1-r5) in approx. 2^{nd}, 3^{rd}, 5^{th}, 7^{th}, and 9^{th} minute of ischemia. Each rotation session lasted approx. 1-1.5 min. Thus, EG recorded in each heart position was of approx. 5-8 s long (depending on actual heart rate).

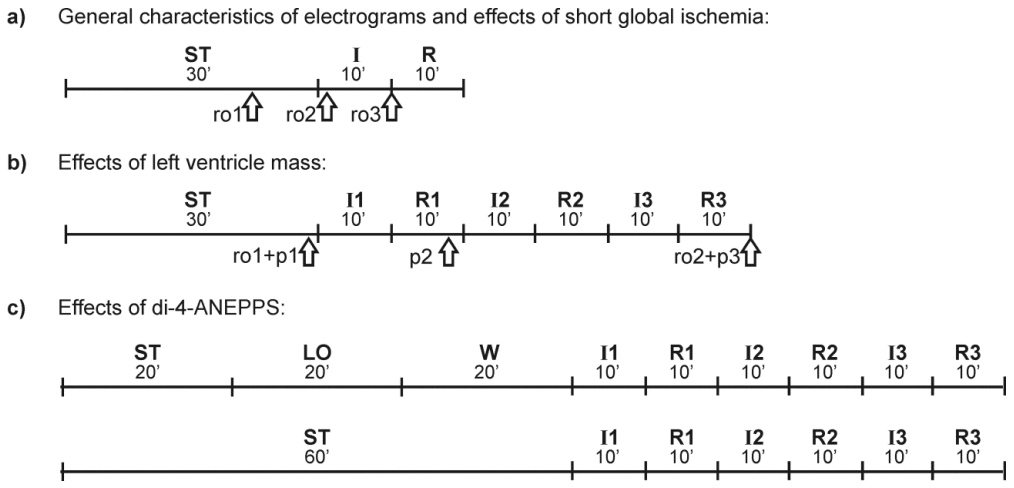

Figure 1. Experimental protocols. Global ischemia in hearts rotated around its longitudinal axis during the whole experiment (arrows depict the beginning of the first rotation session in each experimental period) (a), repeated global ischemia in hearts rotated around its longitudinal axis in stabilization period and at the end of experiment including collection of perfusate samples (b), repeated global ischemia in hearts loaded with voltage-sensitive dye di-4-ANEPPS (top) or without dye administration (bottom) (c). ST – stabilization, LO – loading with the dye, W – washout, I – ischemia, R – reperfusion, ro – rotation of the heart, p – perfusate collection.

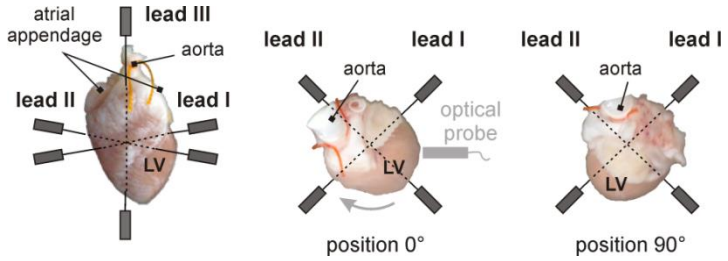

Figure 2. Orthogonal system of electrodes. Front (left part) and top (middle and) views. Lead III is not shown on the top views. Direction of heart rotation is depicted with light grey arrow in the middle part of the figure. LV – left ventricle.

Data processing

The processing of EGs recorded in the hearts in initial position (excluding the segments recorded during heart rotation) is schematically shown in Fig. 3a. EGs recorded with different leads were processed separately except QRS complexes detection and P-QRS-T segments delineation. As a first step, low-frequency baselined wander was eliminated by zero-phase Lynn's filter (cut-off frequency of 0.5 Hz) combined with the padding of EG with flipped, reflected copy (mirror padding) of its beginning and ending parts to reduce the distortion of ST segment which may lead to incorrect interpretation of the records. This method allows avoiding phase distortion, time delay, and start-up and ending transients in the filtered signal. QRS complexes (so called fiducial points) were then detected in filtered signals with the detector based on the wavelet transform adapted to EGs recorded in rabbits [65]; detection results were additionally checked manually. P-QRS-T segments were then selected from EGs as 150 samples before and 700 samples after the points with resulting length of the segments 851 samples (or approx. 426 ms). Manual delineation of the data from 2 h long experiment is very time-consuming; automatic delineation is challenge task itself and is beyond the scope of the dissertation. Therefore, data clustering by UPGMA method ([66]-[69], with number of clusters empirically set at 40 for each experimental period) was performed to divide them into the groups with similar morphological characteristics, such as QRS beginning and QT interval length. If single clustering iteration was not sufficient, the second one was applied in the same manner on data in clusters from previous step to obtained more accurate results. Resulting clusters were delineated manually (including beginning of Q wave, J point and end of T wave, and beginning of P wave in experiments with di-4-ANEPPS) using modified version of software [70]. Presented procedure allows reducing of time required for

data delineation in several times (300-400 clusters instead of 8000-10000 segments for each experiment). The PQ deviation in some initial segments remained after baseline wander elimination could dramatically affect the values of important morphological characteristics of EG. Therefore, P-QRS-T baseline was then shifted exactly to the zero level with respect to detected beginning of QRS complex.

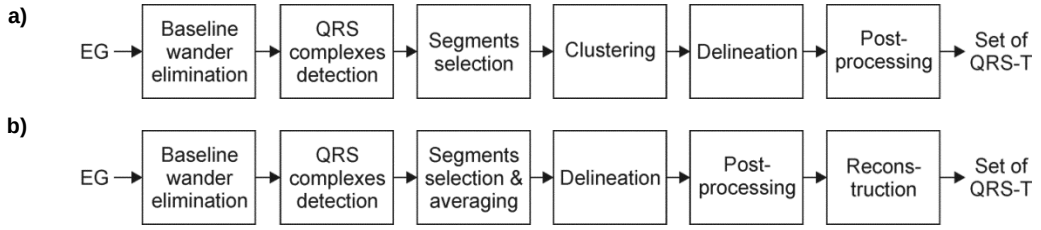

Figure 3. Electrogram processing and analysis: fixed orientation (a) and rotation (b) of the heart.

The processing of EG recorded in the rotated heart is schematically shown in Fig. 3b. Baseline wander elimination and QRS complexes detection were performed in the same way such as in previous case. The parts corresponding with the particular heart position were then selected from EGs. QRS-T segments of 280 ms length were selected from EG parts as 59 samples before and 500 samples after detected fiducial points. Thus, each heart position was represented with group of QRS-T or the averaged QRS-T calculated generally from 10-15 segments (highly correlated with each other, i.e. with Spearman's ρ higher than 0.95) from the middle of corresponding part of the record. Delineation and post-processing of EG segments were then performed such as in previous case, except for clustering: initial groups of highly correlated segments or averaged segments representing particular heart position were delineated individually. The rotation sequence described above is sufficient for reconstruction of EG in the range from -90° to 90° corresponding with the whole LV region using data recorded with horizontal leads during rotation of the heart within the range 0° - 90°. The reconstruction was performed according to Fig. 4a. Each lead position from scheme was finally represented with the averaged QRS-T segment. Heart orientation changes did not affect EG from lead III (ρ for segments from this lead in different heart positions was more than 0.99). Therefore, all available segments from this lead were taken into account to define averaged one representing the positions in the range from -90° to -10°. Indexes of fiducial points and delineation results were reconstructed besides the EG segments. Data from five rotation sessions performed during ischemia and reperfusion (experimental protocol from Fig. 1a) are available for analysis. These sessions are denoted as i1-i5 and r1-r5 for ischemia and reperfusion, respectively (see next chapter).

EG and VCG parameters calculation

Various parameters (32 from each lead and 33 from VCG) were calculated to evaluate ischemic changes in different experimental groups. Three main groups of parameters – namely, those representing interval and voltage characteristics of EGs (Fig. 4b), parameters based on areas under different parts of EGs (AUC-based, Fig. 4c) and VCG-based parameters (Fig. 5) – were calculated in the study. The main reasons of including particular parameters in the study were: a) simple computation without the need of full EG delineation (such as detection of onset and offset of particular QRS peaks, beginning of T wave, etc.); b) use in similar experiments with the same and/or different species or in clinical praxes for comparative analysis; c) easy interpretation of parameters values obtained under different conditions. Full list of parameters can be found in Appendix A.

Note, that ST20 was chosen empirically as an alternative to ST60 used in human ECG analysis, considering the differences in characteristics (mainly QT and ST-T duration) of human ECG and EG of rabbit isolated heart. AUC-based parameters (e.g. AUC_{QRS}) calculated from areas below and above the x-axes gives negative and positive results, respectively, which in some cases may lead to zero value of corresponding parameters (Fig. 4c, left). To avoid this, modified AUC calculated from absolute values of QRS-T were used (e.g. AUC_{QRS}'), too (see Fig. 4c, right). Additionally, the modification by dividing AUC of

particular patterns by AUC calculated from the whole QRS-T or QRS (relative AUC based parameters, e.g. $AUC_{QRS}R'$) was performed to evaluate the pattern's fraction in the whole analysed segment.

In Fig. 5a, conventional VCG [71] derived from experimental data is shown. The vertical axis (Y) stretching from top to down corresponds to lead III axis. For a rotating heart, axes extending from left to right (X) and from front to back (Z) were represented by EG recorded in positions -40° and 40° (Fig. 4a), respectively. In protocols with fixed heart position, EG from lead I and lead II (Fig. 2, left and middle) were used as Z and X leads, respectively (Fig. 5b, left). In this case, XYZ coordinate system is rotated clockwise by approx. 45° relative to conventional one. As a result, the parameters calculated from VCG reconstructed by two approaches are quite different. Nevertheless, it can be acceptable given the experimental context of the study. Moreover, it was found that ischemia induced changes in such data are as much prominent as in case of conventional approach.

As first, QRS and ST-T parts of EG loops were analysed individually using maximal QRS and ST-T spatial vector magnitude and angles in frontal, horizontal and sagittal planes (α, β and γ, respectively, Fig. 5a). 3D perimeters (P_{qrs} and P_{jt}) and areas (A_{qrs} and A_{jt}) of 2D QRS and ST-T loops (in three planes) were then calculated to evaluate the shape of the loops. Loop's areas calculation is rather difficult task due to the loops' values properties: a) the samples sequences forming the loops are not always strictly monotonic; b) the loops are self-intersecting; c) data are scattered (i.e. values are not evenly distributed through the loop).

The conventional methods for calculation the area of irregular closed polygon was insufficient. Use of usual (linear, cubic or spline) interpolation methods is also complicated because of non-monotonic, scattered character of data. Therefore, the natural neighbour based method (based on Voronoi diagram) was applied to perform interpolation of data on a regular grid and calculate loops' areas from the projections of interpolated surface on particular planes. VCG centroid based parameters were additionally proposed to evaluate the relationship between 'mean' and main electrical vectors. Uneven distribution of data within the loop resulted in inaccurate estimation of centroid coordinates as arithmetic means of loop samples, even if QRS and ST-T were selected according to the delineation results (Fig. 5b, top left). Therefore, centroid coordinates $\mathbf{C} = [C_x; C_y; C_z]$ were estimated as mean values of corresponding surfaces (interpolated on evenly sampled grids from previous step) and used for calculation the angle (φ^c_{qrs}, φ^c_{jt}) and distance (D^c_{qrs}, D^c_{jt}) between main (QRS or ST-T) vector and centroid vector. Besides the parameters used for evaluation of depolarization and repolarization processes individually, two additional parameters – the angle (φ) and the distance (D) between main QRS and ST-T vectors (see Fig. 5a, top right) – have been proposed to approximate the relationship between them.

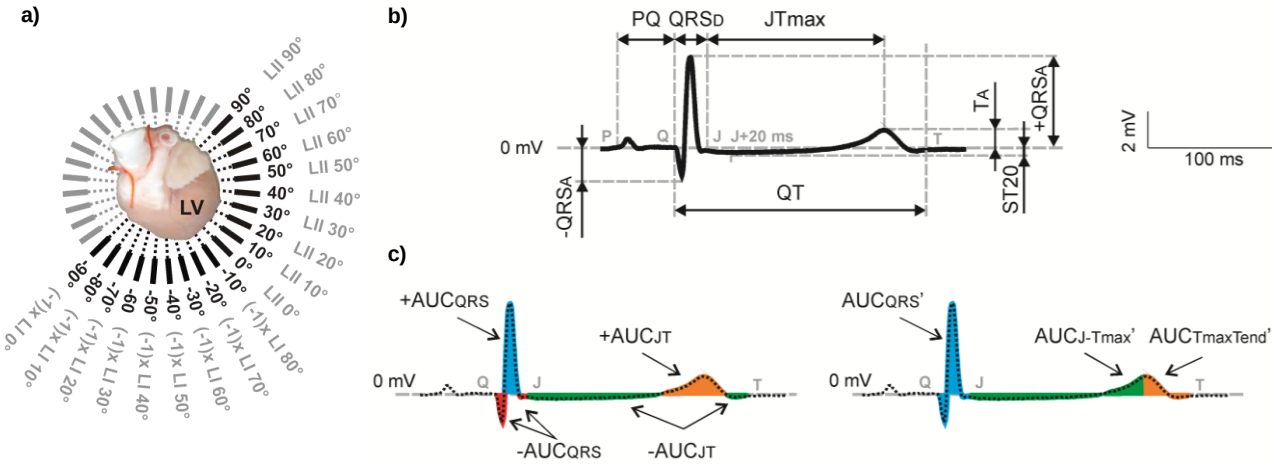

Figure 4. a) Reconstruction in the range from −90° to +90° (black font) using data recorded with two horizontal leads during heart rotation from 0° to 90° (grey font); b) voltage- and interval-based parameters; c) AUC-based parameters.

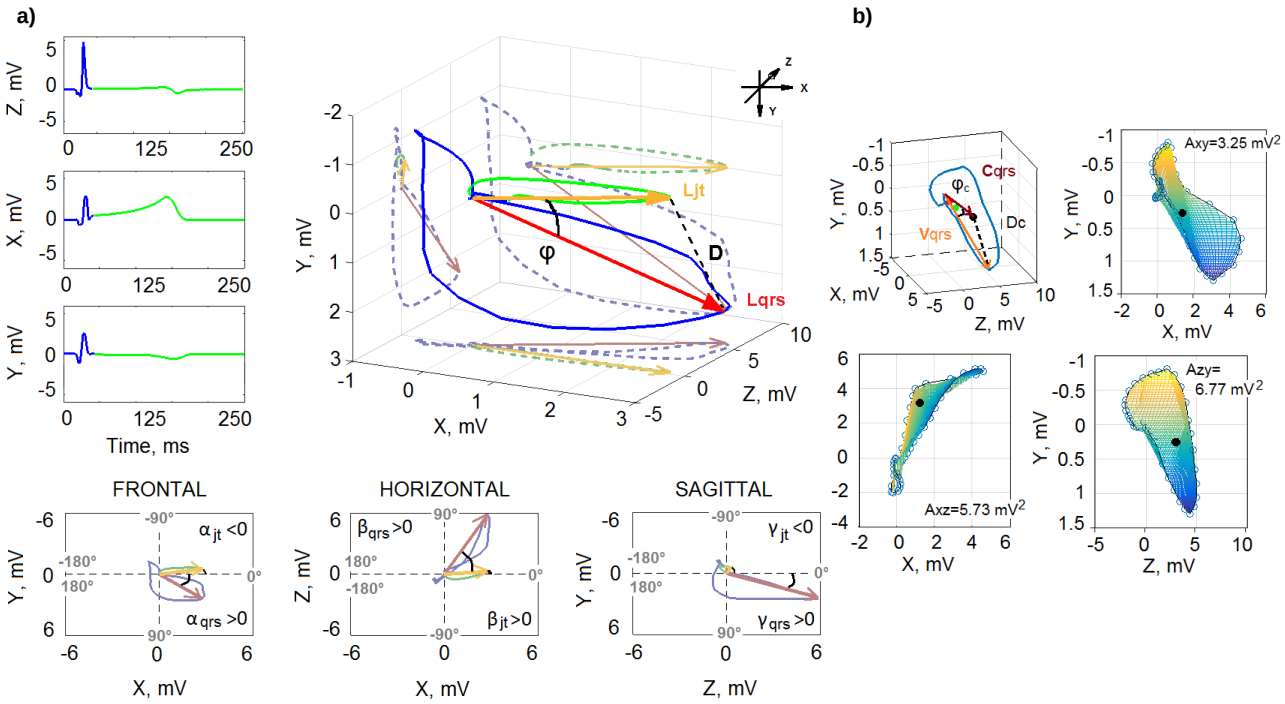

Figure 5. a) Conventional orthogonal leads before ischemia (left), corresponding VCG (right) and three planes (bottom); b) 3D QRS loop (top left) in shifted XYZ coordinate system. Black dots represent centroid derived from interpolated loop surface (top right and bottom).

All above EG parameters excepting interval characteristics can be calculated *without delineation results*. Regions for calculation of particular parameters ('artificial EG patterns') without use of delineation outcomes can be then chosen based on analysis of RR, QT and QRS_D calculated at the end of stabilization and ischemia (where the maximal deviation of parameters as compared to their control values is expected) from all available experiments. Finally, the segments were additionally selected as 59 and 500 samples before and after detected fiducial point, respectively. It results in 'artificial' QRS_D of approx. 60 ms (59 and 60 samples before and after fiducial point, respectively) and QT of approx. 280 ms. This has a minimal impact in case of AUC based parameters from stabilization period, where boundary parts of like-QRS or ST-T patterns usually lie on x-axes and, thus, do not affect resulting AUC value. On the contrary, poor match of boundaries with true onsets and offsets of patterns may lead to parameters distortion. Considering true RR and QT values, beginning of subsequent beat may appear at the end of artificial segments from stabilization period. On the other hand, the end of T wave may be missing in artificial data from ischemia. This may negatively affect parameters and their further analysis, too (see next chapter).

Statistical analysis

The normality and homoscedasticity (where data from different groups have the same standard deviation) of different groups data were checked with *Shapiro-Wilk test* (recommended for analysis of small data sets [72]) and *Levene's test* [73], respectively. It was confirmed, that both assumptions are not precisely hold. Therefore, non-parametric methods were chosen for statistical data analysis.

Wilcoxon signed rank (paired) test was applied in each experimental group (control or L, H, and stained hearts) separately in order to evaluate significant changes of all parameters at the end of each minute during ischemia and reperfusion in comparison with the values immediately before the ischemia onset.

To compare the overall changes in each parameter at the end of particular ischemic (and reperfusion) periods relative to its level in stabilization (i.e. to compare changes induced by different ischemic periods), *Friedman test for repeated measurement accompanied by Tukey-Kramer post-hoc test* (e.g. [74]) was applied to the *delta values* defined as $\Delta = p_E - p_S$, where p_E and p_S is averaged value of the parameter calculated from

20 last samples at the end of particular period (ischemic or reperfusion) and at the end of stabilization, respectively.

General trend of ischemia or reperfusion induced changes during the whole experiment was studied using the *slope* calculated from the line fitted through the normalized parameter's Δ. Significance of slope values (comparing to the zero) was then verified by *one-sample signed-rank test*.

Mann-Whitney U-test (unpaired, e.g. [74]) was used to test the differences between groups in following data sets: 1) EG parameters in different heart positions and VCG parameters, both calculated in stabilization (experiments B); 2) EG and VCG parameters, their Δ and the slopes, and the number of VPBs calculated from data recorded during ischemia and reperfusion (experiments A-C); 3) EG and VCG parameters and the number of VPBs calculated from data recorded during stabilization, staining and wash-out (experiments C); 4) parameters calculated using and without delineation outcomes (experiments A-C).

Analysis of receiver operating characteristics (ROC) curve was performed to assess: a) the overall ability of parameters to distinguish among different phases of ischemia (i.e. different rotation sessions within ischemic period) and the ability of different positions (i.e. recording leads) to provide EG suitable for ischemia detection (experiments A); b) the diagnostic accuracy of different parameters at various cut-off points for the detection of the increased LV mass (experiments B); c) the capacity of the parameters to detect ischemic changes (experiments A-C). In latter case, ROC curves were constructed for data from each minute of ischemia separately for more detailed analysis of the parameters discrimination ability in different ischemic degrees. Additionally, the same analysis was carried out on ROC curve calculated from the whole ischemic period to estimate overall (and, consequently, less optimistic) discrimination ability of particular parameters. Area under ROC curve (AUCROC), sensitivity (Se), specificity (Sp) and optimal cut-off value of each parameter were estimated to quantify the parameters performance [75]. AUCROC of 0.5-0.6 and 0.9-1 represents poor and excellent discrimination accuracy of the method, respectively.

One-way analysis of variance (ANOVA) followed by *Tukey test* for pairwise multiple comparisons were performed to verify group statistical differences in patch-clamp data.

In all tests, p-value less than 0.05 was considered statistically significant.

4 ELECTRICAL ACTIVITY OF THE HEART UNDER NORMAL AND ISCHEMIC CONDITIONS

Results achieved in proposed dissertation mainly contribute to the field of basic electrophysiological research with methodological suggestions associated with the acquisition, analysis and interpretation of data from experiments on rabbit isolated heart undergoing global ischemia.

4.1 GENERAL CHARACTERISTICS OF ELECTROGRAM

Interpretation of ECG is based on the describing of its main interval and amplitude characteristics which represent repolarization and depolarization processes in the heart. The characteristics of particular parts of ECG (such as polarity and shape of the waves and interweaves intervals) can vary based upon gender, activity, age, and used recording leads [76]. Many heart diseases are manifested in ECG, which makes the electrocardiography widespread powerful diagnostics tool.

As was mentioned above, electrocardiographic diagnostics of myocardial ischemia in human is mainly based on assessment of ST segment deviation (elevation or depression). Transient changes associated with QRS duration prolongation or increase of Q wave amplitude may be observed during acute ischemic episode. These observation is not so frequent, but may allow achieving even greater sensitivity and specificity of ischemia detection than in case of ST segment criteria only and seem to be correlated with extent of ischemia [17],[77]. Among other ECG manifestations of ischemia during exercise test are a shortening QTc (i.e. QT interval corrected for heart rate) interval and shifting the mean QRS axis in frontal plane to the right. However, prolonged or non-changed QTc and leftward axis shift (in patients with narrowing of the LAD

coronary artery) in presence of ischemia have also been reported [17]. Generally, the diagnostics of the earliest phase of ischemia is traditionally based on the detection of repolarization changes in ECG (i.e. in ST segment and T wave), whereas the pronounced changes in ventricular depolarization (namely QRS complex morphology) are mainly associated with the onset of necrotic process.

The main electrophysiological characteristics of rabbit are very similar to those of human. Particularly, like in human ECG, there is a well distinguished isoelectric ST segment between QRS complex and T wave in rabbit ECG. It makes rabbit suitable for myocardial ischemia studies. Unlike human electrocardiography, there are no standardized guidelines to assess morphology of ECG/EG in animals (including rabbit), especially under pathological conditions. It is the most probably due to the high interspecies as well as intraspecies differences in anatomy of coronary artery (and especially of collateral circulation) and conduction systems and, last but not least, in used methods for the recording of electrical activity (including such aspects as electrodes type and size and their placement). Furthermore, in case of recordings on isolated hearts, such factors as temperature, pressure, perfusion solution composition, and distance between the heart surface and recording electrodes may affect the heart function or/and morphology of recorded EG. Therefore, the describing of ECG/EG recorded in animal under normal or pathological conditions is rather difficult task, which can be solved by only comprehensive study covering all above aspects.

The main patterns of EGs and VCG recorded in the hearts during experiments under non-ischemic conditions are described in detail by various parameters derived from the records. According to the results of analysis of ST20 (marker of ischemia), longitudinal rotation of the heart in the bath filled with solution does not distort this parameter; thus, electrical activity from different areas of the heart can be accurately recorded by touch-less way using three-lead orthogonal electrode system. Morphology of EG recorded from different site of LV is very similar to that recorded in human with precordial lead V1-V6.

EG and VCG parameters can be successfully used to quantify the heart response to short-term repeated global ischemia which is represented by changes in the signal morphology, as can be seen in Fig. 6 (for EGs and VCG recorded in initial lead positions). Typical observed ischemia manifestations are summarized in Fig. 7. Generally, *ischemia manifestations* found in rabbit isolated heart are very similar to those in human. Particularly, during global ischemia, sinus bradycardia was observed in all experiments, which can be explained by impaired function of SA node. According to the results of the previous study on isolated rabbit SA node, pacemaker cells perfused by 'ischemic' solution (i.e. omission of glucose, pH 6.6 and additional upgrades for evaluation the role of increased serum [K]), reduction of inward Na-Ca exchange current I_{NCX} and T-type Ca current $I_{Ca,T}$ contribute to ischemia-induced bradycardia [78].

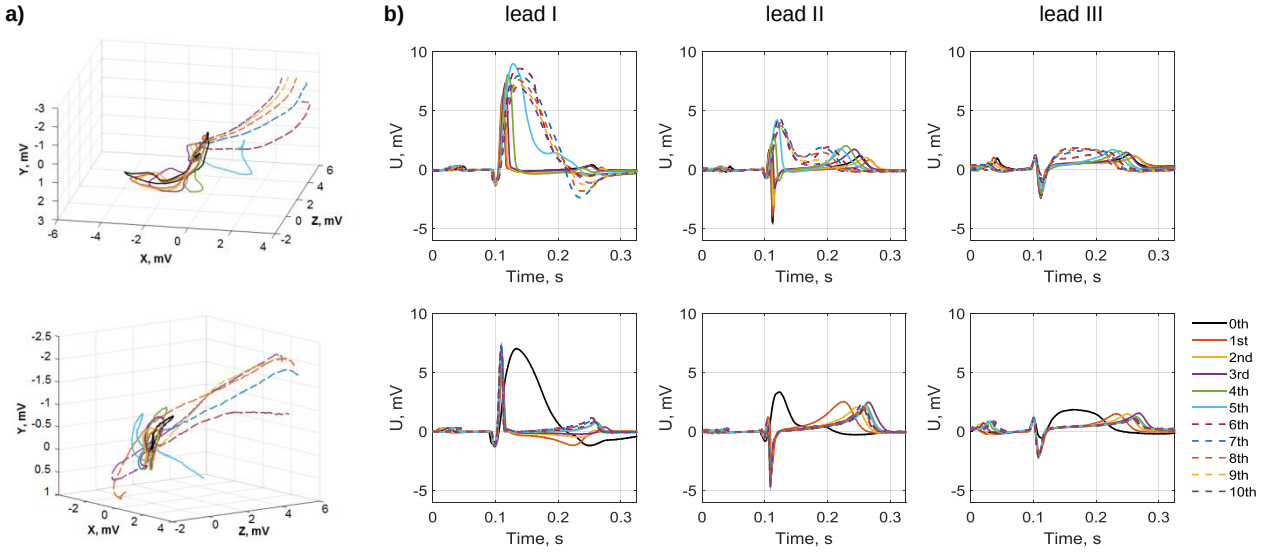

Figure 6. Typical time-course of VCG and EG recorded from rabbit isolated heart during ischemia (top) and reperfusion (bottom). Data from the beginning (0^{th} minute) and end of each minute (1^{st} to 10^{th}) of particular experimental periods.

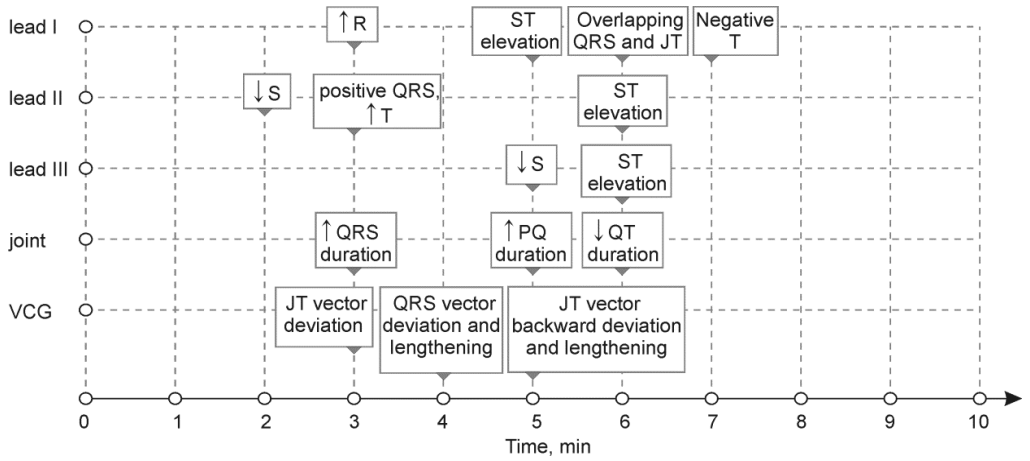

Figure 7. Time progress of the main visual changes in electrograms and VCG of rabbit isolated heart induced by 10 minutes long global ischemia.

Shortening of QT interval after short-term prolongation (immediately after the perfusion stopping), was also observed. This is a result of decreased APD, which was previously reported in the same animal model by Kolářová et al. [54]. In this study, MAPs were recorded by optical method using VSD di-4-ANEPPS. Pronounced shortening of APD recorded in rabbit isolated heart was also observed during first 10 minutes after LDA occlusion (regional ischemia) [60].

The *earliest* (and most prominent) manifestations of global ischemia were found in depolarization part (QRS complex), especially in EG recorded from anterolateral area (the middle of LV), where the change in polarity of QRS was observed besides the QRS widening. The changes in temporal part of QRS were evident in EG from boundary region, which is in accordance with observation in human (see above). QRS duration represents conduction of depolarisation through ventricles. Under ischemia, conduction velocity is decreased due to impaired metabolism in myocardium. In human, acute ischemic injury (myocardial infarction) is caused by significant reduction or even stopping of perfusion usually in one region of the heart. The changes in QRS are usually associated with the late phase of ischemia and ST deviation is used as early marker of injury. Nevertheless in global ischemia, QRS prolongation precedes changes in ST segment (elevation or depression), which are caused by some electric inhomogeneity in ventricles repolarization. In case of global ischemia, whole myocardium is affected in the same time, therefore the development of marked electric inhomogeneity (i.e. 'more' and 'less' ischemic regions) is not so fast and ST changes occur only in 5^{th}-6^{th} minute of ischemic period, whereas significant QRS prolongation ('global' marker) is observed 1-2 minutes earlier. Similar phenomenon associated with severe and global ischemia in human was previously reported by Takaki et al. [22]. Moreover, less steep R peak was observed in EG recorded during ischemia. The changes in these parts of EG are in accordance with the results of AP analysis in rabbits isolated hearts, where increased upstroke duration and decreased amplitude of AP (corresponding to the velocity of impulse conduction through ventricular tissue during depolarisation) were observed in both global and regional ischemia protocols [44],[54],[60]. In the *second half* of ischemia, when ST-T merges with the QRS, the transformation of QRS may be partially regarded as the passive response on the primary changes in repolarization part. In human, this finding is known as so called 'tombstoning pattern of ST segment' or 'monophasic pattern' which most often occurs because of proximal occlusion of LAD coronary artery (leads to the global ischemia of the whole anterior wall of the heart) and accompanies a large infarct [79]. Pronounced ST elevation and 'monophasic pattern' were observed in a broad region, when EG was recorded in different positions (see Appendix B). This is not unexpected because of global character of ischemia induced, where the whole myocardium (including both subendocardial and subepicardial regions) is affected at the same time (transmural ischemia). Thus, the most valuable manifestations in the second half of

ischemic period are characteristic for ST-T. Above observations can be illustrated on AUCROC of parameters from both types of experiments: with rotated (Fig. 8) and fixedly (Fig. 9) placed heart.

Generally, none of EG and VCG parameters was able to detect successfully first minutes of ischemia. It may be due to low sensitivity of evaluated parameters or EG itself to the earliest phase of ischemia. It might be also hypothesized, that the residual oxygen in the myocardium of the non-working heart (i.e. the heart does not pump against the load) is high enough to supply it for a limited time. However, this hypothesis cannot be easily verified. Nevertheless, it is in accordance with other studies on rabbit isolated hearts, where the first pronounced changes in the heart electrical activity were found at 3-5 minutes after the ischemia onset and 30-90-min perfusion stopping was used to induce myocardial infarct [48],[60],[80].

Horizontal *leads* facing LV wall (anterolateral region, initial position of lead II or 0° position in Fig. 2) are preferable for recording EG during ischemia, such as in human, where V3, aVF and V6 seem to be the most suitable for detection of ischemia presented in any territory [20]. It can be seen in overall (through all parameters) AUCROC values calculated in particular positions (Fig. 10). Furthermore, in Fig. 9, AUCROC obtained for QRS-based parameters in lead II are higher at the beginning of ischemia as compared to lead II. On the contrary, ST-T-based parameters provide higher AUCROC at the end phase in lead I as compared to lead II as well as QRS-based parameters from any lead. Lead III is not as sensitive to ischemia as two others and the main manifestation in this lead data is ST elevation occurred 6 min after the perfusion stopping.

Among the most common ischemia markers (ST20, QRS_A, QRS_D, and T_A), QRS_A from lead II is the most earliest. QRS_D, T_A and ST20 from lead I and QRS_A from led II have the best discrimination ability. Generally, AUC-based *parameters* (calculated from absolute values of QRS-T) from both horizontal leads, 3D loop parameters from VCG and interval characteristics (joint for all leads) can be considered as the best for discrimination between non-ischemic and ischemic state (at 5^{th}-6^{th} minute after the onset).

The most prominent ischemia manifestations can be indicated in EG in the middle of ischemic period (i.e. approx. 4^{th}-6^{th} minute). After this period, only slight changes are presented in the most parameters. Thus, *three main degrees of isch*emia may be distinguished in data: 1) 1^{st}-3^{rd} minute, when the prominent changes can be identified mainly in QRS part of EG recorded from the middle of LV; 2) 4^{th}-6^{th} minute, when ischemia is manifested in pronounced ST-T changes in data from the whole LV (especially in its boundary); 3) 7^{th}-10^{th} minute, when marked alterations are present in EGs recorded from any area of LV. Therefore, recording EG in initial positions of lead I (posterolateral) and lead II (anterolateral) seem to be suitable for detection of various phases of ischemia. The issues associated with automatic detection of ischemia (or its different phases) and selection of the most relevant EG and VCG parameters will be addressed later.

The backward changes in *reperfusion* are carried out more quickly than those in ischemia. EG shape in the 3^{rd} minute of reperfusion is almost the same as at the end of stabilization. It is especially valid for QRS morphology. The EG (and VCG) alterations are very similar in all three ischemic-reperfusion repetitions. According to the results of *delta and slopes analysis*, the total changes in EGs morphology during three successive ischemia or reperfusion are the same. However, time moment, where significant alterations were achieved in the records, varies from the first to the third ischemic period.

It can be, therefore, concluded that, 10 minutes long ischemia is manifested in the pronounced modification of the whole QRS-T. These effects nonetheless vanish during the first minutes of reperfusion. 10 minutes of reperfusion is long enough to return the heart function to the control level. It is consistent with the results of biochemical analysis (not published yet), where no significant differences in three markers (e.g. [81]) – creatine kinase, lactate dehydrogenase (both are robust markers of direct myocardial injury and cell necrosis) and 4-hydroxynonenal (marker of lipid peroxidation occurring mainly in reperfusion) – measured at the end of stabilization, the first and the third reperfusion (see Fig. 3b) were observed.

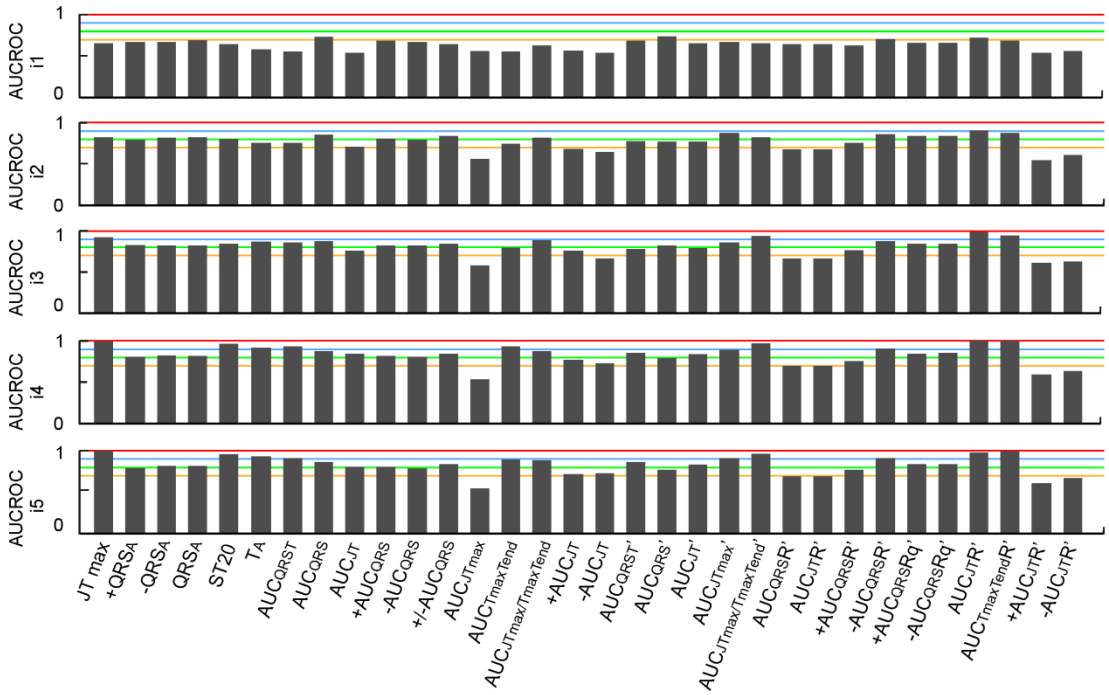

Figure 8. Averaged AUCROC of various EG parameters through all recording positions for different rotation sessions during ischemia (i1-i5). Orange, green, blue, and red lines indicate AUCROC of 0.7, 0.8, 0.9, and 1, respectively.

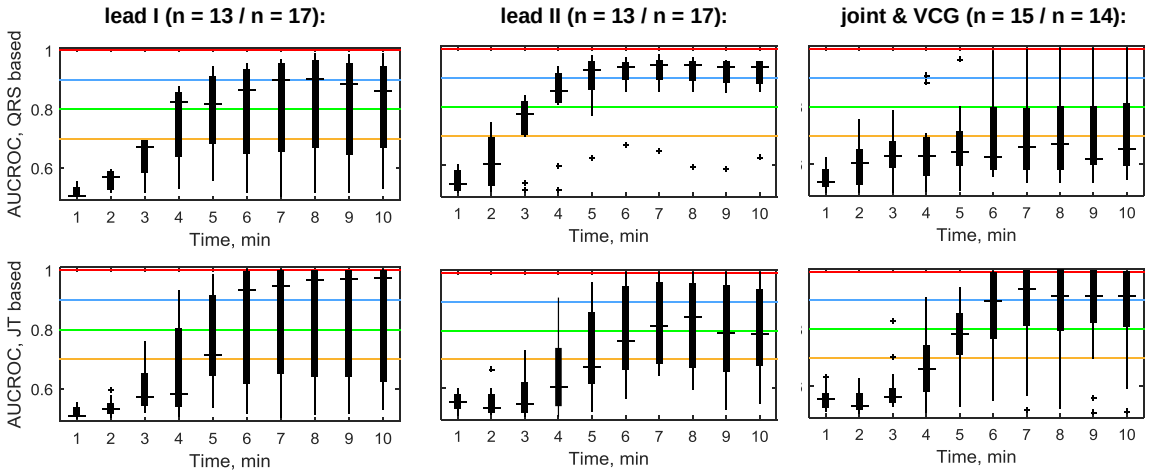

Figure 9. AUCROC for QRS and ST-T (JT) based parameters during the first ischemia.

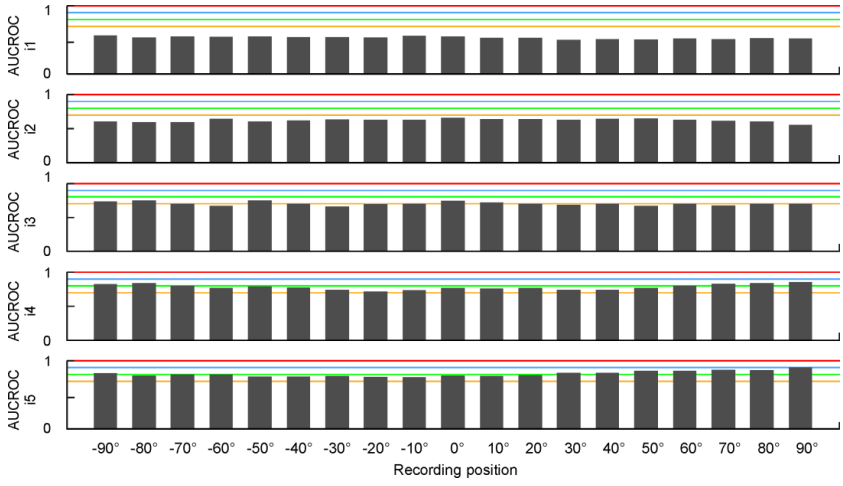

Figure 10. Averaged AUCROC though all EG parameters in different recording positions for different rotation sessions during ischemia (i1-i5). Orange, green, blue, and red lines indicate AUC of 0,7, 0,8, 0,9, and 1, respectively.

Thus, ischemia-reperfusion injury can be successfully studied repeatedly in present animal model. It, in turn, allows studying the preconditioning effect, which is, in this case, characterized by delayed onsets of ischemia-related EGs and VCG changes during the second and the third ischemic periods relative to the first one. Preconditioning also results in the decreased number of detected VPBs (will be discussed later). The significant effect of ischemic preconditioning on the magnitude of the EG and VCG morphology changes was not confirmed.

4.2 EFFECTS OF LEFT VENTRICLE MASS ON ELECTROGRAM

Despite the intensive clinical and preclinical research, both morbidity and mortality associated with myocardial ischemia remain high. Diagnosis of myocardial ischemia might be complicated by co-incidence with other diseases, e.g. myocarditis, hypertension or LV hypertrophy. The association between myocardial ischemia and LV hypertrophy has been intensely discussed during the last few decades. Particularly, the studies elucidated such important aspects as mechanisms of development and prevalence of myocardial ischemia in LV hypertrophy patients, specific character of analysis of ECG with ischemia-like patterns recorded in LV hypertrophy patients with and without evidence of myocardial ischemia, and others [82]-[85]. Nevertheless, detailed quantitative analysis of effect of LV mass changes on myocardial ischemia manifestation in ECG is still missing. Perhaps the only study, where the need of development of special criteria for ST elevation myocardial infarction in patients with LV hypertrophy was addressed, is study of Armstrong et al. [86] Significantly different severity of ST elevation were obtained in LV hypertrophy patients (defined by standard voltage ECG criteria) with and without an angiographic culprit lesion. New diagnostic strategy based on standard criteria was proposed to improve specificity of ST elevation myocardial infarction (by decrease of false positive diagnoses) detection without loss of sensitivity.

In cardiovascular research, particular aspects can be successfully studied on animal models, frequently on isolated heart perfused according to Langendorff [4]. In contrast to human, in animal experiments the myocardial ischemia as well as LV hypertrophy can be simply induced. The development of ischemia in hypertrophic hearts can therefore be investigated and accuracy of its detection in ECG evaluated. Such investigation is, however, complicated since standard ECG criteria for both hypertrophy and ischemia assessment in animals are missing. As was mentioned above, rabbit is one of the most popular models in studies of cardiovascular system due to the similarity of electrophysiological parameters of rabbit hearts to those of human. Moreover, rabbit is characterized with the high sensitivity to spontaneous LV hypertrophy and myocardial coronary vasoconstriction [87].

This study reports that even slight change of LV size can be assessed by analysis of data derived from EG simply recorded with orthogonal electrode system. It is known that the anatomical changes of the heart such as LV hypertrophy produce the changes in ECG morphology including increased amplitude and duration of QRS, the left axis deviation, and QRS patterns associated with the defects of intraventricular conduction [83],[88],[89]. Despite relatively low Se of ECG-based LV hypertrophy detection (in the range of 40-60 %), electrocardiography is still frequently used for LV hypertrophy screening due to its low cost, easy performance and wide availability [90]-[92]. Many electrocardiographic indexes have been proposed for diagnosis of LV hypertrophy in human. Most of them are based on the so called QRS voltage criteria [83],[92]. Thus, diagnostic performance of these indexes particularly depends on the precision of QRS complexes delineation. However, in experimental data, the detailed delineation of QRS is challenging task, especially in case of EG recorded under variable conditions [92],[93]. Moreover, standard indexes used for LV hypertrophy manifestation in human cannot be easily applied to experimental data due to lack of diagnostic criteria specific for different species. Considering the fact that various rabbit models of LV hypertrophy appropriate for studying the congestive heart failure, regional ischemia, LV hypertrophy regression and others, have been reported (e.g. [94],[95],[96]), it would be interesting to investigate this area in detail.

Assessment of incresed LV mass by EG analysis

Mean courses of QRS complexes calculated for L and H group in various heart positions are shown in Fig. 11. In some positions, morphology of mean QRS evidently differs between the groups. It corresponds with the results of statistical analysis of QRS-related parameters.

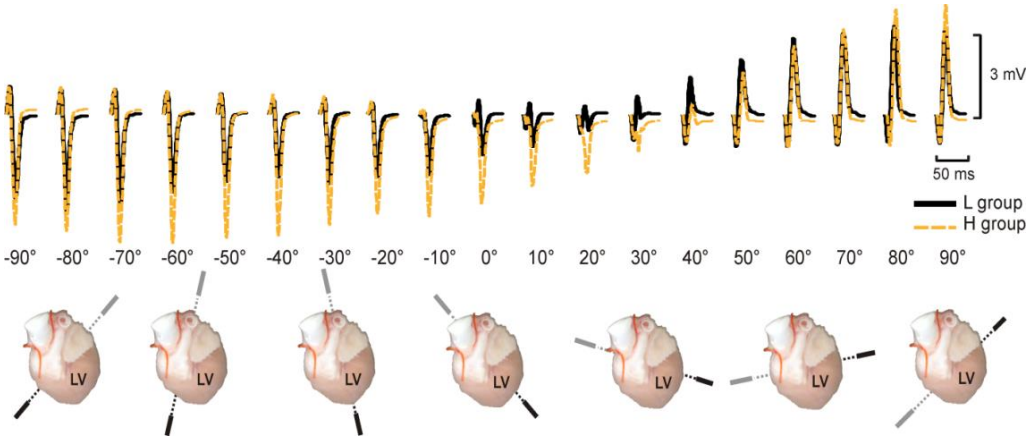

Figure 11. Averaged QRS complexes recorded in hearts with low (L) and high (H) LV mass fraction. Top views of the heart in the range from -90° to +90° illustrate the position of bipolar lead during electrogram recording (bottom).

According to the results, easily calculated EG parameters (without the need of complete delineation of all parts of QRS complex) can be successfully used for detection of increased LV mass. As in human [83], one of such parameters is QRS_A. Nevertheless, AUC_{QRS} seems to be the most sensitive to the changes in electrical activity caused by LV mass increase (compare AUCROC for discrimination between L and H groups for QRS_A, AUC_{QRS} and ST20 in Fig. 12). This is probably due to the method of parameter calculation, where all peaks within the whole QRS complex are taken into account including their polarity. As a result, minor changes in QRS morphology may cause significant change of AUC_{QRS} value that allows detecting increased LV mass with relatively high Se and Sp (both approx. 82 %). Above founding is in agreement with the results of study on 12-lead standard ECG recorded in healthy subjects and patients with LV hypertrophy, where voltage-duration product and true time-voltage QRS area were used instead of standard QRS voltages and duration to calculate Sokolow-Lyon criteria and the 12-lead sum of voltage criteria, which resulted in enhanced results of LV hypertrophy detection [97]. It should be noted that areas with high accuracy of increased LV mass detection in rabbit isolated heart electrogram (<-60°,-30°> and <0°, 20°>) correspond roughly with areas usually used for LV hypertrophy detection in human ECG (precordial leads V1, V2, V5, and V6 [83]).

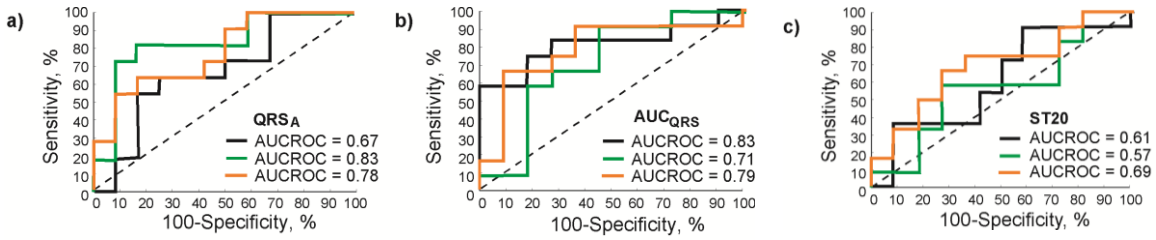

Figure 12. ROC curves of EG parameters proposed for the detection of LV mass increase calculated in the position -30°, 0°, and 20° (black, green and orange, respectively).

Ischemia manifestations in the hearts with unchanged and increased LV mass fraction

In the present model of short-term global myocardial ischemia, the earliest ischemia-induced changes were associated with electrical activity during ventricular depolarisation. In both experimental groups, it was mainly reflected in the values of QRS-related parameters extracted from EG recorded with lead oriented approximately through the anterolateral wall of LV. Some data from this area, however, seem to be sensitive

to LV mass increase, too. If electrophysiological effects of LV mass increase on investigated phenomena are not desired, only EG and/or VCG parameters resistant to such effects should be included in the study (such as ST20, see Fig. 15a). Other possible approach is use of the data recorded from boundary LV areas (lead I in initial position in Fig. 2, middle), where no significant effect of LV mass on the parameters was found. However, ischemia-induced changes in such case can be revealed with some time delay compared to previous one (see Table 1). Thus, appropriate parameters and/or recording area should be carefully chosen depending on the study goal.

Table 1. Onset of significant ischemia-induced changes ($p < 0.05$ for paired test) in selected EG and VCG parameters calculated for the hearts with low and high LV mass fraction.

Parameter	**Onset, min**		
	I1	I2	I3
QRS_A , AUC_{QRS} (L&H, lead II)	1^{st}	3^{rd}	4^{th}
β_{qrs} (L&H)	2^{nd}	4^{th}	4^{th}
QRS_D (L&H) AUC_{QRS} (L&H, lead I)	3^{rd}	4^{th}	4^{th}
α_{qrs} (H)	3^{rd}	5^{th}	6^{th}
ST20 and T_A (L&H, lead I) γ_{qrs} (H)	5^{th}	7^{th}	6^{th}
ST20 and T_A (H, lead II)	6^{th}	7^{th}	7^{th}
ST20 and T_A (L, lead II)	-	7^{th}	7^{th}

L, H – hearts with low and high LV mass fraction, respectively; I – ischemic; '-' – no significant changes

It is worth mentioning, that even recording with leads 'insensitive' to LV mass increase in stabilization period does not ensure that EG alterations indicated in ischemia are associated merely with this pathological condition. The influence of LV anatomical change on the heart electrical activity may appear during ischemia only, which can be seen e.g. on QRS_D and AUC_{QRS} extracted from lead I EG (see Fig. 13), where significant difference in parameters between L and H groups was revealed in the middle of ischemia probably due to certain electrical dyssynchrony based on subtle metabolic changes in slightly increased LV.

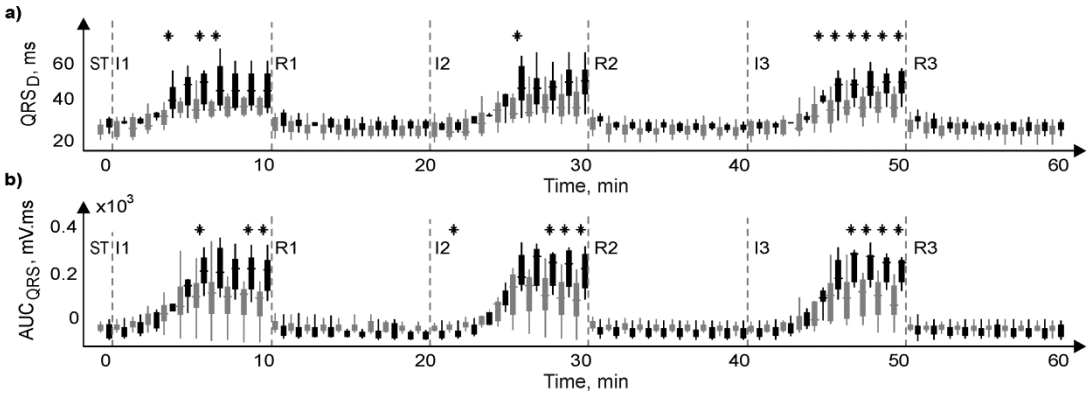

Figure 13. QRS_D (a) and AUC_{QRS} (b) in the hearts with low (grey) and high (black) LV mass fraction during the end of stabilization (ST) and ischemic (I) and reperfusion I periods (* $p < 0.05$ for Mann-Whitney U-test).

It is evident from Fig. 14, that the percent rate of parameters with AUCROC > 0.7 and 0.8 is almost the same in L and H group, whereas the number of parameters with AUCROC > 0.9 is higher in H group in comparison with L one (about 85 % and 35 % at the second half of the first ischemia, respectively). Both the percent of parameters with high AUCROC and the time to particular AUCROC thresholds (AUC > 0.7, 0.8, and 0.9) increase through the experiment in both groups. For lead I parameters, it is valid only for time to threshold and there is no difference in AUCROC course between L and H group. In joint parameters, there are not differences in AUCROC distribution during ischemia. In most parameters calculated in H group and in some parameters from L group, AUCROC increases up to 0.95-1 (perfect discrimination) at the end of

ischemia with corresponding Se and Sp of approx. 75 % - 90 % (even 100 % in some cases not shown). From Table 1 and Fig.14, preconditioning effect is present in both experimental groups.

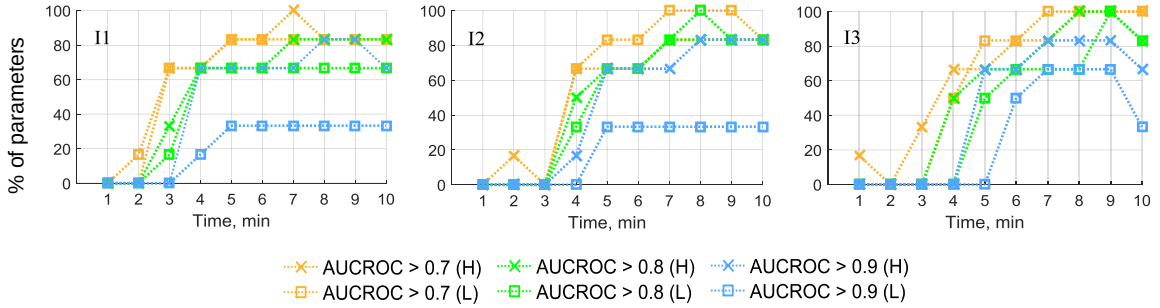

Figure 14. Percentage rate of parameters with AUCROC > 0.7, 0.8, and 0.9 calculated in groups with low (L) and high (H) LV mass fraction.

According to the results of ROC analysis, above phenomenon may have an impact on ischemia assessment, where the detection accuracy depends directly on discrimination threshold. Particularly, if no attention is paid to LV mass and AUC_{QRS} values from L and H groups are analysed together, than resulting Se overestimates by 5 % and underestimates by 6 % that obtained in L and H group, when the 'joint' cut-off value is used in all three cases (see Table 2 and Fig. 15b-d).

Table 2. Accuracy characteristics of myocardial ischemia detection. For the 10th minute of the first ischemia using lead I AUC_{QRS} calculated for hearts with low (L) and high (H) LV mass fraction and both (L&H).

Data group	AUCROC, -	Sensitivity, %	Specificity, %	Cut-off, mV·ms
L	0.88	89	94	-8*
H	1	100	100	39*
L&H	0.94	94	90	-8*
L	0.88	79	98	39
H	1	100	85	-8
L&H	0.94	89	99	39

* Optimal cut-off value derived from receiver operating characteristics curve for corresponding group

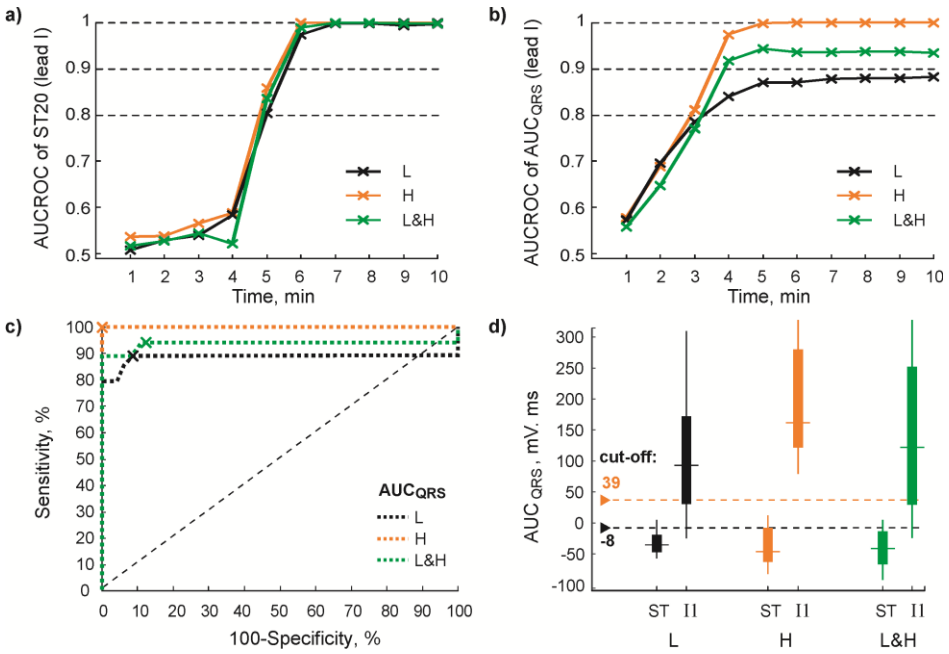

Figure 15. Discrimination ability of ST20 (a) and AUC_{QRS} (b) during the 1st ischemia, ROC curves for AUC_{QRS} at the end of I1 (c), AUC_{QRS} in stabilization (ST) and at the end of I1 and discriminating cut-off values (see text for details). L, H, L&H – hearts with low and high LV mass fraction and united group, respectively.

On the other hand, Sp calculated for joint group underestimates this index for L group by 4 % and overestimates that of H group by 5 %. Use of threshold 'adapted' for H group to detect ischemia in the hearts with high LV mass fraction results in excellent Sp (i.e. 100 %). Thus, the overall decrease of Sp due to unsuitable cut-off value reaches 15 % in this case.

The source of such discrepancies is illustrated in Fig. 15d, where distributions of the parameter in different groups and corresponding thresholds are shown. It is obvious, that use of cut-off calculated from another group data results in increase of false positive or false negative detections and, consequently, in decrease of Sp or Se (or both). Thus, the cut-off value should be carefully set with regard to the type of analysed data. It is generally in agreement with the studies, where increase of false positive detections due to neglecting of various patient-related factors (e.g. gender, age, LV hypertrophy, etc.) affecting ECG morphology at rest was revealed and adaptation (arising) of ST-segment threshold was suggested to improve ischemia detection accuracy [92],[93]. Analysis of anatomical peculiarities of the heart may help to reduce number of incorrect detections and avoid confusions in results interpretation.

4.3 Effects of voltage-sensitive dye di-4-ANEPPS on electrogram

As has been mentioned above, AP is often used in experimental studies to monitor electrical activity of the myocardium. Cardiac AP is generally recorded by two methods. The conventional one – with microelectrodes – is the gold standard for measuring electrical signals on the cellular level [98]. However, this method has one significant disadvantage: insertion of the electrode into the cell leads to its membrane disruption and may negatively affect cell function. Moreover, the procedure of electrode application is rather difficult. Thus, the experimental results depend on the experience and skills of the investigator. Optical method uses fluorescence properties of special chemical compounds, so called fluorescent dyes. Fluorescence of VSD molecules bound on the cell membrane is proportional to its transmembrane potential. Briefly, the procedure of AP measurement using VSD consists of: a) loading the heart with the for a definite time; b) washing the heart with perfusion solution to remove the unbound molecules; c) exposing the heart to excitation light (with halogen lamp, xenon/mercury arc lamp, LED or laser); d) detecting the emission light with some photodetectors (mostly photodiodes, photodiode arrays, photomultiplier tubes, and CCD cameras) [3],[55],[57],[62],[99]. Various fluorescent dyes with different properties are commercially available. The most commonly used VSDs are RH-237 and di-4-ANEPPS. Di-4-ANEPPS allows reaching a time resolution better than 1 ms [3] and exhibits changes in fluorescence of up to 10% per 100 mV [100]. VSD based approach allows noninvasive record of AP from a larger area of heart surface with high spatial resolution.

Despite such benefits, the application scale of optical method is generally limited because of the properties of available fluorescent dyes [62]. One of the most important disadvantages of VSDs is their possible effects on cardiac electrophysiology. Many authors reported various effects of di-4-ANEPPS in different experimental models, among which are the following: a) increasing contractility of cardiac muscle in isolated rabbit heart and human atrial preparation [101]; b) AP duration prolongation in guinea pig isolated ventricle myocytes [102] and in LV midmyocardial myocytes of beagle dog [103]; c) QRS duration prolongation [104], decrease of heart rate [105], and slowing cardiac impulse propagation [106] in guinea pig isolated heart; d) PQ interval prolongation, transient blocks of atrioventricular (AV) conduction, decrease of perfusion pressure due to dilation of coronary arteries [107], decrease of heart rate and slight prolongation of QRS and QTc duration [108] in rat isolated heart; e) vasoconstriction [109] and increase of total activation time [110] in mouse isolated heart. Some above effects are dose dependent [106] and some seem to be caused by phototoxic effect of the dye [103] or by other mechanisms associated with the binding of the dye to the cardiac cell membrane [102]. The most of above observations are the secondary outcomes obtained during experiments and there are only a few studies primarily focused on the evaluation of undesirable effects of VSD.

From above overview, it is evident that the response of myocardium to staining with di-4-ANEPPS is described mainly for small rodents such as mouse, rat and guinea pig. Nevertheless, as was mentioned above, the rabbit model is more suitable for cardiovascular studies due to the high similarity with human in cardiac electrophysiology parameters. One of the areas, where this model is intensively used, is the investigation of myocardial ischemia, infarction and ischemia-related arrhythmia, when the electrical activity is evaluated by conventional or/and optical method (e.g. [3],[5],[43],[44],[46],[56],[58]). In the second approach, unfortunately, the possible side effects of VSD are only briefly discussed or not addressed at all.

With regard to the results obtained for other species and some preliminary observations, various electrophysiological effects can be expected in case of rabbit myocardium. This chapter, therefore, introduces the results of electrical activity analysis in experiments on rabbit isolated heart after administration of di-4-ANEPPS.

Direct effects of di-4-ANEPPS on cardiac electrophysiology

Decrease of spontaneous heart rate and slowing impulse conduction through ventricles were found in stained isolated heart of almost all commonly used laboratory animal species [61],[106],[107], including rabbit (Fig. 16). Decrease of the heart rate may be caused either by effect of di-4-ANEPPS on ion channels in sinoatrial (SA) node or by impairment of coupling between the nodal cells. The SA node is a heterogeneous complex of nodal cells and other tissue [111]. The heterogeneous ion channel expression in different parts of the node and the variation of ion channels within a single nodal cell make the experimental verification of the finding very difficult. Nevertheless, the effect of di-4-ANEPPS is very similar to the effect of specific ion channel blocker ivabradine. Ivabradine selectively inhibits an important sodium depolarization current (the "funny" current, I_f), which controls the rate of spontaneous firing in SA node. It was reported that administration of ivabradine decreases heart rate and reduces severity of ischemia [112]. However, the direct effect of di-4-ANEPPS on I_f has not been studied yet.

For our best of knowledge, evolution of cardiac impulse conduction through atria and AV node in rabbit isolated heart stained with di-4-ANEPPS was addressed for the first time in this study. Besides the rat heart [107], the slowing cardiac impulse conduction through AV node (manifested as increased PQ_D) was observed in rabbit heart. The effect was found in negligible time period during dye loading only.

For the staining of the isolated heart, perfusion with low concentration of the dye lasted approx. 20 min was used. In accordance with the results of patch clamp analysis, significant prolongation of impulse conduction through the ventricles (represented by widening of QRS complex) was observed at the middle of loading procedure. The cell experiment results indicate that the effect of the di-4-ANEPPS on ventricular conduction may depend on the staining procedure, namely on the duration of loading period. Significantly higher inhibition of sodium current density was obtained in case of 30 min staining compared to acute application of the dye in the same concentration (Fig. 17). The change is caused by direct effect of the dye and is not a result neither of phototoxic effect nor an effect of DMSO used for dye dilution.

Only sporadic episodes of arrhythmias were detected in non-stained hearts during stabilization. In stained hearts during washout, junctional rhythm was observed for almost the half of the period. Taking into account the absence of pathological episodes before staining (in stabilisation), the presence of impaired rhythm in following periods seems to be due to the dye. Di-4-ANEPPS may affect various ion channels as well as intracellular connections. Staining leads to conduction velocity decrease and impairment of electrical homogeneity. Decreased heart rate in stained hearts may also lead to onset of junctional rhythm. Above observations were accompanied by the changes in shape of EG and VCG, which were found in repolarization part (ST segment and T wave). It can therefore be assumed that di-4-ANEPPS affects cardiac potassium channels. These alterations were fully washable.

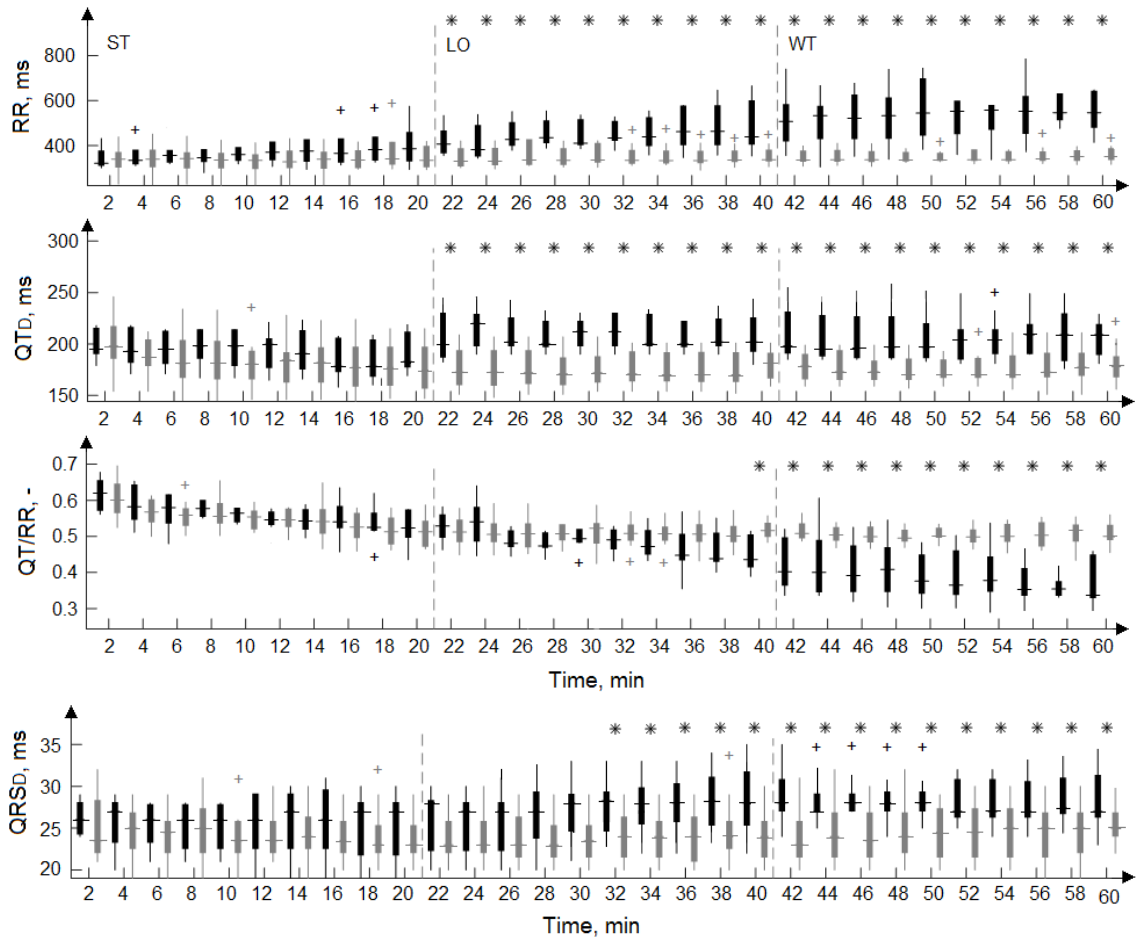

Figure 16. Duration of RR, QT interval, the ratio between them and QRS duration in stained and non-stained hearts. Experiments with (black) and without (grey) dye administration. ST, LO, WT – stabilization, dye loading and washout, respectively. * for $p < 0.05$ (Mann-Whitney U-test). Data from every second minute of the period are shown.

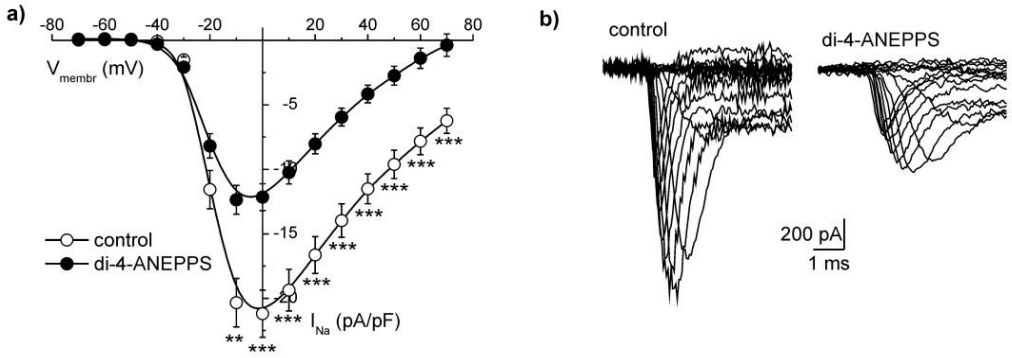

Figure 17. Averaged current-voltage relations for sodium current recorded via patch clamp under the control conditions (○; n=27) or after 30 min long incubation of cells in the presence of 2 μM di-4-ANEPPS (●; n=31). Solid lines represent B-spline fit to the experimental data. ** - $p < 0.01$, *** - $p < 0.001$. b) Current traces recorded under the control conditions or after 30 min long incubation of cells in the presence of 2 μM di-4-ANEPPS.

Some of presented results are in agreement with observations (QRS prolongation, slowing impulse propagation [104],[106]) in guinea pig isolated heart, despite the fact, that the hearts were stained by bolus of highly concentrated dye administered directly to the aorta (i.e. by "fast" staining procedure in contrast to "slow" staining by perfusion with low dye concentration used in present study on rabbit hearts). Similar phenomena caused by "fast" staining with di-4-ANEPPS might be expected in rabbit hearts, since the mechanism of AP propagation (in terms of depolarisation and repolarisation currents involved in the process [113]) in guinea pig and rabbit myocardium is similar. The changes in RR and QT interval duration

accompanied staining the rabbit heart from the beginning of this experimental period (see Fig. 16). It may consequently be supposed that these effects would be present in case of fast dye application, too.

Hence the interpretation of data from the experiments with di-4-ANEPPS (regardless the staining procedure used) should be performed with caution and the results obtained in this case should be validated using different experimental tools if possible. Particularly, the assessment of drug effects in isolated heart stained by di-4-ANEPPS might be complicated due to confounding effects of the dye such as QT and QRS prolongation appeared in the beginning of loading procedure. It is especially important in studies where the rabbit heart is used for the study of the arrhythmogenic potential of drugs such as antipsychotics or antiarrhythmics [34].

The abovementioned observations are not the result of phototoxic effect of the dye. The heart tissue illumination (i.e. dye molecules excitation) was performed locally by 6 optical fibres with diameter of 200 μm after washout period only [54]. During the whole experiment, the heart preparation was kept in the dark. Thus, all the observations can be considered as direct effects of di-4-ANEPPS on the rabbit heart.

An important advantage of this study is that no excitation-contraction uncoupler was used. In other studies, uncouplers (such as 2,3-butanedione monoxime, cytochalasin D and blebbistatin) are frequently used to reduce the motion artefact in AP records. Possible side effects of such agents (e.g. [56],[114],[115]) may complicate the analysis of electrocardiographic data and may lead to incorrect interpretation of the results.

Electrophysiological evaluation of global ischemia in the hearts stained with di-4-ANEPPS

According to above observations, di-4-ANEPPS affects ECG interval characteristics (such as QT_D and RR, Fig. 16). Nevertheless, the relative changes of these parameters in stained hearts during ischemia-reperfusion were almost the same as in controls (Fig. 18). According to ROC analysis, three parameters – RR, JTmax (from lead I) and AUC_{QRS} (from lead II) – provide good discriminating between non-ischemic and ischemic state in both control and stained hearts groups. In control group, besides these parameters, good discrimination capacity was found in some other such as ST20 and T_A (lead I), JTmax and QRS_A (lead II) and α_{qrs}, β_{qrs}, φ, and D. In stained hearts, QRS_A and AUC_{JTmax}R'(from lead I) and QRS_D, L_{qrs}, $D^c_{qrs}xz$ and $A_{qrs}xy$ were suitable for data discrimination besides the parameters observed for both groups.

In about half of evaluated parameters, onset of significant changes during ischemia was 1 – 3 min delayed in case of stained hearts (Table 3). Moreover, in QRS_D (ventricular conduction) as well as in other parameters (such as ST20 from lead I, β_{qrs}, φ, and D) more pronounced changes were found in controls. The total number of VPBs was higher in control hearts, as well (Fig. 19). It can therefore be concluded that di-4-ANEPPS affects the progress of myocardial ischemia: it delays the occurrence of significant ischemic changes and partially attenuates the severity of ischemia.

The progress of EG and VCG parameters in the first ischemia remained almost the same in later ischemic periods. In comparison with the first ischemia, the only difference was that the significant changes were delayed. VPBs number also decreased through three ischemic periods (Fig. 19). Both phenomena can be explained by preconditioning effect.

In reperfusion, the values of parameters affected by ischemia gradually returned to their non-ischemic levels. In stained hearts the recovery was usually faster than in non-stained hearts, where the EG alterations caused by ischemia were vanished during approx. first two minutes of reperfusion, such as in case of ST-T related parameters.

Slower ischemia development in stained hearts may be explained by decreased resting heart rate (see above). It has been reported, that slowing heart rate significantly reduces cardiac energy consumption and therefore may reduce the severity of ischemia and enhance recovery at reperfusion [112],[116],[117]. In patients treated with drugs such as beta blockers and verapamil, which reduce heart rate and systolic arterial blood pressure, false-negative response to exercise test may be obtained due to decreased myocardial oxygen requirements [17].

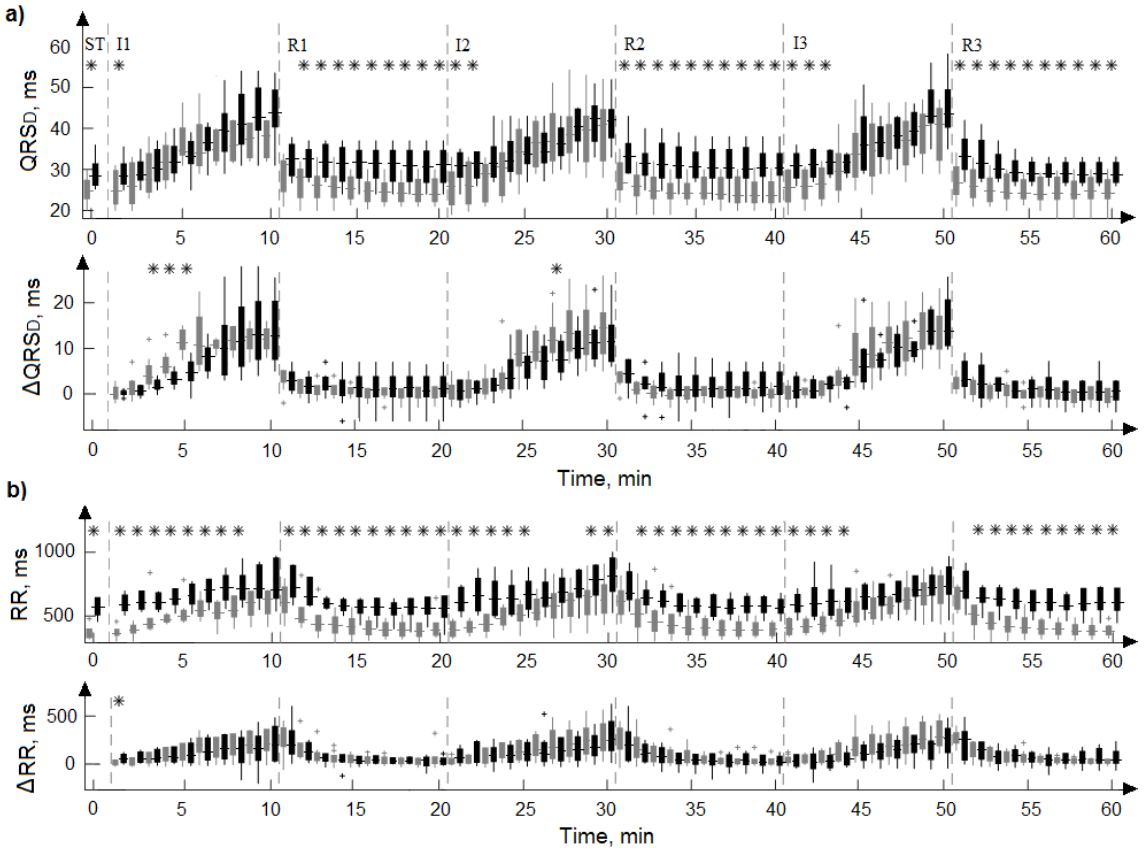

Figure 18. Main interval EG characteristics from stained (black) and non-stained (grey) hearts. Calculated for each minute (mean value) at the end of stabilization (ST) and during three ischemic (I) and reperfusion I periods: QRS and RR and difference (Δ) between actual value and value from the end of ST (bottom part of a, b and c, respectively). * for $p < 0.05$ (Mann-Whitney U-test).

Table 3. Onset of significant ischemia-induced changes ($p < 0.05$, Wilcoxon signed-rank test) in EG and VCG parameters from experiments with and without di-4-ANEPPS administration.

Parameter	**Onset, min**					
	Non-stained hearts			**Stained hearts**		
	I1	**I2**	**I3**	**I1**	**I2**	**I3**
JTmax (LI)	4^{th}	5^{th}	6^{th}	6^{th}	6^{th}	6^{th}
JTmax (LII)	3^{rd}	4^{th}	5^{th}	8^{th}	7^{th}	7^{th}
QRS_A (LI)	tr	tr	tr	5^{th}	7^{th}	8^{th}
QRS_A (LII)	1^{st}	3^{rd}	4^{th}	2^{nd}	3^{rd}	6^{th}
T_A (LI)	5^{th}	7^{th}	6^{th}	7^{th}	10^{th}	10^{th}
T_A (LII)	-	-	-	-	-	-
AUC_{QRS} (LI)	3^{rd}	4^{th}	4^{th}	8^{th}	7^{th}	10^{th}
AUC_{QRS} (LII)	1^{st}	3^{rd}	5^{th}	2^{nd}	9^{th}	9^{th}
$AUC_{JTmax}R'$ (LI)	3^{rd}	5^{th}	5^{th}	6^{th}	8^{th}	7^{th}
$AUC_{JTmax}R'$ (LII)	5^{th}	6^{th}	6^{th}	-	9	-
φ	3^{rd}	6^{th}	6^{th}	10^{th}	9^{th}	-
D	1^{st}	6^{th}	6^{th}	10^{th}	9^{th}	10^{th}
$A_{jt}xz$	4^{th}	5^{th}	4^{th}	tr	9^{th}	8^{th}

I – ischemia; LI, LII – lead I and lead II, respectively; 'tr' – transient changes; '-' – no significant changes

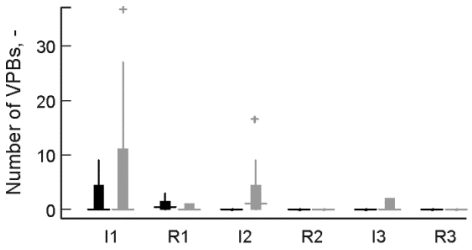

Figure 19. VPBs during ischemia (I) and reperfusion (I) in experiments with (black) and without (grey) di-4-ANEPPS.

Above findings complicate analysis and interpretation of data obtained in experiments with optical mapping by di-4-ANEPPS. Particularly, later and probably less pronounced response to ischemia should be expected in stained hearts, as it was found in present study. According to the results of ROC analysis, AUCROC of parameters from control group are generally higher as compared to stained hearts; moreover, quite good discrimination ability (AUCROC > 0.75 %) is characteristic for parameters from controls already in 4^{th}-5^{th} minute of ischemia, whereas AUCROC in stained hearts reaches similar value in 7^{th} minute only (Fig. 20).

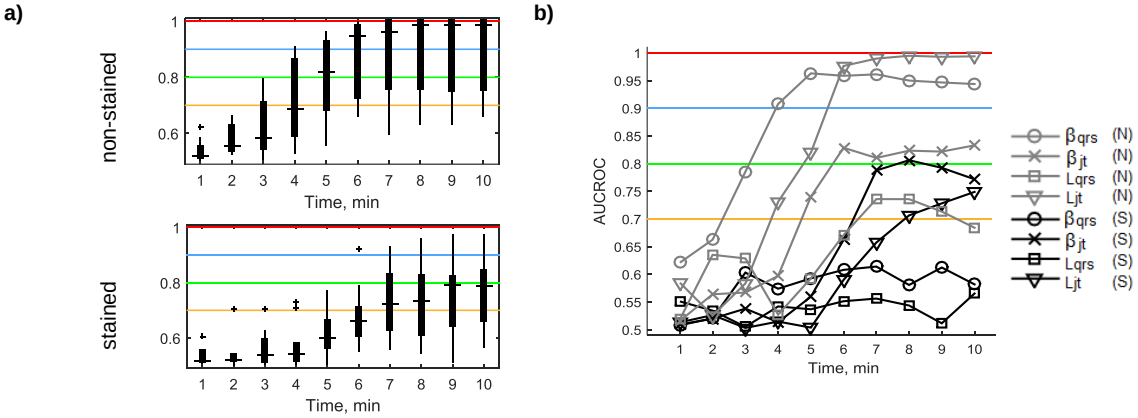

Figure 20. Distribution of AUCROC for main lead I & VCG (a) parameters and courses of AUCROC for main VCG parameters (b) calculated for stained and non-stained hearts.

The examples of distributions of ΔJTmax, ΔQRS_A and ΔT_A in ischemia and reperfusion periods are presented in Fig. 21. Significant differences between ΔJTmax (in both leads) and ΔQRS_A (in lead II) were found in the middle part of ischemia. This trend represents the fact that ischemia-induced changes are time-delayed in stained hearts comparing to the non-stained ones. It is typical for approx. half of analysed parameters. Other trend, namely the difference at the second part of ischemia, was observed in ΔQRS_A (lead I) and other five parameters ($\Delta AUC_{JTmax}R'$ (lead II), $\Delta AUC_{TmaxTend}R'$ (lead II), Δφ, ΔD, and $\Delta\varphi^{c}_{jt}zy$). Only in ΔQRS_A, the values for non-stained hearts were higher than those for stained hearts. In other cases, inverse relation was valid. In the rest (e.g. ΔT_A), no differences between two groups were found. The variability of parameters values within stained group was often much higher in comparison with control group data, especially in ischemia.

In can be, therefore, concluded, that if response to ischemia is under investigation, the prolongation of ischemic period and increase of heart rate by pacing may be considered to achieve appropriate results. To avoid possible discrepancies in results, stained hearts should be used as controls. If the results from experiments with di-4-ANEPPS are compared with those from control group without dye administration, special care should be taken. In this case, possible changes appeared during staining or washout should be identified and appropriate methodological correction (such as analysis of Δ values instead of initial parameters which was proposed in this study) should be performed to avoid wrong interpretation and conclusions.

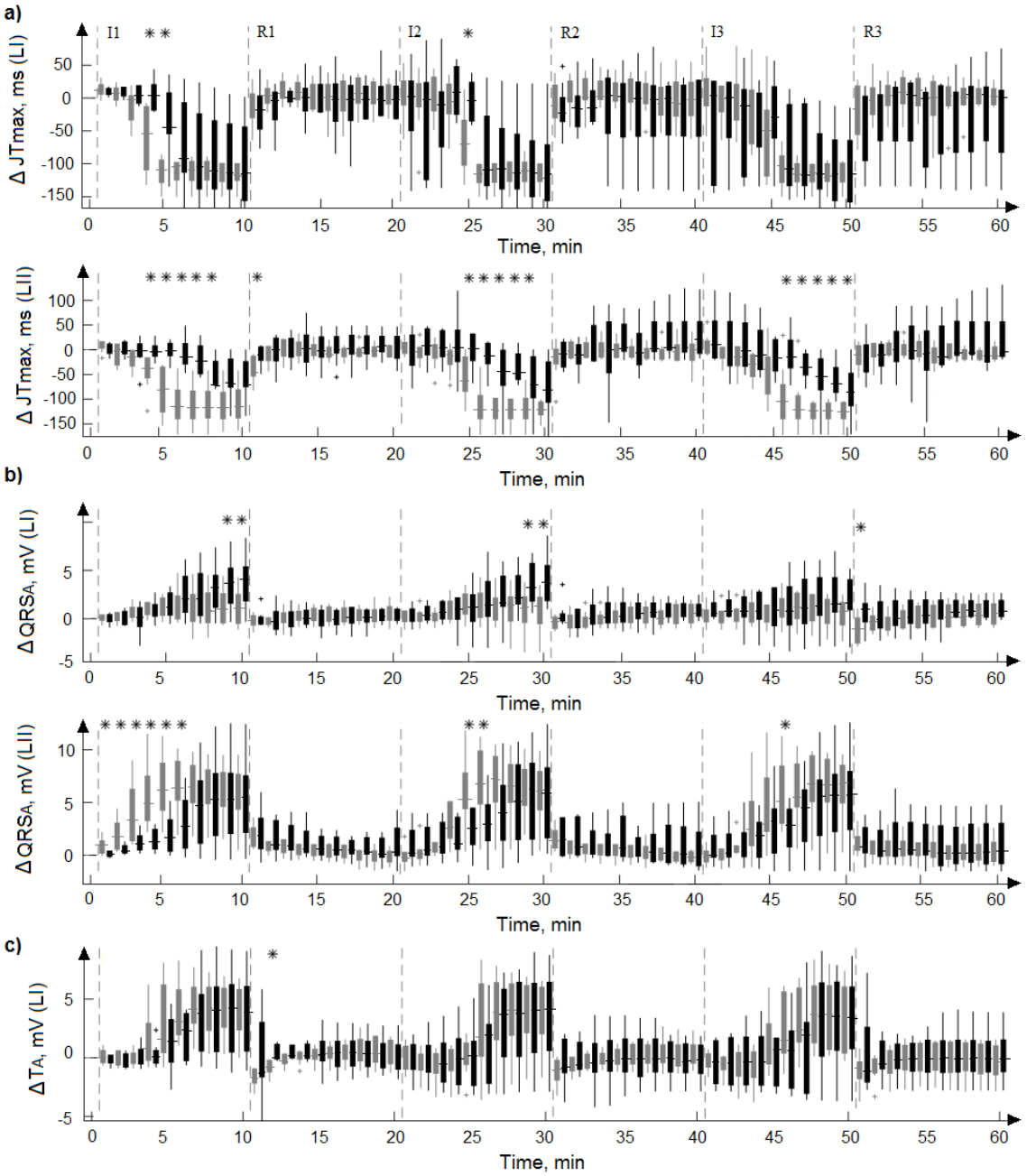

Figure 21. Distribution of the parameters' Δ in stained (black) and non-stained (grey) hearts groups. Δ is the difference between actual value and value from the end of stabilization; calculated for lead I (LI) and lead II (LII) data from three ischemic (I) and reperfusion I periods. * for $p < 0.05$ (Mann-Whitney U-test).

5 AUTOMATIC DETECTION OF ISCHEMIA IN ELECTROGRAMS

Rapid development of computer technologies leads to the intensive automation of various processes traditionally performed by human experts. The long-term records obtain huge amount of data which have to be checked and analysed. Manual (or visual) analysis of the records is a difficult time-consuming process and use of computer interpretation tool can decrease the time required for data analysis by up to 28 % [118]. Moreover, scoring by human expert may not be absolutely correct due to the subjectivity of decision making and accuracy of ECG interpretation ranges approx. from 57 % to 95 % depending on interpretation skills (noncardiologist physicians *vs* more experienced electrocardiologists) and type of ECG abnormality detected [119]. Se and Sp of ST episodes (both elevations and depressions) detection in data from European ST-T Database (commonly used for assessment of algorithms for ST-T changes detection) by the independent

cardiologists are in ranges 70-83 % and 85-93 %, respectively [120]. Therefore, there is an effort to design automated computer-based methods for reliable and timing myocardial ischemia detection.

The detection of myocardial ischemic episodes in ECG can be considered as a classification task, where various parameters derived from ECG (classification features, attributes) are used to discriminate between non-ischemic and ischemic segments by some computational algorithm. Main goal in classification is to assign input vector (feature vector) to one of discrete classes (two or more for binary and multi-class task, respectively). The feature space is divided into decision regions determined by decision boundaries (or decision surfaces). Results of interpretation provided by human expert (gold standard) can be used as so called target (output) values defining the labels of particular classes. The majority of reported tools for automatic ECG analysis use so called supervised learning techniques, which are learned to map the input variables (feature vector) to the target value (class labels) [67]. Use of large feature set for training the classifier may result in its overfitting, which is the situation, when the overly complex model fails by classifying novel samples regardless of the perfect classification results achieved for the training samples [67]. Some features may be redundant or/and irrelevant with respect to the solved problem and can be, therefore, excluded from the analysis by some of feature selectionmethods, which usually allows reducing the complexity of model and time required for its training and testing and, consequently, avoiding the model overfitting [68].

More recent approaches for automatic classification of ECG data including supervised techniques and human-like decision rule-based systems cover a wide range of various methods in terms of used ECG data (from short-term episodic to long-term Holter records [27]-[29],[33],[121]-[127],[129],[130]), features (from simple use of ECG samples to parameters extracted from principle components of ECG [129],[130]), feature selection methods (from use of all calculated features to sequential floating forward selection [29],[128],[131]-[133]), classification algorithms (from the simplest thresholding to more advanced artificial neural networks and support vector machines [27]-[29],[32],[33],[121]-[133]) and methods of performance validation (from simple separation of training and testing sets to leave-one-out cross-validation [131],[132]). Some of techniques will be addressed later.

Data recorded during experiments with induced ischemia include normal (non-ischemic) parts without ischemic patterns as well as those with manifestations of moderate (transitional state) and severe ischemia such as in case of ECG recorded in patients during PTCA available in STAFFIII database [134]. Furthermore, the effect of enlarged LV and drug intervention on properties of the classification approach (e.g. selected features, cut-off values, computational time, etc.) and ischemia detection accuracy can be studied using EG from different experimental groups. Thus, use of experimental data set allows more advanced testing the classification approaches. Parameters calculated from EGs and VCG were used as so called classification features. The part addressed in this chapter includes selection of relevant features from the whole set of parameters, distinguishing of particular classes (e.g. non-ischemic and ischemic) using some classification procedure and evaluation of classification performance. Before analysis, the parameters were scaled to the range <0, 1>; thus, processed parameters contribute to the calculations with the same weight regardless its type, scale and unit which allows obtaining less biased results.

5.1 FEATURE SELECTION

Three types of feature selection were realized. In all cases, parameters without statistical significance between non-ischemic and ischemic values (i.e. with $p \geq 0.05$ for Wilcoxon signed-rank test) were removed from the data set before selection. The first method is based on *correlation coefficient ranking* followed by *forward selection with LDF classification* (thus, hybrid method combining filter and wrapper approaches [135],[136]). Briefly, Spearman's ρ (usable for evaluation of non-linear relationships between the features and robust to outliers [74],[137]) was computed for each pair of the parameters which were then sorted (ranked) according to their averaged (arithmetic mean values) correlation coefficients in ascending order.

Non-significant ($p \geq 0.05$) ρ and those corresponding to the correlation of the parameters with themselves were excluded from the averaged value calculation. Parameters from the sorted sequence were then used to train the LDF (a basic approach ensuring the classification performance depends mainly on features selected) in a stepwise manner, i.e. parameters from the first (less correlated with other) to the last (most correlated with other) were iteratively involved into the model and classification performance indices were calculated within each such iteration. Optimal feature number was then chosen according to the highest Se and Sp achieved. Application of above procedure allows both reducing the dimensionality of the final feature set and decreasing the inter-feature correlation in it.

The second feature set was selected using *PCA-based method*. PCA allows selecting the only features containing the most relevant information (i.e. explaining the most variance in data). To do this, principal components (PCs) were calculated using the parameters and PC coefficients (so called loadings) were analysed such as described in [137]. Up to 12 PCs were required to explain more than 90-95 % of data variance. The first PC provided an explanation of about 33-48 % only and the distribution of loading values of different parameters was inhomogeneous in particular PCs. Simple algorithms based on simple ranking of the parameters according to the averaged values of their loadings calculated through all or several PCs were previously proposed to select relevant features [138]. It, however, does not consider the contribution of the PCs to explanation of the total variance in data and only takes into account the contribution of the parameters to particular PCs, which usually varies greatly. This may lead to incorrect results, where the feature with the high loading lo' in the PC moderately or even minimally contributing to the total variance explanation (usually 3rd-8th PC and later) is considered as more informative than that with the loading lo'': $lo'' < lo'$ from the first or second PC explaining the most of variance, as illustrated in Fig. 22. Therefore, the weighting of loading for k^{th} parameter was proposed as:

$$\overline{lo^k} = \frac{\sum_{i=1}^{M} w_i \cdot |lo_i^k|}{\sum_{i=1}^{M} w_i}, k = \overline{1, N} \quad (1)$$

where w_i is weight defined as percent of total variance in data explained by corresponding i^{th} PC, $|lo_i^k|$ is the absolute value of loading of k^{th} parameter calculated for i^{th} PC, M is the number of PCs explaining together at least 70 % of the total data variance, N is the number of parameters with significantly different values measured under non-ischemic and ischemic conditions. Usually, 3-4 PCs explaining of about 70 % - 75 % from the total variance were used for parameters ranking to eliminate the bias of weighted mean loading estimation. Then, the parameters were ranked according to their averaged loading $\overline{lo^k}$ sorted in descending order and optimal feature set was selected according to Se and Sp obtained by stepwise LDF based classification as in previous case.

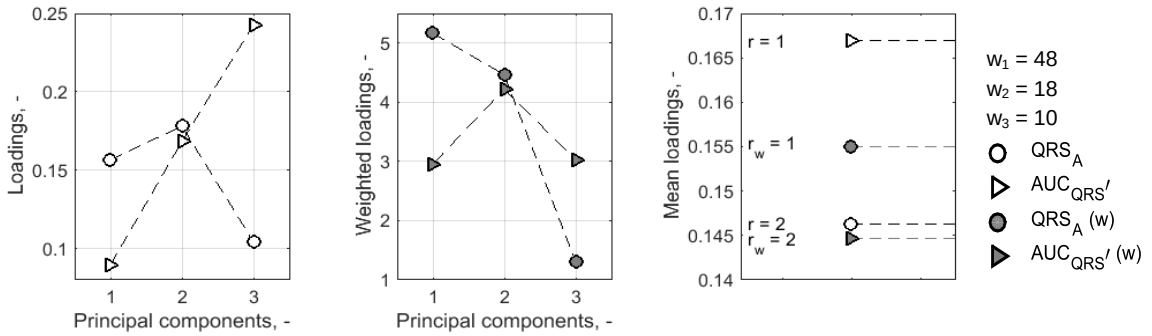

Figure 22. PCA-based ranking of the features.

Principal component (PC) loadings for first three PCs (left); weighted PC loadings (middle) and mean loading values calculated for each parameter through three PCs and corresponding ranks (r) of the parameters (right).

Above two methods were applied for the selection of features from lead I (feature set F3), lead II (F4), joint & VCG (F5), and all parameters (F2), separately. As a result, the number of features was significantly reduced (11 and 5 times as compared to the initial F1 set, for binary and 4-class classification, respectively)

to avoid possible overfitting of classification models, especially in case of binary approach. In all experimental groups, mostly AUC based features were involved in the feature sets from lead I and lead II data and different kinds of features were chosen from joint&VCG parameters. Finally, the parameters providing the best performance using *simple decision rule* (binary case) and *decision tree* (multiclass approach) were included into the feature set F7 (see next section).

Among the features selected by above methods, other sets were tested. The first one (F1) included the parameters with proven difference between their non-ischemic and ischemic values. The second one (F6) was formed by parameters commonly used for ischemia assessment, i.e. deviation of QRS complex, T wave and ST segment and QRS complex duration. All feature sets used for further classification are listed in Table 4 including their notation. Besides F1-F7, each parameter was also used as an input for decision rule based classifier and decision tree to assess its potential usability for single-feature classifier design.

Table 4. List of feature sets selected by proposed approaches.

Feature set:		**Description:**
F1*		All with significant difference between non-ischemic and ischemic value
F2*:	F21	Selected from F1 according to Spearman's ρ
	F22	Selected from F1 according to principal component's (PCs) loadings
F3*:	F31	Selected from lead I based parameters (from F1) according to Spearman's ρ
	F32	Selected from lead I based parameters (from F1) according to PCs loadings
F4*:	F41	Selected from lead II based parameters (from F1) according to Spearman's ρ
	F42	Selected from lead II based parameters (from F1) according to PCs loadings
F5*:	F51	Selected from joint & VCG parameters (from F1) according to Spearman's ρ
	F52	Selected from joint & VCG parameters (from F1) according to PCs loadings
F6**:		Commonly used, i.e. QRS_A, T_A and ST20 (lead I and lead II) and QRS_D
F7*:		Five best parameters according to the results of DR or DT

* different for experimental groups; ** same for experimental groups; DR – decision rule; DT – decision tree

5.2 DATA CLASSIFICATION

Two different classification approaches – *binary and multiclass* – were realized in the thesis. In first case, data from stabilization and ischemic period were used as non-ischemic and ischemic observations, respectively. In the second one, totally 4 (non-ischemic and beginning, moderate and severe ischemia, where ischemic data were selected from the 1^{st}-3^{rd}, the 4^{th}-6^{th} and the 7^{th}-10^{th} minutes of ischemia, respectively) or 11 different classes (non-ischemic and the 1^{st} to the 10^{th} minute of ischemia) were distinguished from each other. Target (known, desired output) values were coded by the sequence from zero to K, where K is the number of classification groups involved in the approach.

Five classification methods, namely simple *decision rule* (or thresholding, analogue of the method used in clinical practice, used for binary classification; DR), *decision tree* (used for multiclass classification; DT), *discriminant function* (linear LDF and quadratic QDF), *k-nearest neighbors* (with various *k*; k-NN), and *support vector machine* (with linear and Gaussian kernel function; SVM) were tested in the study.

Cut-off values involved in DR were determined by analysis of ROC curves calculated from training data set. The optimal point on ROC curve was selected from all points (Se_i > 50 %, Sp_i > 50 %) as a pair providing maximal sum $Se_i + Sp_i$. Above two conditions allows eliminating the cases, when one index is extremely high and another is extremely low, and choosing the compromise, where both indexes are quite high. Then, optimal cut-off was applied on new testing data by LOO validation and average test performance indices, time moment of positive detection (ischemia) and the duration of one validation cycle (including both training and testing procedure) were calculated. For multiclass task, the rules were induced directly from the data extracted from hierarchical decision systems – DT – which were created by standard CART algorithm (generally based on binary splitting the data according to the optimization criterion [67],[139]). Large trees (i.e. with high number of levels, nodes and branches) are predisposed to overfitting. In the thesis,

the depth of tree (leafiness) was optimized by merging leaves on the some tree branch – tree pruning, as has been proposed in [67].

Other tested methods – the statistical parametric approaches LDF and QDF – are based on the concept that different classes generate data based on different distributions. During training phase, the parameters of distribution for each class are estimated by the fitting function and used for calculation the model coefficients. During testing on new data, trained discriminant model finds the class with the smallest misclassification cost. [139]

In case of LDF and QDF, the choice of inappropriate model of density (which is very limited) may lead to poor classification results. In some cases, the classification accuracy can be improved by using of non-parametric approaches, such as k-NN, where decision boundaries are directly constructed based on training data from the neighbourhood determined by *k* [139]. Other non-parametric approach tested in this study was SVM, which constructs a hyperplane in a high dimension – typically much higher than the original feature space – for separation the instances.

5.3 EVALUATION OF CLASSIFICATION PERFORMANCE

To assess the generalization ability of the classification approach on new data set, training of the classifier was performed on only some part of the whole feature set and the rest of data was used to test it. Two different cross-validation (CV) approaches – one-leave-out (LOO) and k-fold (10-fold CV) were chosen in the study [66],[140]. In case of LOO, data from one experiment were used for testing only and the rest was included into the training set iteratively until each signal was used for testing. Resulting number of training and testing samples in each experimental group is summarized in Table 5. Because of quite high inter-subject data variability and low number of available experiments, classification results obtained using this cross-validation method may be very pessimistic. Moreover, since the test set contains data from only one record, the variance of estimated performance indices tends to be high [140].

The second approach is based on random partitioning of data from all experiments into *k* disjoint equal sized subsets, where one of them is then used for testing and rest k-1 subsets are used for training during k iterations (folds). In contrast to LOO, proposed 10-fold CV (where training and testing observations are selected from the same experiment, although not overlapped with each other such as in case of simple resubstitution, where the model is tested using training data) may have overly optimistic bias in estimation of classification performance. This approach may, nevertheless, be helpful for assessment (at least rough) of the model performance, if LOO is not suitable due to small data set and large number of classes to be distinguished (see below).

Table 5. Average size of training and testing data sets in one cycle of LOO validation.

Group	Number of animals	Number of training samples	Number of testing samples
Control	11	14268 ± 188	1585 ± 187
H group	8	10210 ± 167	1702 ± 166
Stained hearts	9	8201 ± 162	1165 ± 160

Sensitivity (Se), specificity (Sp) and accuracy (Acc) were calculated to evaluate the classification performance of particular approaches [141] within each CV interation and were then averaged through the whole CV procedure which results in more accurate estimation of classification performance [66].

Besides cross-validation within a particular experimental group, ‘cross-group’ validation was performed to asses possible effect of data type used for model training on classification performance achieved on different test data.

5.4 BINARY CLASSIFICATION: SINGLE-FEATURE DECISION RULE METHOD

Best results for each parameter group obtained by single-feature decision rule method are summarized in Table 6. According to the best five results obtained in each group, both QRS and ST-T related features

were able to discriminate between non-ischemic and ischemic state. Some features such as JTmax and AUC_{QRST} (lead I), +/-AUC_{QRS} (lead I and lead II), QRS_D, D, and β_{qrs} were selected as one of the best features in at least two from three experimental groups. RR is presented in all groups. However, it is well known that RR is highly sensitive to many external factors (besides perfusion stopping) such as changes in the temperature of preparation, administration of some drugs, etc. Thus, it cannot be recommended as a feature for ischemia detection. It can be seen that the highest classification performance in control and H groups was achieved by using of features from VCG, where two (β_{jt}, β_{qrs}, $A_{jt}xz$, $A_{jt}xy$) or all three leads (QRS_D, D, L_{jt}) were used for calculation. High variability in data recorded in stained hearts (see previous section) results in the high variability of all performance indices as well as the time moment when ischemia can be successfully detected. It should be noted, that common ischemia markers ST20 and QRS_D (not shown) do not provide successful detection in control group. Performance of QRS_D in H group is quite high. The same parameter in L group was among five best features (with still poor performance). It is in accordance with previously findings of visual and ROC analysis, where QRS prolongation was considered as better marker of ischemia than ST-segment deviations in present setup.

Table 6. Best results obtained by decision rule method in control group.Mean ± SD (through LOO cycles).

	Feature	**Cut-off**	**Acc, %**	**Se, %**	**Sp, %**	**TD, min**	**TC, s**
Lead I							
Control	+/-AUC_{QRS}	5 ± 0, -	70 ± 20	67 ± 31	78 ± 20	2.9 ± 2.8	1.14
Control	+AUC_{QRS}Rq’	0.84 ± 0.00, -	71 ± 21	69 ± 31	77 ± 23	2.9 ± 2.7	1.14
H	AUC_{QRST}’	181.2 ± 0.3 mV·ms	81 ± 11	82 ± 16	80 ± 20	1.3 ± 1.2	0.82
Stained	AUC_{JTmax}R’	0.37 ± 0.02, -	65 ± 17	64 ± 26	64 ± 34	2.1 ± 2.0	1.09
Stained	JTmax	128.5 ± 1.4 ms	66 ± 13	63 ± 23	77 ± 23	2.6 ± 2.5	0.15
Lead II							
Control	QRS_A	-1.86 ± 0.23 mV	70 ± 20	66 ± 30	86 ± 13	3.2 ± 3.0	0.57
Control	$AUC_{JTmax/TmaxTend}$	1.84 ± 0.04 mV·ms	72 ± 11	71 ± 19	78 ± 22	1.1 ± 1.0	1.88
H	+AUC_{QRS}	22 ± 2 mV·ms	69 ± 11	65 ± 11	86 ± 14	2.7 ± 2.1	0.82
H	-QRS_A	-3.39 ± 1.17 mV	75 ± 15	74 ± 25	75 ± 25	2.1 ± 1.6	0.30
Stained	AUC_{QRS}	-35.5 ± 0.8 mV·ms	64 ± 27	62 ± 38	70 ± 29	3.8 ± 3.6	0.66
VCG & joint							
Control	β_{qrs}	111 ± 0 °	72 ± 21	65 ± 28	98 ± 2	2.4 ± 2.1	2.28
Control	$A_{jt}xy$	0.34 ± 0.01 mV^2	71 ± 10	69 ± 18	81 ± 19	1.5 ± 1.4	1.13
Control	RR	398 ± 1 ms	74 ± 13	70 ± 18	89 ± 11	2.1 ± 1.5	0.09
Control	D	5.1 ± 0.0 mV	74 ± 12	68 ± 17	96 ± 4	2.8 ± 1.9	2.27
H	β_{qrs}	91 ± 27 °	68 ± 11	66 ± 25	71 ± 29	3.1 ± 2.3	1.63
H	D	6.4 ± 0.02 mV	71 ± 15	64 ± 20	97 ± 3	3.3 ± 2.3	1.62
H	RR	375 ± 9 ms	77 ± 16	79 ± 21	73 ± 25	2.1± 2.0	0.07
H	$D^c_{jt}zy$	0.63 ± 0.03 mV	77 ± 12	75 ± 17	83 ± 16	1.3 ± 1.1	0.82
Stained	RR	31.9 ± 0.4 ms	64 ± 23	64 ± 33	66 ± 24	3.6 ± 3.6	0.02

TD – time moment of ischemia detection; TC – average duration of one LOO iteration (training and testing).

The efficacy of decision rule method was additionally evaluated on the *features calculated without delineation outcomes* (excepting QRS_D and QT_D which in this case have constant values during the whole experiment). According to the results, performance indices obtained in this case were similar (mainly in case of voltage features or VCG features based on voltage VCG characteristics) or slightly lower (mainly in case of AUC based – especially QRS related – features) as compared to the common method. In case of stained hearts, the only feature still providing detection accuracy of about 60 % is AUC_{QRS} calculated from lead II EG. Possible the strongest reducing of performance was obtained in case of AUC_{JTmax}R’ calculated from lead I EG. Despite the fact, that values of this feature calculated using and without delineation outcomes are not significantly different, there are some differences in its distribution before as well as during ischemia,

which leads to different classification results obtained in both cases. Particularly, large number of false positive observations in feature calculated without delineation outcomes results in lower Sp (49 ± 39 %) as compared to common one (64 ± 34 %). Se obtained in both approaches is very similar (64 ± 26 % *vs* 62 ± 40 % in common and proposed method, respectively). In most cases, slight, non-significant time delay (Mann-Whitney U test, $\alpha = 0.05$) in ischemic detection and prolongation of the time required for training and testing (TD and TC in Table 6, respectively) were observed as compared to above method.

It should be noted that the high number of false negatives at the beginning of ischemic experimental period is in fact related to the definition of ischemic data group, mainly to the *definition of the onset of myocardial ischemia injury* in the heart preparation. This time moment cannot be strictly determined because of lack of the guidelines for ischemia detection in rabbit, especially in isolated heart model. In the absence of so called 'golden standard' and since the beginning of perfusion stopping was the only available reliable information, it was considered as the beginning of ischemia injury development in the heart. The effect of above methodological assumption on the detection results is illustrated in Table 7, where the performance indices and cut-off values obtained in case of differently defined beginning of ischemic period are summarized for three features from control and one feature from stained hearts groups. In case of ST20, better performance was achieved if first three or more minutes of period with perfusion stopped were considered as non-ischemic period. However, the results obtained in cases, where 5^{th}-10^{th} minutes of ischemia were considered as non-ischemic, should be accepted with caution. According to the minute-by-minute examination of some EG and VCG parameters by ROC curve, quite high Se and Sp were observed already in the 3^{rd} minute of ischemic period. Thus, such an optimistic performance of ST20 is much likely the result of overestimation due to incorrect definition of ischemia injury onset (too late in comparison with true beginning of ischemia). Quite similar results (with lower performance) were obtained for other features from H group and stained hearts.

Table 7. Performance of DR (ST20 in mV from lead I, control group) for various definition of ischemia beginning.

Indices	**Minute/s of period with perfusion stopped considered as a non-ischemic period**								
	1^{st}	1^{st}-2^{nd}	1^{st}-3^{rd}	1^{st}-4^{th}	1^{st}-5^{th}	1^{st}-6^{th}	1^{st}-7^{th}	1^{st}-8^{th}	1^{st}-9^{th}
Acc,%	64 ± 8	71 ± 9	78 ± 13	85 ± 15	86 ± 14	87 ± 12	89 ± 7	83 ± 9	76 ± 11
Se,%	58 ± 22	60 ± 22	69 ± 20	80 ± 18	88 ± 12	96 ± 4	99 ± 1	88 ± 11	86 ± 14
Sp,%	82 ± 18	90 ± 25	90 ± 10	90 ± 10	87 ± 13	85 ± 15	87 ± 9	83 ± 12	79 ± 14
Cut-off	0.6±0.3	0.6±0.2	0.7±0.1	0.6±0.1	0.8±0.2	0.7±0.1	1.2±0.0	1.4±0.1	1.4±0.1

As a next step, *cross-group validation* of above approaches was performed to assess the effect of data type used for training (i.e. control, H or stained hearts group) on classification results and to select the most 'universal' method/s suitable for classification of data from any experimental group. Example of the performance indices of decision rule determined using the features from different groups obtained by testing on data from the other two groups are shown in Table 8. The only way to obtain successful performance in all three groups is to use features from lead II EG, namely QRS_A (or $-QRS_A$, same in lead II) and $AUC_{TmaxTend}R'$ or QRS_D (not shown) from the control group. The best total performance (average through all groups) was obtained by using of QRS_A. When the cut-offs were determined from H group data, the successful performance was found in only one group from two others. The best total classification performance for training on stained hearts data was obtained in case of $+/-AUC_{QRS}$. However, Se calculated for stained hearts was even worse than in case of cut-off value determined for various features from the control group.

Finally, the results obtained for the first ischemic period were verified using data from the other two ischemic periods. The results of such *'cross-ischemia' analysis* for $+AUC_{QRS}Rq'$ from the control group are partially shown in Table 8, right. The best performance of ischemia detection was obtained for testing on the feature from the first ischemic period regardless the period used to derive the training data set. As the cut-offs calculated for different ischemic periods are almost the same (not shown), this observation is most likely

due to the above mentioned preconditioning effect, where appearance of ischemia manifestations in EG in the second and the third ischemic periods is time delayed in comparison with the first one. It leads to higher number of false negatives at the beginning and middle of these ischemic periods and, consequently, quite low Se obtained. It was also found that the indices calculated for later ischemic periods are quite similar, which is probably due to the similarity between EG recorded during the second and third ischemia. Similar results were obtained for other parameters from all experimental groups.

Table 8. Results of cross-group and cross-ischemia validation of single-feature decision rule method.

	Cross-group validation:						**Cross-ischemia:**		
Indices DR	**Training = QRS_A from lead II (control)** (cut-off: -1.9±0.2 mV)			**Training = +/-AUC_{QRS} from lead II (stained)** (cut-off: 0.24 ± 0.02, -)			**Training = I1 control (+AUC_{QRS}Rq' lead I)** Cut-off: 0.84 ± 0.00, -		
	Test: Control	Test: H	Test: Stained	Test: Stained	Test: Control	Test: H	Test: I1	Test: I2	Test: I3
Acc,%	70 ± 20	74 ± 1	63 ± 2	60 ± 25	71 ± 0	75 ± 1	71 ± 21	68 ± 1	65± 1
Se,%	66 ± 30	72 ± 1	63 ± 3	58 ± 38	72 ± 1	75 ± 1	69 ± 31	65 ± 1	61 ± 1
Sp,%	86 ± 14	85 ± 0	65 ± 4	63 ± 37	70 ± 5	76 ± 7	77 ± 23	78 ± 1	78 ± 1

5.5 BINARY CLASSIFICATION: MULTI-FEATURE SUPERVISED TECHNIQUES

The performance indices obtained by LDF and QDF using the same feature set were quite similar. QDF gave slightly lower Sp in all data groups. Therefore, LDF was chosen for further comparison with other classification approaches. It moreover enables the comparison of the results with those from the literature, where LDF is frequently used for ischemia detection in ECG.

As regards k-NN, the performance of this approach may significantly vary depend on number *k* of the closest training examples used for assignment of training observations to the classes [66],[67]. Generally, the rule of thumb is based on choosing this value as squared root of the training samples number [67]. Number of training samples in this study reached approx. 8200-14300 depending on experimental group (see Table 5). Therefore, k = 91 (the closest odd value calculated as squared root of the smallest training samples number) was chosen as starting value for further search of optimal *k*. The sequence from 11 to 301 (with step of 20) was used to search the optimal *k* providing the best overall performance indices (through the whole cross-validation) [142]. Low values were excluded from the search because of the classifier overfitting (i.e. high number of misclassifications during testing, especially at the beginning of ischemia, despite zero resubstitution – or training, error) which was present in all groups in case of *k* chosen from 1 to 10. Finally it was confirmed, that k = 91 is high enough to avoid the overfitting and low enough to keep the generalization ability of k-NN. This setting was applied in all experimental groups and feature sets.

Among two different types of SVM, namely regular (linear) one and that with Gaussian kernel (or radial basis function kernel), regular type was more successful (Gaussian kernel SVM was predisposed overfitting) and less complexity expensive. Therefore, SVM without kernel was chosen for further analysis.

The best overall performance indices obtained by binary multi-feature supervised classification techniques are summarized in Table 9. Generally, use of multi-feature methods (even the simplest LDF based classifier) helped to improve the results of one-feature approach in terms of the classification performance (accuracy up to 87-89 %) and also time moment of successful detection of ischemia (approx. during the first minute after perfusion stopping). SVM based approaches allow achieving high classification performance (and the best in control and H groups) in all experimental groups. One disadvantage of SVM is it's time-consuming as compared to LDF (not shown) and k-NN. In most cases, k-NN model was overfitted, which resulted in poor classification Sp. In stained hearts, nevertheless, the best approach was based on k-NN classification. Among all feature sets, F51 and F7 seem to be the most reliable for classification, even in case of H group, where F51 included only three uncommon features (QT_D, RR and $A_{qrs}xy$). Surprisingly, F32 set consisting of only three features (all of them are QRS related derived from lead I EG) provided quite

good classification in H group by the simplest model – LDF. It should be noted that features commonly used for ischemia detection (F6 set with the same content for all experimental groups) provided quite good results by classification using SVM (Acc = 85 ± 10 %, Se = 85 ± 13 % and Sp = 88 ± 30 % in control group and Acc = 82 ± 9 %, Se = 87 ± 7 % and Sp = 61 ± 44 % in stained hearts) and LDF (Acc = 72 ± 5 %, Se = 64 ± 7 % and Sp = 100 ± 0 % in H group). An important advantage of these small feature sets (as compared to F1 or F2) is in lower computational complexity and lower probability of classifier overfitting. The earliest detection of ischemia in control group is possible using F41 set (not shown), which is in agreement with above findings, where the earliest ischemia manifestations were presented mostly in lead II and corresponding parameters.

Table 9. Overall performance indices of the best binary multi-feature classification approaches. Mean ± SD through all cycles of LOO validation on test set.

Experimental group	**Classifier & feature set**	**Overall performance indices**			**Time moment of ischemia detection, min**	**Computational time, s**
		Acc, %	Se, %	Sp, %		
Control	SVM & F7	**89 ± 8**	**90 ± 9**	**86 ± 14**	**0.8 ± 0.8**	**12.49**
		88 ± 8	88 ± 10	88 ± 11	1.3 ± 1.2	8.69*
H group	SVM & F7	**87 ± 7**	**87 ± 7**	**90 ± 8**	**0.9 ± 0.8**	**5.87**
		81 ± 5	88 ± 9	64 ± 19	0.6 ± 0.5	5.78*
Stained	k-NN & F7	**87 ± 8**	**91 ± 9**	**68 ± 30**	**0.8 ± 0.4**	**2.47**
		81 ± 5	100 ± 0	58 ± 34	0.1 ± 0.1	0.16*

* – results obtained using parameters calculated without manual delineation outcomes

The usefulness of the best methods was also evaluated on the features calculated *without delineation outcomes* (Table 9). Classification performance obtained in this case was slightly lower (in terms of Se or Sp) in all cases than in common method. Nevertheless, the overall performance still remained higher in comparison with single-feature approach.

As in previous case, *shift of the moment which is considered as the beginning of ischemic injury* in preparation results in increasing Se and on the same time decreasing Sp (with improvement of about 5 % and 3 % for Se and Sp, respectively). If samples from first 8-9 minutes of the period were used as non-ischemic, the detection failed (all samples were classified as non-ischemic). Similar results were obtained for other classifiers and experimental groups.

According to the results of *cross-group validation*, LDF is the most appropriate for classification regardless the type of data (SVM was not able to generalize well on data from other experimental groups). Training LDF using data from stained hearts is the best choice. In this case, the performance calculated for control and H group is very close to those obtained by LDF trained on corresponding groups' data. Probably the main benefit of this approach is successful results achieved for stained heart group as compared to other methods. F51 based classification was found as the best, which is probably due to the fact that parameters from VCG provided successful classification performance in all experimental groups.

According to the results of *cross-ischemia validation*, as in single-feature method, the best performance was achieved for data from the first ischemic period regardless type of training data. Generally, the differences in Acc, Se and Sp obtained in different cases are not so prominent such as in previous case which is probably due to quite well generalization ability and flexibility of SVM as compared to simple decision rule application.

5.6 4-CLASS CLASSIFICATION: SINGLE-FEATURE DECISION TREE

The best results obtained by DTs constructed for various features calculated using and without delineation outcomes are summarized in Table 10. As compared to binary decision-rule method (Table 6), the performance of 4-class classification by DT is generally lower by 5-15 %. Some of present features, such as QRS_A, D^c_{jt}zy and JTmax (for control, H and stained hearts groups, respectively), are the same as in binary

approach which confirms their capacity to detect myocardial ischemia. Unfortunately, none of feature measured in stained hearts gave accuracy higher than 52-55 %. In most features (from all experimental groups), such a low overall performance is due to very low Se obtained for non-ischemic and middle ischemic data and very low Sp in case of other two classes (both indices less than 30 %). It can be seen that the optimal trees consisted of relatively low number of levels which resulted in short duration of one validation cycles including training and testing (mostly shorter than 1 s) which is similar or even less than in cut-off determination using ROC curve analysis. In all cases, the decrease of performance was observed by using of the features calculated *without delineation outcomes*, especially in AUC_{QRST} which is strongly depend on the definition of the beginning and the end of QRS-T segments.

Table 10. Best results obtained by single-feature DT. Shown as mean ± SD (through all classes and LOO cycles).

	Feature	**Acc, %**	**Se, %**	**Sp, %**	**Computational time, s**	**Tree levels number**
Control	QRS_A (lead II)	61 ± 15 61 ± 15	60 ± 14 59 ± 16	60 ± 16 60 ± 16	0.98 1.08	4 ± 2 6 ± 4*
Control	φ	65 ± 10 66 ± 11	63 ± 10 64 ± 11	65 ± 10 65 ± 11	1.27 1.33	20 ± 19 7 ± 7*
H	AUC_{QRST} (lead I)	62 ± 10 59 ± 2	60 ± 9 54 ± 2	61 ± 10 58 ± 2	0.78 0.98	3 ± 1 5 ± 3*
H	$D^c_{jt}zy$	63 ± 5 62 ± 5	62 ± 6 60 ± 6	63 ± 5 61 ± 5	0.85 0.94	5 ± 1 6 ± 2*
Stained	JTmax (lead I)	52 ±12 48 ± 12	48 ± 13 45 ± 12	51 ± 13 48 ± 13	0.19 0.28	6 ± 4 4 ± 2*
Stained	JTmax (lead II)	50 ± 18 45 ± 14	45 ± 17 40 ± 13	49 ± 18 44 ± 14	0.13 0.13	10 ± 5 8 ± 6*

* – results obtained using parameters calculated without manual delineation outcomes

Cross-group validation of all features resulted in poor (lower than 55 %) overall performance obtained in different experimental groups. Thus, the 4-class classification model should be trained and applied on the same data.

As in case of testing DT on data from experimental group different from that used for training set definition, use of DT trained on features from the *first ischemic period* to classify data from other periods resulted in poor classification performance. The best performance can be achieved only by tree trained on data from corresponding ischemic period.

5.7 4-CLASS-CLASSIFICATION: MULTI-FEATURE SUPERVISED TECHNIQUES

The best 4-class classification results obtained for different experimental groups are listed in Table 11. In all groups, resulting performance indices are slightly higher than in DT method. The largest improvement (up to 5 %) was obtained in control group. SVM is evidently the best classification technique. The computational time is similar to that of multi-feature binary method (Table 9).

Table 11. Overall performance indices of the best 4-class multi-feature approaches. Shown as mean ± SD.

Experimental Group	**Classifier & feature set**	**Overall performance indices**			**Computational time, s**
		Acc, %	Se, %	Sp, %	
Control	SVM & F6	**68 ± 10** 64 ± 8	**67 ± 11** 63 ± 8	**68 ± 11** 64 ± 8	**7.58** 8.20*
H group	SVM & F32	**62 ± 22** 59 ± 16	**63 ± 21** 58 ± 15	**63 ± 22** 59 ± 16	**6.71** 6.67*
Stained	SVM & F51	**57 ± 15** 35 ± 21	**52 ± 12** 33 ± 18	**56 ± 14** 35 ± 21	**6.14** 7.79*

* – results obtained using parameters calculated without manual delineation outcomes

Se and Sp obtained by the best approaches are shown in Fig. 23a. There are a large number of experiments, where the classification failed, even in the middle and ending phase of ischemia. The graphs of desired and 'real' outcomes and confusion matrixes showing a detailed distribution of the misclassified observations are shown in Fig. 23b and Fig. 23c, respectively. According to the latter, the greatest number of incorrectly assigned samples given by SVM in the control group corresponded to those belonging to the beginning and the ending phases of particular classes. These approaches provide good results despite utilizing of sets with only 7, 10 and 5 features (F6, control group; F32, H group; F51, stained hearts). For comparison, best classification accuracy of the largest set F1 was 55 ± 11 % in control group, 56 ± 11 % in H group and 46 ±13 % in stained hearts, which is even worse than that obtained by small sets.

In control group, use of F6 consisted from parameters calculated *without delineation outcomes* resulted in only slight performance decreasing despite the fact that QRS_D was removed from the feature set in this case. On the contrary, pronounced decrease in performance indices was observed in stained hearts group, where only three features remained in the set F51 after removing QRS_D and QT_D from it.

As in previous case, no approach was able to provide proper classification *regardless the type of testing data.* As for *cross-ischemia validation*, the best results for control and H group were obtained by LDF trained on F51 from control data, whereas the only useful method for stained hearts data classification was LDF trained on F51 derived from corresponding experimental group.

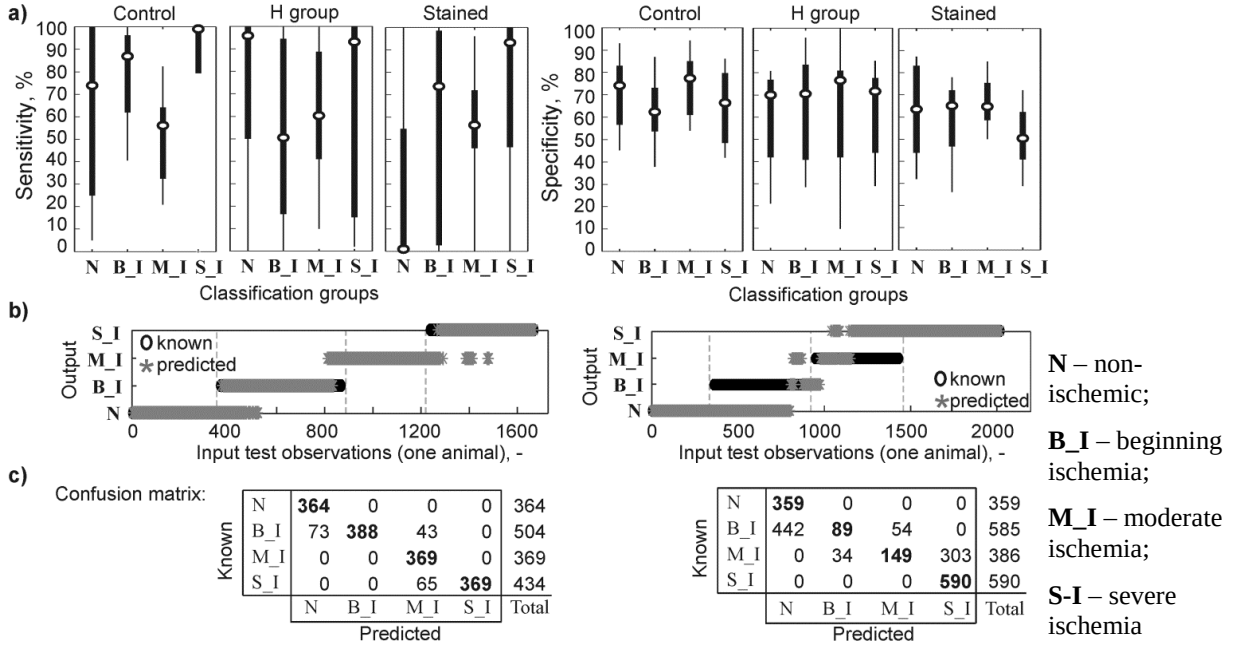

Figure 23. Outcomes of the best 4-class SVM based classifiers. Se and Sp (LOO validation) of the best approaches(a). SVM response on control group testing data from two different animals (b) and corresponding confusion matrixes (c).

5.8 11-CLASS CLASSIFICATION

As regards *11-class approach*, it can be, unfortunately, concluded that no technique was able to provide successful classification in particular experimental groups, which is most probably due to the small data set (in terms of number of available experiments). Thus, poor results were achieved by LOO validating procedure even using the largest feature set F1. On the contrary, highly optimistic and nonetheless not perfect results were obtained by 10-fold CV (not shown). In control and H groups, low Se at the end of ischemia can be explained by misclassifications between particular minutes within this part of experiment (i.e. between 7^{th} – 10^{th} minutes of ischemia). As expected, these results are poorer in comparison with binary as well as 4-class approaches.

OVERALL CONCLUSIONS

Results achieved in proposed dissertation mainly contribute to the field of basic electrophysiological research with methodological suggestions associated with the acquisition, analysis and interpretation of data from experiments on rabbit isolated heart undergoing global ischemia. Particularly, the main patterns of EGs and VCG recorded in the hearts under non-ischemic conditions are described in detail by various parameters derived from the records. These parameters are then used to quantify the heart response to short-term repeated global ischemia. It is shown, that electrical activity from different areas of the heart can be accurately recorded by touch-less way using three-lead orthogonal electrode system during longitudinal rotation of the heart. One of the most valuable results in this part is that the earliest global ischemia is mostly manifested in the depolarization phase, in contrast to the regional ischemia induced by occlusion of some coronary artery, when the pronounced changes are usually observed in repolarization period. Nevertheless, moderate and severe global ischemia results in marked changes of ST-T part of EG. As regards the spatial organization of global ischemia, the beginning and moderate phase are distinguishable mainly in EG from middle part of LV (anterolateral region), whereas the severe degree is represented in the records from any site of LV wall, with most pronounced manifestations in boundary part of LV (posterolateral region). Therefore, recording of EG by at least two leads facing above LV regions or three-lead VCG is suggested for accurate and timely assessment of all grades of ischemia.

Next contribution is associated with the evaluation of the effect of increased LV mass (which is relatively frequently seen in rabbits because of their high sensitivity to spontaneous LV hypertrophy) on cardiac electrical activity under both non-ischemic and ischemic conditions. Area under QRS complex (AUC_{QRS}) calculated for leads facing anterior or anterolateral area of the heart is proposed as electrophysiological marker of increased (even slightly) LV mass providing Se = 75 % and Sp = 82 %. In contrast to ECG indices commonly used in clinical practice for detection of LV hypertrophy (such as Sokolow-Lyon criteria, etc.), AUC_{QRS} does not require detection of particular peaks in QRS, which is a challenging task in case of experimental EG. Thus, increased LV mass mainly affects ventricular depolarization phase, which may lead to QRS patterns similar to those caused by ischemia. Manifestations of both phenomena are lead-dependent, which makes it possible to select data from lead ‘insensitive’ to LV mass changes, if study is focused on impact of ischemia itself and effects of LV mass on EG should be eliminated. However, it is shown, that some electrophysiological effects of increased LV may appear in ischemia only, which may negatively affect the accuracy of ischemia detection due to unsuitable discrimination criteria. For example, use of AUC_{QRS} cut-off calculated in the heart with normal LV (from ‘insensitive’ lead) results in perfect Se (100 %), but reduced Sp (85 % against 100 % in case of cut-off calculated for corresponding group of hearts with increased LV mass). Use of cut-off calculated for the hearts with changed LV leads to decrease of Se (by 10 %) and increase of Sp (by 4%) by discriminating ischemia in data from control group. ST-T based parameters (such as ST20 and others) seem to be more robust to changes of LV and, consequently, more suitable for ischemia detection in studies on the hearts with increased LV or if no information about LV mass is available. However, as was mentioned above, these parameters have less capacity to detect early phase of ischemia, as compared to those derived from QRS.

In recent animal studies, VSD di-4-ANEPPS is widely used for recording cardiac MAP. Nevertheless, the side-effects of the dye on cardiac electrical activity have been described mainly in small animals, such as rat, mouse and guinea pig. According to the results of previous studies, the electrophysiological effects of the dye are mainly present in EGs recorded during staining and washout periods of experiment. Ideally, these changes are reversible and disappear by the end of washout. Results addressed in thesis show, nevertheless, that some changes in heart activity caused by the dye are irreversible. This may affect the results obtained during the part of experiment following the washout. Among the most significant direct effects (not associated with dye phototoxicity) of di-4-ANEPPS observed in rabbit myocardium are: a) decrease of spontaneous heart rate manifested in EG as RR interval prolongation, which, in turn, results in increased QT

duration; b) slowing impulse conduction through the ventricles represented by significant QRS prolongation, which can be explained by the inhibition of I_{Na} in presence of the dye (validated by patch-clamp experiments); c) non-sustained slowing cardiac impulse conduction through AV node manifested as increased PQ duration during staining procedure. Prolongation of QT and QRS should be taken into account especially in cases, where the rabbit heart is used for the study of the arrhythmogenic potential of drugs. First two above mentioned phenomena are not reversible and, therefore, the progress of ischemia in stained preparations differs from that in control group (non-stained hearts). Namely, the dye delays the occurrence of significant ischemic changes, partially attenuates the severity of ischemia and enhance recovery at reperfusion in rabbit isolated heart, most likely due to reduced cardiac energy consumption caused by decreased resting heart rate. It is reflected in slower and less pronounced progress of EG and VCG parameters in stained hearts during 10-min long ischemia, as compared to the controls. This finding complicates analysis and interpretation of data obtained in experiments with di-4-ANEPPS. Particularly, significant ischemia-induced changes in EG and VCG can be expected by 1-3 min later than in controls and the number of parameters with the good ability to discriminate ischemia is much smaller in stained hearts. Among the parameters capable to detect ischemia in stained hearts, there are AUC_{QRS} and QRS_D, which, however, should be used with special care because of their sensitivity to LV enlargement. Therefore, other parameters should be preferred to avoid undesirable cross-effects of three factors – myocardial ischemia, VSD, and increased LV mass. The morphology of EG recorded in stained hearts varies quite widely among the preparations, which results in high variability of parameters values and, consequently, worsening of their discrimination ability. This additionally complicates the diagnosis of ischemia. Generally, to achieve appropriate results in ischemia studies, the prolongation of ischemic period or increase of heart rate by pacing may be considered. Possible discrepancies in results may be eliminated by using stained hearts as controls if possible; if not, appropriate methodological correction of evaluated parameters, such as analysis of values corrected by their stabilization levels instead of initial ones, should be performed to avoid wrong interpretation.

Finally, the dissertation contributes to the recent state-of-the-art in computer-based detection of myocardial ischemia by proposing of several classification approaches and validating them on data recorded during progressing ischemia. The effects of increased LV mass, VSD and preconditioning on efficacy of ischemia detection in electrophysiological data are quantified for the first time. Some methodological aspects, such as definition of the beginning of ischemic injury, method of feature calculation (using or without previous detailed delineation of EG), number (single- *vs* multi-feature approach) and type of the features (common – such as ST20, QRS_A and QRS_D, *vs* uncommon, such as those used recently for classification of different types of arrhythmias rather than ischemia and newly proposed, based on relative AUC values of EG and VCG patterns), number of classes (common binary *vs* non-conventional 4- or 11-class for more detailed analysis of particular grades of ischemia), type of algorithms for feature selection (correlation- vs PCA-based ranking) and classification (simple thresholding, decision tree, discriminant functions, k-NN, and SVMs), and method for cross-validation (LOO *vs* 10-fold) are also addressed (some of them for the first time). The most interesting and useful observations are summarized below. According to the content of feature sets obtained by correlation- and PCA-based selection methods, parameters calculated as relative AUC values are the least correlated with others; QRS-related parameters explain the most variance in data (i.e. they are potentially the most informative for further classification). AUC- (calculated from QRS and ST-T) and VCG-based features (representing information about spatial orientation of cardiac electrical vectors) seem to be the most promising. Both feature types belong to uncommon group and allow obtaining similar or even better results in comparison with conventional ST20 and QRS_D. Small sets (7 and less features) provide good classification results, whereas large sets are not suitable for binary as well as multi-class approaches mainly due to model overfitting. Besides the elimination of overfitting, use of small feature sets significantly reduces computational complexity of the method, which is important in both off-

line and real-time applications. Other technique allowing dramatic decrease of time-consuming of EG interpretation (by several times) consists in calculation of the parameters using empirically defined the beginning and the end of QRS complex and T wave. It is shown that classification performance achieved using such parameters is usually similar or only slightly reduced as compared to the conventional features. Nevertheless, the estimation of some features (such as AUC-based from QRS) via this method may be quite biased, which results in worsening of classification accuracy. Thus, more robust features (e.g. representing EG or electrical vectors deviation, etc.) should be preferred to avoid this effect. As in many previous reports, linear types of both discriminant function and SVM have better discrimination ability as compared to their non-linear alternatives (quadratic discriminant and SVM with Gaussian kernel). Along with k-NN, these types of classifier seem to be predisposed to overfitting, even in case of small feature sets. In most cases, SVM provides the best results. Nevertheless, if the low computational time is desirable, LDF may be used instead, without significant loss of detection quality. Besides all above factors affecting the efficacy of ischemia detection, there is other one, may be the most important, that is related to the heart condition itself. This is associated with above mentioned changes in cardiac electrical activity caused by increased LV mass or side-effects of chemical agents, such as VSD di-4-ANEPPS. According to the results, the most accurate ischemia detection can be performed in control group and hearts with changed LV, whereas slowed ischemia progress and high intra- and inter-subject variability in data results in quite poor detection performance in stained hearts. Thus, if there is a need to build the universal tool providing successful detection regardless data type, features from the group with the most complicated classification (and as a result the lowest performance achieved, such as in stained hearts) are suggested for training the model. Generally, such a tool can be suitable, if no information is available about LV anatomy or if classification is provided for hearts undergoing some chemical intervention, that changes (attenuates) the severity of ischemia. Preconditioning effect presented in all experiments should be also taking into account, when heart response to different subsequent ischemic periods is evaluated. Occurrence of ischemia manifestations in EG in the second and third ischemic periods is time delayed in comparison with the first one. As a result, low Se is obtained in second and third ischemia because of high number of false negative answers at the beginning and middle of these periods. Classifier trained on data from the first ischemic period provides quite good performance for data from subsequent ischemic episodes. Generally, in comparison with the reported results achieved in studies with PTCA data (where progressing ischemia is represented, such as in case of experimental data used in the thesis), the performance of proposed classification approaches is comparable or slightly better, even when data recorded immediately after perfusion stopping were considered as ischemic. In present setup employing simple thresholding (analogue to the decision in clinical practice), ischemia detection is possible at 2^{nd}-3^{rd} minute after perfusion stopping (with Se and Sp of approx. 68 % and 85 %, respectively) in control hearts and those with increased LV mass and at 3^{rd}-4^{th} minute after ischemia onset (with Se and Sp of approx. 63 % and 70 %, respectively) in stained hearts. Use of more advanced classifier – SVM – improves the time (detection in 1^{st}-2^{nd} minute of ischemic period in all experimental groups) and the performance (approx. Se and Sp are 89 % and 81 %, respectively) of the detection. In case of 4-class approach, the most difficult task is distinguishing of moderate ischemia, where the first part of this period is usually assigned as the beginning grade and the latter as the severe grade of ischemia.

The study limitations are associated with various its aspects. Data clustering performed at the beginning affects the time resolution of the method, where the real courses of parameters during experiment are smoother than those obtained by the proposed procedure. On the other hand, this technique allows significant reducing of time required for manual delineation of EG (by several hours). Other possible source of distortion is in the delineation itself, where the main difficulty is associated with J point detection (especially in progressing ischemia), which is crucial for accurate calculation of important parameters. The delineation was, nevertheless, provided by one reader and possible systematic error in detection of particular points is nearly constant. Proposed approach for estimation of parameters without outcomes of manual

delineation allows avoiding above errors; however, important interval characteristics, such as QRS_D and QT_D representing electrical depolarization and repolarization of the ventricles, are not informative in this case (constant during the whole experiment). Classification results are negatively affected by the concept used for determining the beginning of ischemic injury. According to this concept, data recorded immediately after perfusion stopping are considered as ischemic because of lack of gold standard for accurate assessment of ischemia in present experimental setup. It can be assumed, that the onset of ischemic injury in preparation is actually delayed due to reserve of oxygen in heart tissue. Thus, enhancement of the detection performance (due to less number of false negatives at the beginning of ischemic period) might be expected, if results of some other test would be available.

Further research might be focused on the verification of above results in subjects with evident LV hypertrophy (with significant changes in anatomy and/or function of LV) and on the investigation of gender and age dependence of phenomena associated with progressing ischemia in the hearts with unchanged and increased LV, which would be useful for support of ischemia diagnosis in patients with one or both these disorders. Validation of the dose-dependence of di-4-ANEPPS effects in the same heart model could be informative for effective experimental setup, reliable data acquisition and accurate interpretation of the results. Further development of ischemia detection methods can be based on other features, which seem to be promising according to published results. One of possible choices is investigation of high-frequency content of experimental QRS. However, there is no standardized method for quantification of the components even in human; moreover, signal averaging is required to obtain successful results, which may negatively affect the analysis of progressing ischemia. As shown in pilot study (see [143]), there is a high inter-subject variability in HF-QRS parameters. Thus, more experiments are needed to validate the findings and to appreciate the potential practical usefulness of this approach.

In view of aforementioned, comprehensive approach taking into account both anatomical and electrical characteristics of the heart and its orientation within the electrode system is required for proper analysis of heart electrical activity under normal and pathological conditions. Computer-based methods may be useful adjuncts in processing and analysis of ECG/EG and detecting various electrophysiological abnormalities.

REFERENCES

[1] Townsend N, Wilson L, Bhatnagar P, et al. Cardiovascular disease in Europe: epidemiological update 2016. Eur Heart J 2016.

[2] Wagner GS, Macfarlane P, Wellens H, et al. AHA/ACCF/HRS recommendations for the standardization and interpretation of the electrocardiogram: part VI: acute ischemia/infarction: a scientific statement from the American Heart Association Electrocardiography and Arrhythmias Committee, Council on Clinical Cardiology; the American College of Cardiology Foundation; and the Heart Rhythm Society: endorsed by the International Society for Computerized Electrocardiology. Circulation 2009; 119: e262–70.

[3] Dhein S, Mohr DW, Delmar M. Practical methods in cardiovascular research. Springer Berlin Heidelberg, 2005, p. 997, ISBN 978-3-540-40763-8.

[4] Olejnickova V, Novakova M, Provaznik I. Isolated heart models: cardiovascular system studies and technological advances. Med Biol Eng Comput 2015; 53: 669-678.

[5] Kang C, Brennan JA, Kuzmiak-Glancy, et al. Technical advances in studying cardiac electrophysiology – role of rabbit models. Prog Biophys Mol Biol 2016: 121: 97-109.

[6] Bers DM. Excitation-contraction coupling and cardiac contractile force (2nd edition). Dordrecht: Kluwer Academic Publisher, 2001, p. 427, ISBN 0-7923-7157-7.

[7] Lee HC, Mohabit R, Smith N, et al. Effect of ischemia on calcium-dependent fluorescence transient in rabbit hearts containing indo 1. Correlation with monophasic action potentials and contraction. Circulation 1988; 78: 1047-1059.

[8] Leirner AA, Cestari IA. Monophasic action potential. New uses for an old technique. Arc Bras Cardiol 1999; 72: 237- 242.

[9] Kusumoto F. ECG interpretation: from pathophysiology to clinical application. Springer, 2009, p. 298, ISBN 978-0-387-88879-8.

[10] Nasario Junior O, Benchimol Barbosa PR, Trevizani GA, et al. Effect of aerobic conditioning on ventricular activation: a principal components analysis approach to high-resolution electrocardiogram. Comput Biol Med 2013; 43: 1920-1926.
[11] Riera AR, Uchida AH, Filho CF, et al. Significance of vectorcardiogram in the cardiological diagnosis of the 21st centrury. Clin Cardiol 2007; 30: 319-323.
[12] Carmeliet E. Cardiac ionic currents and acute ischemia: from channels to arrhythmias. Physiol Rev 1999; 79: 917-1017.
[13] Dekker LRC, Coronel R, Van Bavel E, et al. Intracellular Ca^{2+} and delay of ischemia-induced electrical uncoupling in preconditioned rabbit ventricular myocardium. Cardiovasc Res 1999; 44: 101-112.
[14] Kalogeris T, Baines CP, Krenz M, et al. Cell biology of ischemia/reperfusion injury. Int Rev Cell Mol Biol 2012; 298: 229-317.
[15] Gorgels APM. ST-elevation and non-ST-elevation acute coronary syndromes: should the guidelines be changed? J Electrocardiol 2013; 46: 318-323.
[16] Gibbons RJ, Balady GJ, Bricker JT, et al. Acc/AHA 2002 guideline update for exercise testing: summary article: a report of the American College of Cardiology/American Herat Association Task Force on Practice Guidelines. Circulation 2002; 106: 1883-1892.
[17] Surawicz B, Tavel M. Stress test. In: Surawicz B, Knilans TK, editors. Chou's electrocardiography in clinical practice, Philadelphia: Saunders Elsevier, 2008, p. 221-255, ISBN 978-1-4160-3774-3.
[18] Man S, Haar CC, Schalij MJ, et al. The dependence of the STEMI classification on the position of ST-deviation measurement instant relative to the J point. In Computing in Cardiology 2015; 42: 837-840.
[19] Fayn J. A classification tree approach for cardiac ischemia detection using spatiotemporal information from three standard ECG leads. IEEE Trans Biomed Eng 2011; 58: 95-102.
[20] Haeberlin A, Studer E, Niederhauser T, et al. Electrocardiographic ST-segment monitoring during controlled occlusion of coronary arteries. J Electrocardiol 2014; 47: 29-37.
[21] Michaelides AP, Dilaveris PE, Psomaraki ZD, et al. QRS prolongation on the signal-averaged electrocardiogram versus ST-segment changes in the 12-lead electrocardiogram: which is the most sensitive electrocardiographic marker of myocardial ischemia? Clin Cardiol 1999; 22: 403-408.
[22] Takaki H, Tahara N, Miyazaki, et al. Exercise-induced QRS prolongation in patients with mild coronary artery disease. J Electrocardiol 1999; 32: 206-211
[23] Goldberger AL, Bhargava V, Froelicher V, et al. Effect of myocardial infarction on high-frequency QRS potentials. Circulation 1981; 64:3 4-42.
[24] Abboud S, Cohen RJ, Selwyn A, et al. Detection of transient myocardial ischemia by computer analysis of standard and signal-averaged high-frequency electrocardiograms in patients undergoing percutaneous transluminal coronary angioplasty. Circulation 1987; 76: 585-596.
[25] Amit G, Granot Y, Abboud S. Quantifying QRS changes during myocardial ischemia: Insights from high frequency electrocardiography. J Electrocardiol 2014; 47: 505-511.
[26] Sharir T, Merzon K, Kruchin I, et al. Use of electrocardiographic depolarization abnormalities for detection of stress-induced ischemia as defined by myocardial perfusion imaging. Am J Cardiol 2012; 109: 642-650.
[27] Pueyo E, Sörnmo L. QRS slopes for detection and characterization of myocardial ischemia. IEEE Trans Biomed Eng 2008; 55: 468-477.
[28] Garciá J, Sörnmo L. Autimatic detection of ST-T complex changes on the ECG using filtered RMS difference series: application to ambulatory ischemia monitoring. IEEE Trans Biomed Eng 2000; 47: 1195-1201.
[29] Firoozabadi R, Gregg RE, Babaeizadeh S. Identification of exercise-induced ischemia using QRS slopes. J Electrocardiol 2016; 49: 55-59.
[30] Matveev M, Naydenov S, Krasteva V, et al. Assessment of the infract size in high-resolution electrocardiograms. In Computing in Cardiology 2006; 3: 461-464.
[31] Treskes RW, Cato Ter Haar C, Man S, et al. Performance of ST and ventricular gradient difference vectors in electrographic detection of acute myocardial ischemia. J Electrocardiol 2015; 48: 498-504.
[32] Correa R, Arini PD, Valentinuzzi ME, et al. Novel set of vectorcardiographic parameters for the identification of ischemic patients. Med Eng Phys 2013; 35: 16-22.
[33] Correa R, Arini PD, Correa L, et al. Acute myocardial ischemia monitoring before and during angioplasty by a novel vectorcardiographic parameter set. J Electrocardiol 2013; 46: 635-643.
[34] Kaese S, Frommeyer G, Verheule S, et al. The ECG in cardiovascular-relevant animal models of electrophysiology. Herzschr Electrophys 2013; 24: 84-91.
[35] Gralinski MR. The Dog's role in preclinical assessment of QT interval prolongation. Toxicol Pathol 2003; 31: 11-16.
[36] Pogwizd SM, Bers DM. Rabbit models of heart desease. Drug Discovery Today: Disease Models 2008; 5: 85-93.
[37] Bell RM, Mocanu MM, Yellon DM. Retrograde heart perfusion: the Langendorff technique of isolated heart perfusion. J Mol Cell Cardiol 2011; 50: 940-950.
[38] Podesser B, Wollenek G, Seitelberger R, et al. Epicardial branches of the coronary arteries and their distribution in the rabbit heart: the rabbit heart as a model of regional ischemia. Anat Rec 1997; 247: 521-527.

[39] Verdow P, Doel MA, Zeeuw S, et al. Animal models in the study of myocardial ischaemia and ischaemic syndromes. Cardiovasc Res 1998; 39: 121-135.
[40] Abarbanell AM, Herrmann JL, Weil BR, et al. Animal models of myocardial and vascular injury. J Surg Res 2010; 162: 239-249.
[41] Cascio WE, Yang H, Muller-Borer BJ, et al. ischemia-induced arrhythmia: the role of connexions, gap junctions, and attendant changes in impulse propagation. J Electrocardiol 2005; 38: 55-59.
[42] Garg V, Taylor T, Warren M, et al. β-Adrenergic stimulation and rapid pacing mutually promote heterogeneous electrical failure and ventricular fibrillation in the globally ischemic heart. Am J Physiol Heart Circ Physiol 2015; 308: H1155-H1170.
[43] Mandapati R, Asano Y, Baxter WT, et al. Quantification of effects of global ischemia on dynamics of ventricular fibrillation in isolated rabbit heart. Circulation 1998; 98: 1688-1696.
[44] Matiukas A, Pertsov AM, Cram KP, et al. Optical mapping of electrical heterogeneities in the heart during global ischemia. Conf Proc IEEE Eng Med Biol Soc 2009; 6321-6324.
[45] Kazbanov IV, Clayton RH, Nash MP, et al. Effect of global cardiac ischemia on human ventricular fibrillation: insights from a multi-scale mechanistic model of the human heart. PLoS Comput Biol 2014; 10: e1003891.
[46] Qian YW, Sung RJ, Lin SF, et al. Spatial heterogeneity of action potential alternans during global ischemia in the rabbit heart. Am J Physiol Heart Circ Physiol 2003; 285: H2722-H2733.
[47] Ferdinandy P, Hausenloy DJ, Heusch G, et al. Interaction of risk factors, comorbidities, and comedications with ischemia/reperfusion injury and cardioprotection by preconditioning, postconditioning, and remote conditioning. Pharmacol Rev 2014; 66: 1142-1174.
[48] Bernardo NL, D'Angelo M, Okubo S, et al. Delayed ischemic preconditioning is mediated by opening of ATP-sensitive potassium channels in the rabbit heart. Am J Physiol 1999; 45: H1323-H1330.
[49] Botsford MW, Lukas A. Ischemic preconditioning and arrhythmogenesis in the rabbit heart: effects on epicardium versus endocardium. J Mol Cel Cardiol 1998: 30: 1723-1733.
[50] Dickson EW, Lorbar M, Porcaro WA, et al. Rabbit heart can be 'preconditioned' via transfer of coronary effluent. Am J Physiol 1999; 277: H2451-H2457.
[51] Walker DM, Walker JM, Yellon DM. Global myocardial ischemia protects the myocardium from subsequent regional ischemia. Cardioscience 1993; 4: 263-266.
[52] Zhang X, Xiano Z, Yao J, et al. Participation of protein kinase C in the activation of Nrf2 signaling by ischemic preconditioning in the isolated rabbit heart. Mol Cell Biochem 2013; 372: 169-179.
[53] Gutbrod SR, Sulkin MS, Rogers J, et al. Patient-specific flexible and stretchable devices for cardiac diagnostics and therapy. Prog Biophys Mol Biol 2014; 115: 244-251.
[54] Kolářová J, Fialová K, Janoušek O, et al. Experimental methods for simultaneous measurement of action potentials and electrograms in isolated heart. Physiol Res 2010; 59: S71-S80.
[55] Attin M, Clusin WT. Basic concepts of optical mapping techniques in cardiac electrophysiology. Biol Res Nurs 2009; 11: 195-207.
[56] Brack KE, Narang R, Winter J, et al. The mechanical uncoupler blebbistatin is associated with significant electrophysiological effects in the isolated rabbit heart. Exp Physiol 2013; 98: 1009-1027.
[57] Efimov IR, Nikolski V, Salama G. Optical imaging of the heart. Circ Res 2004; 94: 21-33.
[58] Holcomb MR, Woods MC, Uzelac I, et al. The potential of dual camera systems for multimodel imaging of cardiac electrophysiology and metabolism. Exp Biol Med 2009; 234: 1-34.
[59] Kelly A, Ghouri IA, Kemi OJ, et al. Subepicardial action potential characteristics are a function of depth and activation sequence in isolated rabbit hearts. Circ Arrhythm Electrophysiol 2013; 6: 809-817.
[60] Martišiene I, Jurevičius J, Vosyliute R, et al. Evolution of action potential altrenans in rabbit heart during acute regional ischemia. Biomed Res Int 2015: 1-12.
[61] Novakova M, Bardonova J, Provaznik I, et al. Effect of voltage sensitive dye di-4-ANEPPS on guinea pig and rabbit myocardium. Gen Physiol Biophys. 2008; 27: 45-54.
[62] Ronzhina M, Čmiel V, Janoušek O, et al. Application of the optical method in experimental cardiology: action potential and intracellular calcium concentration measurement. Physiol Res 2013; 62: 125-137.
[63] Curtis MJ, Hancox JC, Farkas A, et al. The Lambeth Conventions (II): Guidelines for the study of animal and human ventricular and supraventricular arrhythmias. Pharmacol Ther 2013; 139: 213-248.
[64] Kolářová J, Nováková M, Ronzhina M, et al. Isolated Rabbit Hearts – Databases of EGs and MAP Signals. In Computing in Cardiology 2013: 551-554.
[65] Vítek M., Kozumplík J. QRS SEEKER: Software for QRS complexes detection, 2010.
[66] Bishop CM. Pattern recognition and machine learning. Springer, 2006, p. 738, ISBN-10: 0-387-31073-8.
[67] Duda RI, Hart PE, Stork DG. Pattern classification (2nd edition). Wiley-Interscience, 2000, p. 680, ISBN 0-471-05669-3.
[68] Theodoridis S, Koutroumbas K. Pattern recognition (4th edition). Elsevier, 2009, p. 961, ISBN 978-1-59749-272-0.
[69] Tibshirani R, Walther G, Hastie T. Estimating the number of clusters in a data set via the gap statistics. J R Statist Soc 2001; 63: 411-423.
[70] Ronzhina M., Potočňák T., Kolářová J., et al. Software for annotation of heart beats ANEG, 2011.

[71] Drew BJ, Califf RM, Funk M, et al. Practice standards for electrocardiographic monitoring in hospital settings. Circulation 2004; 110: 2721-2746.
[72] Saculinggan M, Balase EA. Empirical power comparison of goodness of fit tests for normality in the presence of outliers. J Phys Conf Ser 2013; 435: 1-11.
[73] Gastwirtth JL, Gel YR, Miao W. The impact of Levene's test of equality of variances on statistical theory and practice. Statistical Science 2009; 24: 343-360.
[74] Sheskin DJ. Handbook of parametric and nonparametric statistical procedures (2nd edition). Chapman&Hall, 2000, p. 1016, ISBN 1-58488-133-X.
[75] Fawcett T. An introduction to ROC analysis. Pattern Recogn Lett 2006; 27: 861-874.
[76] Clifford DG, Azauaje F, McSharry PE. Advanced methods and tools for ECG data analysis. Artech House, Inc., 2006, p. 384, ISBN-10 1-58053-966-1.
[77] Thygesen K, Alpert JS, Jaffe AS, et al. Third universal definition of myocardial infarction. JACC 2012; 60:1581-1598.
[78] Du Y-M, Nathan RD. Ionic basis of ischemia-induced bradycardia in the rabbit sinoatrial node. J Mol Cell Cardiol 2007; 42: 315-325.
[79] Surawicz B, Knilans T. Acute ischemia: electrocardiographic patterns. In: Chou's electrocardiography in clinical practice (6th edition). Philadelphia: Saunders Elsevier, 2008, p. 124-161, ISBN 978-1-4160-3774-3.
[80] Feng Y, Cona MM, Vunckx K, et al. Detection and quantification of acute reperfused myocardial infarction in rabbits using DISA-SPECT/CT and 3.0 T cardiac MRI. Int J Cardiol 2013; 168: 4191-4198.
[81] Eaton P, Li JM, Hearse DJ, et al. Formation of 4-hydroxy-2-nonenal modified proteins in ischemic rat heart. Am J Physiol – Heart C 1999; 276: H935-H943.
[82] Dunn FG, Pringle SD. Left ventricular hypertrophy and myocardial ischemia in systemic hypertension. Am J Cardiol 1987; 60: 19 I-22 I.
[83] Hancock EW, Deal BJ, Mirvis DM, et al. AHA/ACCF/HRS recommendations for the standardization and interpretation of the electrocardiogram. Part V: Electrocardiogram changes associated with cardiac chamber hypertrophy. JACC 2009; 53: 992-1002.
[84] Otterstad JE. Ischaemia and left ventricular hypertrophy. Eur Heart J 1993; 14: 2-6.
[85] Zehender M, Faber T, Koscheck U, et al. Ventricular tachyarrhythmias, myocardial ischemia, and sudden cardiac death in patients with hypertensive heart disease. Clin Cardiol 1995; 18: 377-383.
[86] Armstrong EJ, Kulkarni AR, Prashant DB, et al. Electrocardiographic criteria for ST-elevation myocardial infarction in patients with left ventricular hypertrophy. Am J Cardiol 2012; 110: 977-983.
[87] Weber HW, Van der Walt JJ. Cardiomyopathy in crowded rabbits: a preliminary report. S Afr Med J 1973; 47: 1591-1595.
[88] Bacharova L, Szathmary V, Kovalcik M, et al. Effect of changes in left ventricular anatomy and conduction velocity on the QRS voltage and morphology in left ventricular hypertrophy: a model study. J Electrocardiol 2010; 43: 200-208.
[89] Estes EH, Jacksin KP. The electrogram in left ventricular hypertrophy: past and future. J Electrocardiol 2009; 42: 589-592.
[90] Budhwani N, Patel S, Dwyer EM. Electrocardiographic diagnosis of left ventricular hypertrophy: the effect of left ventricular wall thickness, size, and mass on the specific criteria for left ventricular hypertrophy. Am Heart J 2005; 149: 709-714.
[91] Schillaci G, Battista F, Pucci G. A review of the role of electrocardiography in the diagnosis of left ventricular hypertrophy in hypertension. J Electrocardiol 2012; 45: 617-623.
[92] Hejč J, Vítek M, Ronzhina M, et al. A wavelet-based ECG delineation method: adaptation to an experimental electrograms with manifested global ischemia. Cardiovasc Eng Technol 2015; 6: 364-375.
[93] Kozumplík J, Ronzhina M, Janoušek O, et al. QRS complex detection in experimental orthogonal electrograms of isolated rabbit hearts. In Computing in Cardiology 2014: 1085-1088.
[94] Corno AF, Cai X, Jones CB, et al. Congestive heart failure: experimental model. Front Pediatr 2013; 1:33.
[95] Wolk R, Sneddon KP, Dempster J, et al. Regional electrophysiological effects of left ventricular hypertrophy in isolated rabbit hearts under normal and ischaemic conditions. Cardiovasc Res 2000; 48: 120-128.
[96] Zhao Z, Chen L, Xiao Y-B, et al. A rabbit model to study regression of ventricular hypertrophy. Heart Lung Circ 2013; 22: 373-382.
[97] Okin PM, Roman MJ, Devereux RB, et al. Time-voltage QRS area of the 12-lead electrocardiogram: detection of left ventricular hypertrophy. Hypertension 1998; 31: 937-942.
[98] Richardson ES, Xiao Y. Electrophysiology of Single Cardiomyocytes: Patch Clamp and Other Recording Methods. In Cardiac Electrophysiology Methods and Models (1st edition). DC Sigg, PA Iaizzo, Y-F Xiao, B He (eds). New York: Springer, 2010, p. 329-348, ISBN 978-1-4419-6657-5.
[99] Salama G. Optical mapping: background and historical perspective. In Optical Mapping of Cardiac Excitation and Arrhythmias. D.S. Rosenbaum, J. Jalife (eds). New York: Futura Publishing Company. Futura Publishing Company, 2001, p. 9-33, ISBN 0-87993-481-6.

[100] Johnson PL, Smith W, Bayhnam TC, et al. Errors caused by combination of di-4-ANEPPS and fluo 3/4 for simultaneous measurements of transmembrane potentials and intracellular calcium. Annals of Biomedical Engineering 1999; 27: 563-571.
[101] Cheng Y, Van Wagoner DR, Mazgalev TN, et al. Voltage-sensitive dye RH421 increases contractility of cardiac muscle. Can J Physiol Pharmacol 1998; 76: 1146–1150.
[102] Hardy MEL, Lawrence CL, Standen NB, et al. Can optical recordings of membrane potential be used to screen for drug-induced action potential prolongation in single cardiac myocytes? J Pharmacol Toxicol Methods 2006; 54:173-82.
[103] Hardy MEL, Pollard CE, Small BG, et al. Validation of a voltage-sensitive dye (di-4-ANEPPS)-based method for assessing drug-induced delayed repolarisation in beagle dog left ventricular midmyocardial myocytes. J Pharmacol Toxicol Methods 2009; 60: 94–106.
[104] Larsen AP, Olesen SP, Grunnet M, et al. Pharmacological activation of IKr impairs conduction in guinea pig hearts. J Cardiovasc Electrophysiol 2010; 21: 923-929.
[105] Fialová K, Kolařová J, Provazník I, et al. Comparison of voltage-sensitive dye di-4-ANEPPS effects in isolated hearts of rat, guinea pig, and rabbit. In Computing in Cardiology 2010; 37: 565-568.
[106] Larsen PL, Sciuto KJ, Moreno AP, et al. The voltage-sensitive dye di-4-ANEPPS slows conduction velocity in isolated guinea pig hearts. Heart Rhythm. 2012; 9: 1493-1500.
[107] Nygren A, Kondo C, Clark RB, et al Voltage-sensitive dye mapping in Langendorff-perfused rat hearts. Am J Physiol Heart Circ. 2003; 284: H892-H902.
[108] Fialová K, Kolařová J, Janoušek O, et al. Effects of voltage-sensitive dye di-4-ANEPPS on isolated rat heart electrogram. In Computing in Cardiology 2011; 38: 721-724.
[109] Nygren A, Clark RB, Belke DD, et al. Voltage-sensitive dye mapping of activation and conduction in adult mouse hearts. Ann Biomed Eng 2000; 28: 958–967.
[110] Liang Q, Sohn K, Punske BB. Propagation and electrical impedance changes due to ischemia, hypoxia and reperfusion in mouse hearts. In Conf Proc IEEE Eng Med Biol Soc 2006; 1: 1560–1563.
[111] Shattock MJ, Rosen MR. The control of heart rate: the Physiology of the sinoatrial node and the role of the I_f current. Dialogues Cardiovasc Med. 2006; 11: 5-17.
[112] Ng FS, Shadi IT, Peters NS, et al. Selective heart rate reduction with ivabradine slows ischaemia-induced electrophysiological changes and reduces ischaemia-reperfusion-induced ventricular arrhythmias. J Mol Cell Cardiol 2013; 59: 67-75.
[113] Varró A, Lathrop DA, Hester SB, et al. Ionic currents and action potentials in rabbit, rat, and guinea pig ventricular myocytes. Basic Res Cardiol 1993; 88: 93-102.
[114] Baker LC, Wolk R, Choi BR, et al. Effects of mechanical uncouplers, 48iacetyl monoxime, and cytochalasin-D on the electrophysiology of perfused mouse hearts. Am J Physiol Heart Circ Physiol 2004; 287: H1771-H1779.
[115] Swift LM, Asfour H, Posnack NG, et al. Properties of blebbistatin for cardiac optical mapping and other imaging applications. Pflugers Arch 2012; 464: 503-512.
[116] Bernier M, Curtis MJ, Hearse DJ. Ischemia-induced and reperfusion-induced arrhythmias: importance of heart rate. Am J Physiol 1989; 256: H21–H31.
[117] Ceconi C, Cargnoni A, Francolini G, et al. Heart rate reduction with ivabradine improves energy metabolism and mechanical function of isolated ischaemic rabbit heart. Cardiovasc Res 2009; 84: 72–82.
[118] Brailer DJ, Kroch E, Pauly MV. The impact of computer-assisted test interpretation on physician decision making: the case of electrocardiogram. Med Decis Making 1997; 17: 80-86.
[119] Salerno SM, Alguire PC, Waxman HS. Competency in interpretation of 12-lead electrocardiograms: a summary and appraisal of published evidence. Ann Intern med 2003; 138: 751-760.
[120] Taddei A, Distante G, Emdin M, et al. The Europen ST-T Database: standard for evaluating systems for the analysis of ST-T changes in ambulatory electrocardiography. European Heart Journal 1992; 13: 1164-1172.
[121] Park J, Pedrcycz W, Jeon M. Ischemia episode detection in ECG using kernel density estimation, support vector machine and feature selection. Biomed Eng Online 2012; 11: 1-22.
[122] Exarchos TP, Tsipouras MG, Exarchos CP, et al. A methodology for the automated creation of fuzzy expert systems for ischaemic and arrhythmic beat classification based on a set of rules obtained by a decision tree. Artif Intell Med 2007; 40: 187-200.
[123] Goletsis Y, Papaloukas C, Fotiadis DI, et al. Automated ischemic beat classification using genetic algorithms and multicriteria decision analysis. IEEE Trans Biomed Eng 2004; 51: 1717-1725.
[124] Llamedo M, Martínez JP. Heartbeat classification using feature selection driven by database generalization ctireria. IEEE Trans Biomed Eng 2011; 58: 616:625.
[125] Murugan S. Rule based classification of ischemic ECG beats using ANT-Miner. IJEST 2010; 2: 3929-3935.
[126] Xu M, Wei S, Qin X, et al. Rule-based method for morphological classification of ST segment in ECG signals. J Med Biol 2015; 35: 816-823.
[127] Kumar A, Singh M. Ischemia detection using isoelectric energy function. Comput Biol Med 2016; 68: 76-83.
[128] Dranca L, Goni A, Illarramendi A. Tuning real-time detector of transient cardiac ischemic episodes on the Long-Term ST Database according to the annotation protocol B. In Computing in Cardiology 2013; 40: 583-586.

[129] Papaloukas C, Fotiadis DI, Likas A, et al. An ischemia detection method based on artificial neural networks. Artif Intell Med 2002; 24: 167-178.
[130] Murthy HSN, Meenakshi M. ANN, SVM and KNN classifiers for prognosis of cardic ischemia – a comparison. IJRCE 2015; 5: 7-11.
[131] Llamedo M, Martínez JP, Albertal M, et al. Morphologica features of the ECG for detection of stress-induced ischemia. In Computing in Cardiology 2013; 40: 591-594.
[132] Garciá J, Wagner G, Sörnmo L, et al. Identification of the occluded artery in patients with myocardial ischemia induced by prolonged percutaneous transluminal coronary angioplasty using traditional vs transformed ECG-based indexes. Comput Biomed Res 1999; 32: 470-482.
[133] Tseng Y-L, Lin K-S, Jaw F-S. Comparison of support-vector machine and sparse representation using a modified rule-based method for automated myocardial ischemia detection. Comput Math Methods Med 2016: 1-8.
[134] Laguna P, Sörnmo L. The STAFF III ECG database and its significance for methodological development and evaluation. J Electrocardiol 2014; 47: 408-417.
[135] May R, Dandy G, Maier H. Review of input variable selection methods for artificial neural networks. In Artificial neural networks – methodological advances and biomedical applications. K. Suzuki (eds.). InTech, 2011, p. 374, ISBN 978-953-307-243-2.
[136] Guyon I, Elisseeff A. An introduction to variable and feature selection. J Mach Learn Res 2003; 3: 1157-1182.
[137] Meloun M, Militký J. Statistická analýza experimentálních dat. Academia, 2004, p. 953, ISBN 80-200-1254-0.
[138] Jolliffee IT. Principal component analysis (2nd edition). Springer, 2002, p. 487, ISBN 0-387-95442-2.
[139] Dougherty G. Pattern recognition and classification. An introduction. Springer, New York, 2013, p. 196, ISBN 978-1-4614-5322-2.
[140] Arlot S. A survey of cross-validation procedures for model selection. Statistics Suveys 2010; 4: 40-79.
[141] Labatut V, Cherifi H. Accuracy measures for the comparison of classifiers. In Proceedings of The 5th International Conference on Information Technology 2011, 1-5.
[142] Ghosh AK. On optimum choice of k in nearest neighbor classification. Comput Stat Data Anal 2006; 50: 3113-3123.
[143] Hejč J, Ronzhina M, Janoušek O, et al. The effect of heart orientation on high frequency QRS components in multiple bandwidths. In Computing in Cardiology 2015: 1121-1124.

SELECTED AUTHOR PUBLICATIONS:

[1] Ronzhina M, Čmiel V, Janoušek O, et al. Application of the optical method in experimental cardiology: action potential and intracellular calcium concentration measurement. Physiol Res 2013; 62: 125-137.
[2] Janoušek O, Kolářová J, Ronzhina M, et al. Motion artefact in voltage-sensitive fluorescent dye emission during repeated ischemia of isolated heart. Physiol Res 2013; 62: 371-378.
[3] Maršánová L, Ronzhina M, Vítek M. Automatická klasifikace EKG s použitím morfologických parametrů. Elektrorevue 2015; 17: 115-123.
[4] Maršánová L, Ronzhina M, Smíšek R, et al. Použití kumulantů vyšších řádů pro automatickou klasifikaci EKG. Elektrorevue 2016; 18: 103-111.
[5] Kolářová J, Nováková M, Ronzhina M, et al. Isolated Rabbit Hearts – Databases of EGs and MAP Signals. In Computing in Cardiology 2013: 551-554.
[6] Ronzhina M, Olejníčková V, Janoušek O, et al. Effects of heart orientation on isolated hearts electrograms. In Computing in Cardiology 2013: 543-546.
[7] Ronzhina M, Olejníčková V, Stračina T, et al. Evaluation of repeated global ischemia in isolated rabbit heart. In Proceedings of the 41st International Congress on Electrocardiology 2014: 175-178.
[8] Ronzhina M, Potočňák T, Janoušek O, et al. Spectral and higher-order statistics analysis of ECG: application to study of ischemia in rabbit isolated hearts. In Computing in Cardiology 2012: 645-648.
[9] Ronzhina M, Maršánová L, Smíšek R, et al. Classification of ventricular premature and ischemic beats in animal electrograms. In Computing in Cardiology 2015: 1137-1140.
[10] Olejníčková V, Ronzhina M, Paulová H, et al. Susceptibility of isolated rabbit hearts with various left ventricular mass to short ischemic periods. In Computing in Cardiology 2014; 1097-1100.
[11] Hejč J, Ronzhina M, Janoušek O, et al. The effect of heart orientation on high frequency QRS components in multiple bandwidths. In Computing in Cardiology 2015: 1121-1124.
[12] Janoušek O, Ronzhina M, Hejč J, et al. The effect of voltage-sensitive dye di-4-ANEPPS on heart rate variability in Langendorff-perfused isolated rabbit heart. In Computing in Cardiology 2015: 1049-1052.
[13] Olejníčková V, Ronzhina M, Janoušek O, et al. Voltage sensitive dye di-4-ANNEPS prolongs impulse conduction through ventricles, but not through AV node in isolated rabbit heart. In Computing in Cardiology 2015: 1-4.
[14] Veselý P, Ronzhina M, Fialová , et al. The effect of voltage sensitive dye di-4-ANEPPS on the RT/ RR coupling in rabbit isolated heart. In Computing in Cardiology 2015: 1137-1140.

APPENDIX A – PARAMETERS CALCULATED FROM ELECTROGRAMS AND VECTORCARDIOGRAMS

Table A-1. Groups of electrogram based parameters.

Name	Description, unit
Interval parameters(joint for all leads):	
RR	RR interval duration, ms
QRS_D	QRS complex duration, ms
QT	QT interval duration, ms
JTmax	Time interval from J point to maximal deviation of ST-T, ms
PQ	PQ interval duration, ms
Voltage parameters:	
QRS_A	Maximal absolute deviation of QRS complex, mV
$+QRS_A$	Maximal positive deviation of QRS complex, mV
$-QRS_A$	Maximal negative deviation of QRS complex, mV
ST20	Deviation of ST-T at J+20 ms point, mV
T_A	Maximal deviation of ST-T, mV
AUC based parameters I:	
AUC_{QRST}	Area under QRS-T, mV·ms
AUC_{QRS}	Area under QRS complex, mV·ms
AUC_{JT}	Area under ST-T, mV·ms
$+AUC_{QRS}$	Area under positive part of QRS complex, mV·ms
$-AUC_{QRS}$	Area under negative part of QRS complex, mV·ms
$+/- AUC_{QRS}$	Ratio between areas under positive and negative parts of QRS complex: $+AUC_{QRS} / -AUC_{QRS}$, -
AUC_{JTmax}	Area under curve from J point to maximal deviation of ST-T, mV·ms
$AUC_{TmaxTend}$	Area under curve from maximal deviation of ST-T to the end of T wave, mV·ms
$AUC_{JTmax/TmaxTend}$	Ratio between areas under ST-T curve before and after maximal deviation of ST-T: $AUC_{JTmax} / AUC_{TmaxTend}$, -
$+AUC_{JT}$	Area under positive part of ST-T, mV·ms
$-AUC_{JT}$	Area under negative part of ST-T, mV·ms
AUC based parameters II:	
AUC_{QRST}'	Area under |QRS-T|, where |.|- absolute value, mV·ms
AUC_{QRS}'	Area under |QRS|, mV·ms
AUC_{JT}'	Area under |ST-T|, mV·ms
AUC_{JTmax}'	Area under absolute values from J point to maximal deviation of ST-T, mV·ms
$AUC_{TmaxTend}'$	Area under absolute values from maximal deviation of ST-T and end of T wave, mV·ms
AUC based parameters III:	
$AUC_{QRS}R'$	Relative AUC_{QRS}': AUC_{QRS}' / AUC_{QRST}', -
$AUC_{JT}R'$	Relative AUC_{JT}': AUC_{JT}' / AUC_{QRST}', -
$+AUC_{QRS}R'$	Relative $+AUC_{QRS}$: $+AUC_{QRS} / AUC_{QRST}'$, -
$-AUC_{QRS}R'$	Relative $\|-AUC_{QRS}\|$: $\|-AUC_{QRS}\| / AUC_{QRST}'$, -
$+AUC_{QRS}Rq'$	Relative $+AUC_{QRS}$: $+AUC_{QRS} / AUC_{QRS}'$, -
$-AUC_{QRS}Rq'$	Relative absolute value of $-AUC_{QRS}$: $\|-AUC_{QRS}\| / AUC_{QRS}'$, -
$AUC_{JTmax}R'$	Relative AUC_{JTmax}': $AUC_{JTmax}' / AUC_{QRST}'$, -
$AUC_{TmaxTend}R'$	Relative $AUC_{TmaxTend}'$: $AUC_{TmaxTend}' / AUC_{QRST}'$, -
$+AUC_{JT}R'$	Relative $+AUC_{JT}$: $+AUC_{JT} / AUC_{QRST}'$, -
$-AUC_{JT}R'$	Relative absolute value of $-AUC_{JT}$: $\|-AUC_{JT}\| / AUC_{QRST}'$, -

Table A-2. Groups of VCG based parameters.

Name	**Description, unit**
Common parameters:	
L_{qrs}	Maximal QRS spatial vector magnitude, mV
L_{jt}	Maximal ST-T spatial vector magnitude, mV
α_{qrs}	Angle of maximal QRS vector in frontal plane, °
β_{qrs}	Angle of maximal QRS vector in horizontal plane, °
γ_{qrs}	Angle of maximal QRS vector in sagittal plane, °
α_{jt}	Angle of maximal ST-T vector in frontal plane, °
β_{jt}	Angle of maximal ST-T vector in horizontal plane, °
γ_{jt}	Angle of maximal ST-T vector in sagittal plane, °
3D loop parameters:	
P_{qrs}	Perimeter of 3D QRS loop, mV
P_{jt}	Perimeter of 3D ST-T loop, mV
D	Distance between maximal QRS and ST-T vector, mV
φ	Angle between maximal QRS and ST-T spatial vector, °
2D loop area based parameters:	
$A_{qrs}xy$	Area of 2D QRS loop in frontal plane, mV^2
$A_{qrs}xz$	Area of 2D QRS loop in horizontal plane, mV^2
$A_{qrs}zy$	Area of 2D QRS loop in sagittal plane, mV^2
$A_{jt}xy$	Area of 2D ST-T loop in frontal plane, mV^2
$A_{jt}xz$	Area of 2D ST-T loop in horizontal plane, mV^2
$A_{jt}zy$	Area of 2D ST-T loop in sagittal plane, mV^2
2D loop centroid based parameters:	
$D^c_{qrs}xy$	Distance between main QRS and centroid vectors in frontal plane, mV
$D^c_{qrs}xz$	Distance between main QRS and centroid vectors in horizontal plane, mV
$D^c_{qrs}zy$	Distance between main QRS and centroid vectors in sagittal plane, mV
$D^c_{jt}xy$	Distance between main ST-T and centroid vectors in frontal plane, mV
$D^c_{jt}xz$	Distance between main ST-T and centroid vectors in horizontal plane, mV
$D^c_{jt}zy$	Distance between main ST-T and centroid vectors in sagittal plane, mV
$\varphi^c_{qrs}xy$	Angle between main QRS and centroid vectors in frontal plane, °
$\varphi^c_{qrs}xz$	Angle between main QRS and centroid vectors in horizontal plane, °
$\varphi^c_{qrs}zy$	Angle between main QRS and centroid vectors in sagittal plane, °
$\varphi^c_{jt}xy$	Angle between main ST-T and centroid vectors in frontal plane, °
$\varphi^c_{jt}xz$	Angle between main ST-T and centroid vectors in horizontal plane, °
$\varphi^c_{jt}zy$	Angle between main ST-T and centroid vectors in sagittal plane, °